Information Sciences 320 (2015) 244–287

Contents lists available at ScienceDirect

Information Sciences

journal homepage: www.elsevier.com/locate/ins

Differential evolution with hybrid linkage crossover

Yiqiao Cai [a,*], Jiahai Wang [b]

[a] College of Computer Science and Technology, Huaqiao University, Xiamen 361021, China
[b] Department of Computer Science, Sun Yat-sen University, Guangzhou 510006, China

A R T I C L E   I N F O

Article history:
Received 2 March 2014
Received in revised form 5 February 2015
Accepted 15 May 2015
Available online 27 May 2015

Keywords:
Differential evolution
Linkage learning
Crossover
Grouping
Numerical optimization

A B S T R A C T

In the field of evolutionary algorithms (EAs), differential evolution (DE) has been the subject of much attention due to its strong global optimization capability and simple implementation. However, in most DE algorithms, crossover operator often ignores the consideration of interactions between pairs of variables. That is, DE is linkage-blind, and the problem-specific linkages are not utilized effectively to guide the search process. Furthermore, linkage learning techniques have been verified to play an important role in EA optimization. Therefore, to alleviate the drawback of linkage-blind in DE and enhance its performance, a novel linkage utilization technique, called hybrid linkage crossover (HLX), is proposed in this study. HLX utilizes the perturbation-based method to automatically extract the linkage information of a specific problem and then uses the linkage information to guide the crossover process. By incorporating HLX into DE, the resulting algorithm, named HLXDE, is presented. In order to evaluate the effectiveness of HLXDE, HLX is incorporated into six original DE algorithms, as well as several advanced DE variants. Experimental results demonstrate the high performance of HLX for the DE algorithms studied.

1. Introduction

Differential evolution (DE), proposed by Storn and Price [55], is a simple and powerful evolutionary algorithm (EA) for global optimization over continuous space. In the field of EA, DE has been the subject of much attention due to its attractive characteristics, such as its compact structure, ease of use, speediness and robustness. In the last few years, DE has been extended for handling multiobjective, constrained, large scale, dynamic and uncertain optimization problems [11,40] and is now successfully used in various scientific and engineering fields [47,66,19,85], such as chemical engineering, engineering design, and pattern recognition.

When DE is applied to a given optimization problem, there are two main factors which significantly affect the behavior of DE: control parameters (i.e., population size *NP*, mutation scaling factor *F* and crossover rate *Cr*) and evolutionary operators (i.e., mutation, crossover and selection). During the last decade, many researchers have worked to improve DE by adopting self-adaptive strategies for the control parameters [48,30,13], devising new mutation operators [23,5,67], developing ensemble strategies [68,25,6], and proposing a hybrid DE with other optimization algorithms [73,46,64], etc. Many studies related to the evolutionary operators of DE have focused on the mutation operator [48,30,23,5,68,25]. In contrast, there have been few studies on the crossover operator of DE [43,24,69].

* Corresponding author.
E-mail addresses: caiyq@hqu.edu.cn (Y. Cai), wjiahai@hotmail.com (J. Wang).

http://dx.doi.org/10.1016/j.ins.2015.05.026
0020-0255/

Linkages or inter-dependencies between pairs of variables have been studied and utilized in genetic algorithm (GA) and EAs to improve performance on difficult problems [8,65]. From the perspective of GA, tight linkage refers to the identified building blocks (BBs) on a chromosome, and the genes belonging to the same BB should be inherited together by the offspring at a higher probability. According to the existing work, linkage identification or recognition of BBs plays an important role in GA optimization [8,65]. Many linkage learning techniques have been proposed for combinatorial optimization [8,65,17], while techniques for global numerical optimization have been rarely discussed [84,7]. In addition, to the best of our knowledge, studies explicitly using linkage information to enhance the performance of DE are scarce. Therefore, most DE algorithms are not able to effectively utilize problem-specific linkages for guiding the search.

Based on these considerations, we present a novel linkage utilization technique, called hybrid linkage crossover (HLX), to utilize the problem-specific linkages to guide the crossover process of DE. First, HLX uses a perturbation-based method, an improved differential grouping (DG) method [44], to adaptively extract the linkage information between pairs of variables. The linkage information is stored in a linkage matrix (*LM*). In *LM*, each element stands for "linkage strength" which measures the likelihood of a pair of variables being tightly linked. Then, with *LM*, the BBs are identified by automatically decomposing the problem variables into different groups without overlaps. Here, BB is a group of tightly interactive variables. Finally, two group-wise crossover operators are designed to explicitly use the identified BBs for guiding the crossover process. One is named group-wise binomial crossover (GbinX). Different from the conventional binomial crossover of DE, GbinX exchanges the variables based on the detected groups. The second one is referred to as group-wise orthogonal crossover (GorthX), which combines the orthogonal design [27,38] and the identified BBs to make a systematic search in a region defined by a pair of the target and mutant vectors. In this way, both GbinX and GorthX can avoid the disruption of BBs during crossover. By incorporating HLX into DE, the resulting algorithm, named HLXDE, is proposed. In HLXDE, the conventional binomial crossover operator and the two group-wise crossover operators are implemented together in a cooperative manner.

In order to evaluate the effectiveness of HLXDE, HLX is incorporated into six original DE algorithms, as well as several advanced DE variants. Experimental studies are carried out on a suite of benchmark problems, including the classical functions [74], the functions from the IEEE congress on evolutionary computation (CEC) 2005 special session on real-parameter optimization [56] and the functions from the IEEE CEC 2012 special session on large-scale global optimization [60]. The results indicate that HLX can effectively enhance the performance of most DE algorithms studied.

The major contributions of this study include the following:

- An improved differential grouping technique is presented to address the linkage learning problem for global numerical optimization. It provides some insights on how the idea of grouping variables can be extended beyond the cooperative coevolution framework.
- Two group-wise crossover operators, GbinX and GorthX, are designed to explicitly utilize the identified BBs to guide the crossover process of DE.
- HLXDE effectively combines two group-wise crossover operators with the binomial crossover in a cooperative manner, which effectively maintains the advantages of the binomial crossover and utilizes the BBs of good or promising individuals.
- HLX can be easily applied to other advanced DE variants and cooperated with different kinds of modifications in the advanced DE variants. It provides a new promising approach for optimization.

The rest of this paper is organized as follows. Section 2 briefly describes the original DE algorithm, the related work to the crossover operator of DE and the linkage learning techniques. Then, HLX and HLXDE are presented in detail in Section 3. In Section 4, the experimental results for a suite of benchmark functions are reported and analyzed. Finally, the conclusions are drawn in Section 5.

2. Related work

In this section, the original DE algorithm is introduced first. Then, the related work to the crossover operator of DE and the linkage learning techniques are reviewed.

2.1. DE

DE is for solving the numerical optimization problem. Without loss of generality, we consider the following optimization problem: *Minimize* $f(X), X \in S$, where $S \subseteq R^D$ and D is the dimension of the decision variables. DE evolves a population of vectors, and each vector is denoted as $X_{i,G} = (x_{1,i,G}, x_{2,i,G}, \ldots, x_{D,i,G})$, where $i = 1, 2, \ldots, NP$, NP is the size of the population and G is the number of current iteration. Here, the initial value of the jth parameter of $X_{i,G}$ can be generated by:

$$x_{j,i,G} = L_j + rndreal(0,1) \cdot (U_j - L_j) \tag{1}$$

where $rndreal(0,1)$ represents a uniformly distributed random variable within the range [0, 1] and L_j (U_j) represents the lower (upper) bound of the jth variable.

During each generation, DE uses three main operators for population reproduction: mutation, crossover and selection.

(1) *Mutation:* DE employs the mutation strategy to generate a mutant vector $V_{i,G}$ with respect to each individual $X_{i,G}$ (called the target vector) in the current population. The general notation for mutation strategy is "*DE/x/y*", where *DE* stands for differential evolution algorithm, *x* represents the vector to be perturbed and *y* represents the number of difference vectors considered for perturbation of *x*. Two commonly used strategies are as follows:

- "DE/rand/1"

$$V_{i,G} = X_{r1,G} + F \cdot (X_{r2,G} - X_{r3,G}) \tag{2}$$

- "DE/best/1"

$$V_{i,G} = X_{best,G} + F \cdot (X_{r2,G} - X_{r3,G}) \tag{3}$$

where F is called the mutation scaling factor, and $r1, r2$ and $r3$ are distinct integers randomly selected from the range $[1, NP]$ and are different from i. There are various well-known and widely used mutation strategies in the literature, such as "DE/rand/2", "DE/current-to-best/1", "DE/rand-to-best/1" and "DE/best/2". More details of them can be found in [55,11].

(2) *Crossover:* The crossover operator is applied to each pair of $X_{i,G}$ and the corresponding $V_{i,G}$ to generate a trial vector $U_{i,G}$. There are two types of crossover scheme: binomial and exponential. Here, only the binomial crossover (BinX) is outlined, as it is more widely used. BinX is shown as follows:

$$u_{j,i,G} = \begin{cases} v_{j,i,G} & \text{if } rndreal(0,1) \leqslant Cr \text{ or } j = j_{rand} \\ x_{j,i,G} & \text{otherwise} \end{cases} \tag{4}$$

where $Cr \in [0, 1]$ is called the crossover rate, and j_{rand} is an integer randomly selected from the range $[1, D]$. In this study, if $u_{j,i,G}$ is out of the boundary, it will be reinitialized within the range $[L_j, U_j]$.

(3) *Selection:* DE uses a one-to-one selection operator to select the better one between $X_{i,G}$ and $U_{i,G}$ to survive into the next generation. The selection operator is described as follows:

$$X_{i,G+1} = \begin{cases} U_{i,G} & \text{if } f(U_{i,G}) \leqslant f(X_{i,G}) \\ X_{i,G} & \text{otherwise} \end{cases} \tag{5}$$

2.2. Crossover operator in DE

DE has drawn many researchers' attention, which has resulted in many variants with improved performance [11,41]. According to [41], these DE variants can be divided into two categories: DE with an extra component and DE with modified structures. In the existing work of DE, the mutation operator has been studied in various ways. In contrast, there are few studies on the crossover operator of DE [11,41]. In this section, we focus on the work related to the crossover operator in the context of DE. Table 1 provides a list of some previous studies on the crossover operator in DE along with different facets (i.e., tuning *Cr* value, parameter adaption technique and crossover scheme).

Many researchers focus on tuning *Cr* to improve the performance of DE. From Table 1, we can find that these empirical suggestions for setting *Cr* are different and lack sufficient experimental justifications. However, some interesting observations can be obtained from these findings. A small *Cr* value (e.g., $Cr \leqslant 0.2$) is more appropriate for the separable functions, and a large *Cr* value (e.g., $Cr > 0.9$) is the best for non-separable functions. For the role of *Cr* in optimizing functions with interacting parameters, the greater the number of interacting parameters, the higher *Cr* must be. In addition, from the analysis in [39], DE with low values of *Cr* (near 0) results in very small exploratory moves that are orthogonal to the current axes, while DE with high values of *Cr* (near 1) makes large exploratory moves that are at angles to the search space's axes. That is, both extremes are able to produce effective moves [39]. In order to avoid manual tuning *Cr*, many parameter adaption techniques have been developed [48,30,33,80,4,34,79,61,31]. These researches presented the effective methods to adaptively tune the *Cr* value.

On the other hand, from Table 1, we can see that the studies on the new crossover scheme in DE are relatively few. In most of the DE variants, BinX is employed as the default. As mentioned above, the crossover operator has always been regarded as the primary search operator in GA, and the linkage identification or recognizing BBs plays an important role in the GA optimization [8,65]. However, in most of the crossover operators of DE, the linkage information is not effectively identified and used to enhance the performance of DE. Based on these analyses, in this study, we develop HLX to utilize the problem-specific linkages to guide the crossover process of DE.

2.3. Linkage learning

In GA and EAs, the identification and preservation of important interactions among variables have a desirable effect on the evolutionary process, which is generally called linkage learning. In biological systems, linkage refers to the level of association in inheritance of two or more non-allelic genes on the same chromosome [28]. These linked genes have a higher chance of being inherited from the same parent. In GA, linkage is used to describe and measure the interrelationships

Table 1
Previous studies on crossover operator in DE.

Taxonomy	Reference work	Approaches
Tuning *Cr*	Storn and Price [55]	*Cr* could be set to 0.1 or 0.9 to obtain good performance
	Mezura-Montes et al. [36]	A low value of $Cr = 0.1$ was often the best chosen
	Roňkkoňen et al. [50]	$Cr \leqslant 0.2$ was more appropriate for the separable functions and *Cr* close to 1.0 (e.g., $Cr > 0.9$) was the best for non-separable functions
	Montgomery and Chen [39]	DE behaved differently with low and high values of *Cr* and both extremes are able to produce effective moves
Parameter adaption technique	Qin et al. [48], Zhang et al. [83]	*Cr* was gradually self-adapted by learning from their previous experiences in generating promising solutions
	Liu and Lampinen [33]	Fuzzy logic controllers were used to adapt the *Cr* value
	Zaharie [80]	Adaptive control was based on the idea of controlling the population diversity
	Brest et al. [4]	Self-adaptive settings by extending individuals with the *Cr* value
	Mallipenddi et al. [34]	A pool of *Cr* values was taken in the range of 0.1–0.9
	Yu et al. [79]	Two-level adaptive parameter control scheme based on the optimization states and the individual's fitness value
	Tang et al. [61]	Individual-dependent parameter setting with a rank-based scheme and a value-based scheme
Crossover scheme	Storn and Price [55]	Two kinds of well-known crossover schemes, binomial and exponential crossover
	Zaharie [81]	A systematic analysis of the influence of binomial and exponential crossover on the behavior of DE
	Zhao et al. [86]	A linearly scalable exponential crossover operator based on a number of consecutive dimensions to crossover
	Weber and Neri [71]	A contiguous binomial crossover with the exchange of contiguous block in a fashion similar to the exponential crossover
	Lin et al. [32]	The choice of crossover method and parameters were related to the mathematical features of the problems
	Gou et al. [26]	Eigenvector-based crossover operator by utilizing eigenvectors of covariance matrix of individual solutions
	Noman and Iba [43]	A simplex crossover-based adaptive local search operator
	Gong et al. [24], Wang et al. [69]	An orthogonal crossover combined with the conventional crossover

existing between the genes. These highly interactive genes belong to a BB. When GA is applied to a given optimization problem, Holland [29] suggested that the genes belonging to the same BB should be tightly linked together on the chromosome to improve performance. Otherwise, if these linked genes spread all over the chromosome, the BBs are very hard to create and are easy to be disrupted during crossover, for example, single-point crossover. This suggestion is also supported in some studies [8,21,62]. Furthermore, for the continuous optimization, Chen et al. [7] suggested that the crossover with dynamic linkage technique is beneficial to utilizing the obtained linkage information. Therefore, identifying or recognizing BBs plays an important role in crossover of GA and EAs. However, it is often difficult to know the linkage information of a specific problem in the real world a priori. As a consequence, linkage learning has been studied in both the discrete and continuous GA and EAs [8,65,7,12,63]. Table 2 provides a list of some previous studies on linkage learning for discrete and continuous optimization problems.

For the discrete optimization problems, there are many linkage learning techniques proposed to improve the performance of GA and EAs. From Table 2, these linkage learning techniques can be classified into three categories based on different aspects of GA and EAs: how to distinguish between the good and bad linkages, how to express or represent linkage information and how to store linkage information [8]. More details of other linkage learning techniques in GA and EAs can be found in [8].

For the continuous optimization problems, linkage learning has been studied less. As shown in Table 2, there are several linkage learning methods for continuous optimization, such as dynamic linkage discovery [7], estimation of distribution algorithms (EDAs) [84], perturbation-based methods (PMs) [12,44] and data mining techniques [63]. In dynamic linkage discovery, the linkage configuration is adapted by assigning the linkage groups randomly [7]. Hence, dynamic linkage discovery does not rely on a systematic or smart procedure to discover the interactions among variables. It may happen that the problem-specific BBs are very hard to create and are destroyed easily during the crossover process. While identifying linkage in a statistical manner, EDAs generally tend to ignore BBs with a relatively low fitness contribution [9,63], and the computational cost of them is usually very high, for example, the Bayesian optimization algorithm (BOA) [45]. Recently, in the context of PMs for continuous global optimization, differential grouping (DG) which is an automatic decomposition strategy, was superimposed on a cooperative co-evolutionary framework in [44]. Based on the above analysis and the effectiveness of DG, a new linkage utilization technique based on DG is developed for the continuous optimization problems in this study.

3. Differential evolution with hybrid linkage crossover (HLXDE)

3.1. Motivation

As discussed above, the crossover operator plays an important role in the performance of DE [81,86,71,32,43,24,69]. The existing work [8,65,7,9,12] also demonstrates that the crossover with linkage learning can effectively prevent the linkages between pairs of variables from being destroyed and promote the cooperation of individuals of population. In most DE algorithms, BinX (see Eq. (4)) is employed to generate a trial vector from a pair of target and mutant vectors. As we can find, each variable of the trial vector in BinX is randomly and independently inherited from either target vector or mutant vector based on *Cr*. In this way, the linkage information between pairs of variables is ignored during the crossover process. That is, DE is linkage-blind, and thus the problem-specific linkages cannot be utilized to guide the evolutionary process. As discussed in [39,86,81,58], although DE can solve the non-separable functions with a high value of *Cr*, DE with a high *Cr* value will cause rapid and perhaps premature convergence unless the population size is large enough. In addition, DE with high values of *Cr* will take a longer time to solve these non-separable functions than that with low values of *Cr* [39]. That is, DE has difficulty on functions that are not linearly separable, and the linkage learning techniques might be used to further improve the performance of DE on these functions. Therefore, in order to alleviate this drawback and utilize the problem-specific linkages for enhancing the performance of DE, we propose HLX and then incorporate it into DE to present HLXDE in this study. The details of HLX and the complete framework of HLXDE are described as follows.

3.2. HLX

For many problems, the problem-specific knowledge does not exist in the individual variables but in the linkages between pairs of variables. In order to detect the underlying interaction structure of these variables and to guide the crossover process with the problem-specific linkage, HLX consists of three main operators: (1) constructing the linkage matrix to extract and store the linkage information; (2) adaptively grouping the problem variables to detect BBs; (3) applying group-wise crossover to explicitly use BBs for guiding the crossover process.

Algorithm 1. Linkage Matrix Construction (LMC)

Initialize a vector $C^0 = (c_1^0, \ldots, c_i^0, \ldots, c_D^0)$ and set c_i^0 as $lbound_i, i = 1, \ldots, D$
Initialize $\Delta_{max} = 0$
  // calculate difference value of pair variables
For $i = 1$ to $D - 1$ **do**
  Set c_i^0 as $ubound^i$ and name the new vector as C^1
  Calculate $\Delta_{1,x_i}[f](X) = f(C^1) - f(C^0)$
  For $j = i + 1$ to D **do**
    Set c_j^1 as $midbound_j$ and name the new vector as C^2
    Set c_i^2 as $lbound_j$ and name the new vector as C^3
    Calculate $\Delta_{2,x_i}[f](X) = f(C^2) - f(C^3)$
    Calculate $\Delta_{x_i,x_j}[f](X)$ using Eq. (8)
    If $|\Delta_{x_i,x_j}[f](X)| < f(C^0) \times 10^{-3}$ **Then**
      Set $\Delta_{x_i,x_j}[f](X) = 0$
    End if
    If $|\Delta_{x_i,x_j}[f](X)| > \Delta_{max}$ **Then**
      Set $\Delta_{max} = \Delta_{x_i,x_j}[f](X)$
    End if
  End for
End for
  // normalize difference values and store them in *LM*
For $i = 1$ to D **do**
  For $j = 1$ to D **do**
    calculate $LM[i,j]$ using Eq. (9)
  End For
End For

Table 2
Previous studies on linkage learning in discrete and continuous optimization problems.

Taxonomy	Reference work	Approaches
Discrete optimization problems	Salman et al. [51–53]	The probabilistic inference framework was used for modeling crossover operators and proposed an adaptive linkage crossover
	Goldberg et al. [20,22], Bandyopadhyay et al. [3]	Messy genetic algorithm (mGA) was proposed to solve problems by combining relatively short and well-tested building blocks to form longer and more complex substructures
	Emmendorfer and Pozo [14]	A simple EDA based on low-order statistic and a clustering technique was combined to propose a new evolutionary algorithm, φ-PBIL
	Yu et al. [75–78]	A dependency structure matrix GA (DSMGA) was proposed by utilizing a dependency structure matrix (DSM) to analyze and explicitly decompose the problem and using the BBs information to accomplish crossover
	Fan et al. [17,16], Nikanjam et al. [42]	Improved variants were proposed to enhance the performance of DSMGA
Continuous optimization problems	Chen et al. [7]	Dynamic linkage discovery was proposed to adapt the linkage configuration by employing the selection operator without extra judging criteria irrelevant to the objective function
	Zhange et al. [84]	A regularity model-based multiobjective estimation of distribution algorithm (RM-MEDA) for continuous multiobjective optimization problems with variable linkages
	Devicharan and Mohan [12]	Problem specific linkages was learned by examining a randomly chosen collection of points in the search space to determine the correlations in fitness changes resulting from perturbations in pairs of components of particle positions
	Omidvar et al. [44]	Differential grouping was proposed to automatically decompose an optimization problem into a set of smaller problems for large scale optimization
	Ting et al. [63]	Linkage was mined based on the analogy between building blocks and association rules

3.2.1. Linkage matrix construction (LMC)

By detecting the fitness changes from perturbing pairs of variables, the perturbation-based methods are employed to identify the interactive variables. Recently, differential grouping (DG) has been proposed to decompose the problem automatically, deriving from the definition of partial separability [44]. Due to its theoretical basis and effectiveness, DG is adopted and improved in HLX to detect the underlying structure of a specific problem. With the linkage information obtained by the improved DG, a linkage matrix (*LM*) is constructed to explicitly represent the linkage information between pairs of variables.

Given a function $f(x)$, two difference values with respect to variable x_i are calculated as follows [44]:

$$\Delta_{\delta,x_i}[f](X)|_{x_i=a,x_j=b} = f(\ldots,x_{i-1},a+\delta,x_{i+1},\ldots,x_{j-1},b,x_{j+1},\ldots) - f(\ldots,x_{i-1},a,x_{i+1},\ldots,x_{j-1},b,x_{j+1},\ldots) \quad (6)$$

$$\Delta_{\delta,x_i}[f](X)|_{x_i=a,x_j=c} = f(\ldots,x_{i-1},a+\delta,x_{i+1},\ldots,x_{j-1},c,x_{j+1},\ldots) - f(\ldots,x_{i-1},a,x_{i+1},\ldots,x_{j-1},c,x_{j+1},\ldots) \quad (7)$$

where a is an arbitrary value for x_i, $\delta \neq 0$ is a nonzero interval value, and b and c are two arbitrary different values for x_j. In Eqs. (6) and (7), $\Delta_{\delta,x_i}[f](X)|_{x_i=a,x_j=b}$ and $\Delta_{\delta,x_i}[f](X)|_{x_i=a,x_j=c}$ refer to the forward difference of $f(x)$ with respect to x_i with δ. Then, the difference value between them is calculated as follows:

$$\Delta_{x_i,x_j}[f](X) = \Delta_{\delta,x_i}[f](X)|_{x_i=a,x_j=b} - \Delta_{\delta,x_i}[f](X)|_{x_i=a,x_j=c} \quad (8)$$

After that, the difference value of each pair of variables is normalized and stored in *LM*, as follows:

$$LM[i,j] = \frac{\Delta_{x_i,x_j}[f](X)}{\Delta_{max}} \quad (9)$$

where Δ_{max} is the maximum value in *LM*. If $LM[i,j]$ is zero, x_i and x_j are regarded to be independent of each other or separable. Otherwise, they will be considered to be interacting or non-separable.

In this way, *LM* construction (LMC) operator extracts and stores the linkage information between pairs of variables in *LM*. Each element of *LM* stands for "linkage strength", which measures the likelihood of a pair of variables being tightly linked. The pseudo-code of LMC is described in Algorithm 1 where $lbound_i$, $ubound_i$ and $midbound_i$ represent the lower, upper and center bound of x_i respectively. Note that these values can be set randomly as long as they are not identical with each other so as to obtain the nonzero difference value. Additionally, if the difference value between x_i and x_j is smaller than $f(C^0) \times 10^{-3}$, they are regarded to be independent of each other in this study (see *steps 11–13* in Algorithm 1).

In order to illustrate how LMC works, a simple example based on Noisy Quartic function at $D = 8$ is shown here. The definition of Noisy Quartic function is as follows [74]:

$$f(X) = \sum_{i=1}^{8} ix_i^4 + random[0,1), \quad -1.28 \leqslant x_i \leqslant 1.28 \tag{10}$$

Firstly, a vector is initialized as $C^0 = (-1.28, \ldots, -1.28)$ and the difference values for pairs of variables are calculated using Eq. (8) (Here, $a = b = -1.28, \delta = 2 * 1.28 = 2.56, c = 0$), as follows:

$$\Delta_{x_1,x_2}[f](X) = (f(1.28, -1.28, \ldots, -1.28) - f(C^0)) - (f(1.28, 0, -1.28, \ldots, -1.28) - f(-1.28, 0, -1.28, \ldots, -1.28))$$

$$\begin{aligned}\Delta_{x_1,x_3}[f](X) = {} & (f(1.28, -1.28, \ldots, -1.28) - f(C^0)) - (f(1.28, -1.28, 0, -1.28, \ldots, -1.28) \\ & - f(-1.28, -1.28, 0, -1.28, \ldots, -1.28))\end{aligned}$$

...

$$\begin{aligned}\Delta_{x_7,x_8}[f](X) = {} & (f(-1.28, \ldots, -1.28, 1.28, -1.28) - f(C^0)) - (f(-1.28, \ldots, -1.28, 1.28, 0) \\ & - f(-1.28, \ldots, -1.28, -1.28, 0))\end{aligned}$$

Secondly, a difference matrix (DM) is used to store all the difference values, as follows:

$$\begin{pmatrix} 0.00 & 1.21 & 0.32 & 0.78 & 1.55 & 0.78 & 0.78 & 0.78 \\ 1.21 & 0.00 & 1.54 & 1.54 & 1.54 & 1.54 & 1.61 & 1.68 \\ 0.32 & 1.54 & 0.00 & 1.54 & 1.54 & 1.54 & 1.61 & 1.68 \\ 0.78 & 1.54 & 1.54 & 0.00 & 0.56 & 0.56 & 0.94 & 2.13 \\ 1.55 & 1.54 & 1.54 & 0.56 & 0.00 & 1.04 & 1.04 & 1.04 \\ 0.78 & 1.54 & 1.54 & 0.56 & 1.04 & 0.00 & 1.61 & 1.68 \\ 0.78 & 1.61 & 1.61 & 0.94 & 1.04 & 1.61 & 0.00 & 1.48 \\ 0.78 & 1.68 & 1.68 & \mathbf{2.13} & 1.04 & 1.68 & 1.48 & 0.00 \end{pmatrix} \tag{11}$$

Finally, all the difference values are normalized with $\Delta_{max} = 2.13$ using Eq. (9), and LM is constructed as follows:

$$\begin{pmatrix} 0.00 & 0.57 & 0.15 & 0.37 & 0.73 & 0.37 & 0.37 & 0.37 \\ 0.57 & 0.00 & 0.72 & 0.72 & 0.72 & 0.72 & 0.76 & 0.79 \\ 0.15 & 0.72 & 0.00 & 0.72 & 0.72 & 0.72 & 0.76 & 0.79 \\ 0.37 & 0.72 & 0.72 & 0.00 & 0.26 & 0.26 & 0.44 & 1.00 \\ 0.73 & 0.72 & 0.72 & 0.26 & 0.00 & 0.49 & 0.49 & 0.49 \\ 0.37 & 0.72 & 0.72 & 0.26 & 0.49 & 0.00 & 0.76 & 0.79 \\ 0.37 & 0.76 & 0.76 & 0.44 & 0.49 & 0.76 & 0.00 & 0.69 \\ 0.37 & 0.79 & 0.79 & 1.00 & 0.49 & 0.79 & 0.69 & 0.00 \end{pmatrix} \tag{12}$$

3.2.2. Adaptive grouping (AG)

After LMC, BBs are identified by AG to decompose the variables of a problem into different groups without overlap. Here, BB is a group of highly interactive variables. The pseudo-code of AG is described in Algorithm 2 where a state vector (i.e., Z) is used to examine whether the variable has been grouped. The algorithm starts by checking the linkage strength of the first variable with other variables based on LM. If the state value of the jth variable ($j = 2, 3, \ldots, D$) is marked as not being grouped (i.e., $z_j = 0$) and $LM[1, j]$ is greater than a threshold value (ϵ), the jth variable is placed into the same group with the first variable and its state value is changed to 1 (i.e., $z_j = 1$). This process is repeated until all the variables are grouped. In this study, ϵ is adaptively set as the mean value of all the elements in LM, which is shown in *step 2* of Algorithm 2. Additionally, in order to enhance the search ability of HLX, grouping is not carried out in sequential order but in a random order π. That is, let $\pi(i)$ be a random permutation of $i = 1, 2, \ldots, D$ and grouping is carried out following the order given by the permutation $\pi(i)$.

Although employing a similar way of detecting the interaction between pairs of variables, AG has some differences from DG [44]. First, as discussed in [44], without prior knowledge about the problem, the decomposition with a specified threshold value is not effective for all the problems, and how to set the threshold value is still a difficult problem. In DG, the threshold value is pre-set, while the threshold value (ϵ) in AG is set adaptively for different problems. The effectiveness of adaptive ϵ value will be studied in Section 4.7. Second, grouping in AG is carried out based on LM. In LM, each element represents the linkage strength between a pair of variables. In addition, randomness is also introduced into AG to generate different decompositions for the same problem. The benefit of randomness will be studied in Section 4.8 empirically. Third, AG is just as a linkage learning strategy for HLX, which is different from DG as a decomposition strategy for large scale optimization. In a sense, AG is an improved method of DG. Detailed discussions between HLXDE and the cooperative co-evolution with DG (CCDG) [44] will be given in Section 3.3.3.

Algorithm 2. Adaptive Grouping (AG)

Initialize the state vector as $Z = (0, \dots, 0, \dots 0)$
Set ϵ as the mean value of $\sum_{i=1}^{D}\sum_{j=1}^{D} LM[i,j]$
Initialize the number of groups as $num = 1$
For $i = 1$ to D **do**
  If $z_{\pi(i)} = 0$ **Then**
    Set $z_{\pi(i)} = 1, Group_{num} = \{\pi(i)\}$
    For $j = 1$ to D **do**
      If $z_{\pi(j)} = 0$ and $LM[\pi(i), \pi(j)] \geqslant \epsilon$ **Then**
        Set $z_{\pi(j)} = 1$
        $Group_{num} \leftarrow Group_{num} \cup \{\pi(j)\}$
      End if
    End for
  End if
  Set $num = num + 1$
End For

3.2.3. Group-wise crossover

In order to explicitly use the identified BBs, two group-wise crossover operators, named as group-wise binomial crossover (GbinX) and group-wise orthogonal crossover (GorthX), are introduced into HLX.

Algorithm 3. Group-wise Binomial Crossover (GbinX)

For $i = 1$ to $NumofGroup$ **do**
  If $rndreal(0,1) < Cr_G$ **Then**
    For $j \in Group_i$ **do**
      $u_j = v_j$
    End for
  Else
    For $j \in Group_i$ **do**
      $u_j = x_j$
    End for
  End if
End For

GbinX: Different from BinX in DE, GbinX exchanges the variables based on the identified BBs. The pseudo-code of GbinX is described in Algorithm 3 where Cr_G is the crossover rate for groups. When GbinX is applied to a pair of X_i and V_i, all variables belonging to the selected group in X_i will be replaced with the corresponding variables of V_i if a group is selected for exchange. In this way, GbinX can avoid the disruption of the problem-specific BBs during the crossover process. For simplicity, Cr_G is set as Cr of DE.

Algorithm 4. Group-wise Orthogonal Crossover (GorthX)

Generate an $L_M(2^N)$ OA
Make up M tested solutions $O_i (i = 1, \dots, M)$ by selecting the variables in the corresponding group from V_i or X_i according to the OA
Evaluate each tested solution $O_i (i = 1, \dots, M)$ and record the best vector, denoted as O_{best}
Calculate the effect of each level on each factor, and determine the best level for each factor using Eq. (10)
Derive a predictive solution O_{pr} with the identified best level of each factor
Compare $f(O_{best})$ with $f(O_{pr})$, and output the better solution as U_i

GorthX: An efficient way to study the effect of several factors simultaneously is to use orthogonal experimental design (OED) with both orthogonal array (OA) and factor analysis (FA) [27,38]. OED utilizes the properties of fractional factorial experiments to efficiently determine the best combination levels for different factors with a reasonably small number of experimental samples. Therefore, OED with OA and FA is regarded as a systematic reasoning experimental design method. For more details of OED, see [27,38]. In order to make a systematic search in a region defined by a pair of parent vectors, GorthX is designed by using OED and BBs together to generate offspring. Here, OED is used to discover the best combination of a target vector and its mutant vector. Based on the identified BBs, each group of variables is regarded as a factor of OED in GorthX. The pseudo-code of GorthX is described in Algorithm 4. In Algorithm 4, the two-level OA is first generated as $L_M(2^N)$ where L means OA, N means the number of identified groups, and $M = 2^{\lceil \log_2(N+1) \rceil}$ is the number of combinations of the test cases. The way of constructing OA can be found at [27,38,82] and a number of OAs can also be found in http://www2.research.att.com/~njas/oadir/. Then, the M combinations (i.e., individuals) are constructed according to OA. After that, FA is used to discover the best combination of levels based on the experimental results of all the M combinations. The effect of each level on each factor is calculated as follows:

$$S_{nq} = \frac{\sum_{m=1}^{M} f_m \times z_{mnq}}{\sum_{m=1}^{M} z_{mnq}} \tag{13}$$

where S_{nq} denotes the effect of the qth level in the nth factor and f_m denotes the result of the mth combination. z_{mnq} is 1 if the mth combination is with the qth level of the nth factor, otherwise, z_{mnq} is 0. When all the S_{nq} values are calculated, the best level of each factor can be determined by selecting the level of each factor that provides the highest-quality S_{nq}. After that, a predictive solution is derived with the identified best level of each factor. Finally, the best combination among the M combinations and the predictive solution is output as the trial vector. A simple example from chemical experiments for illustrating how to use OED is shown in [82]. Note that OED used in GorthX is different from that in [82]. The variables belonging to the same group are regarded as a factor in GorthX, while each variable is regarded as a factor in [82].

Algorithm 5. HLXDE with "DE/rand/1" (HLXDE/rand/1)

Generate the initial population P and set $G = 1$;
Evaluate the fitness for each individual in P;
$*$ Apply **LMC** (Algorithm 1)
While the terminated condition is not satisfied **do**
$*$ Select an index OX_{index} from $\{1,\ldots,NP\}$ using the roulette wheel selection method based on the individuals' fitness
  For each individual $X_{i,G}$ **do**
    Mutation:
    Randomly select $r_1 \neq r_2 \neq r_3 \neq i$
    Generate $V_{i,G}$ using Eq. (2)
    Crossover:
$*$ **If** $X_{i,G} \neq X_{OX_{index},G}$ **Then**
$*$ **If** $rndreal(0,1) < e^{-2*(G-1)/G_{max}}$ **Then**
$*$ Generate $U_{i,G}$ using **BinX** (Eq. (4))
$*$ **Else**
$*$ Apply **AG** (Algorithm 2)
$*$ Generate $U_{i,G}$ using **GbinX** (Algorithm 3)
$*$ **End if**
$*$ **Else**
$*$ Apply **AG** (Algorithm 2)
$*$ Generate $U_{i,G}$ using **GorthX** (Algorithm 4)
$*$ **End if**
    Selection:
    Select the vector in the next generation using Eq. (5)
  End For
  Set $G = G + 1$
End while

3.3. HLXDE

Combining HLX with DE, HLXDE is presented. The pseudo-code of HLXDE with "DE/rand/1" (HLXDE/rand/1 for short) is shown in Algorithm 5, where the differences with respect to the original DE/rand/1 are highlighted with "$*$". From Algorithm 5, it is clear that HLXDE differs from the original DE algorithm only in the crossover operator.

In Algorithm 5, to save the computational cost and keep the implementation simple, GorthX is only applied to one individual which is selected by the roulette wheel selection method [2] based on the individual's fitness. That is, the individual with a better fitness value has a higher probability of being selected for GorthX. In addition, BinX has more chances to be executed at the beginning of HLXDE, and GbinX is activated more and more frequently along with the evolutionary process of DE. In this way, HLXDE can effectively maintain the advantages of BinX and utilize the BBs of good or promising individuals through group-wise crossover.

3.3.1. Algorithmic functioning

As pointed out in [41], reasons for the success of the DE variants are mainly due to the additional and alternative search moves integrating into the DE structure. Based on the discussions in [41], the algorithmic functioning of HLXDE is given as follows:

The use of GorthX in HLXDE can be seen as an increase of the exploitation moves. Concretely, GorthX uses both OED and the identified BBs to make a systematic search in the promising region defined by better parent vectors. In this way, GorthX can assist DE to promote the exploitation ability.

GbinX and BinX are performed in a cooperative manner. Here, a question may arise firstly: why GbinX does not completely replace BinX in HLXDE. The reason lies in that the population at the beginning of the evolutionary process has poor quality; thus the linkage information learned from the population cannot effectively reflect the underlying structure of a specific problem. By this way, BinX can maintain the exploration ability of DE by keeping population diversity at the beginning of the evolutionary process, while GbinX can utilize the identified BBs of good or promising individuals to guide the choice of possible search moves. Therefore, combining them together in HLXDE can not only maintain the advantages of BinX, but also utilize the BBs by GbinX.

In summary, by combining these three crossover operators, HLXDE can employ the linkage learning technique to enhance the search ability of DE. Therefore, it is expected that HLXDE can achieve a good balance between exploration and exploitation.

3.3.2. Complexity analysis

The additional complexity of HLXDE depends on HLX, which consists of LMC, AG and group-wise crossover. For LMC, the complexity lies in the calculation and normalization of difference value for each pair of variables. The complexity of the former is $O(D \times (D-1)/2)$, and the complexity of the latter is $O(D \times (D+1)/2)$. Thus, the total complexity of LMC is $O(D \times D)$. One may find that LMC will lead to additional fitness evaluations (FEs), and the number is $D \times D + D$. Note that the termination criterion of the algorithm is set on the basis of number of FEs. Therefore, the additional FEs of LMC have been included in the total number of FEs. It will be confirmed in the experimental study that the additional FEs of LMC are worthwhile for enhancing DE. For AG, the complexity is $O(D \times NG)$, where NG is the number of groups. When AG is applied to the separable function, NG is D. This is the worst-case scenario for NG, and the complexity of AG in this case is $O(D \times D)$. For the group-wise crossover, the complexity of GbinX and GorthX is $O(D)$ and $O((M+1) \times D)$ where $M = 2^{(\lceil log_2(NG+1)\rceil)}$, respectively. Note that LMC is only carried out once at each run and GorthX is also only employed once at each generation. Since the complexity of the original DE algorithm is $O(Gmax \times NP \times D)$ where $Gmax$ is the maximal number of generation, the total complexity of HLXDE is $O(G_{max} \times NP \times D \times NG)$.

In order to analyze the computational overhead of DE and HLXDE empirically, a run-time based performance comparison is carried out here. The results are shown in Tables 3 and 4. Note that these results are approximate. The measure of algorithm complexity used here is from [56]. Table 3 shows that the complexities of HLXDE/rand/1 is higher than DE/rand/1, especially for $f6$ and $f13$. The reason is that HLX requires additional cost to extract the linkage information and execute the group-wise crossover. However, with the increase of dimension, the relative time required by HLX decreases with respect to the total run-time of HLXDE, especially for $F11$ and $F13$. Table 4 also shows that HLXDE/rand/1 can reach the predefined threshold value with less run-time in most cases, compared with DE/rand/1. These results indicate that the computational cost of HLX is worthwhile for enhancing the performance of DE.

3.3.3. Comparison with cooperative co-evolution with DG (CCDG) [44]

In CCDG [44], DG, as a decomposition strategy, is superimposed on CC to improve the performance for large scale optimization problems. As discussed in Section 3.2.2, AG in HLXDE is similar to DG in CCDG. However, there are three major differences between HLXDE and CCDG. First, the difference values are represented and normalized as linkage strength in AG, which might make it easier to tune the ϵ value than CCDG. This will be confirmed in Section 4.7. In addition, by introducing randomness, the grouping structure will be changed dynamically. As stated in [7], the configuration of BBs may dynamically change along with the search stages. In this sense, AG with randomness in HLX may be more reasonable and provide a benefit to numerical optimization. The benefit of randomness in AG will be studied in Section 4.8. Second, in HLXDE, group-wise crossovers (GbinX and GorthX) are used to make a systematic search in the region defined by the pair of trial vector and parent vector, while DG with CC is used to decompose the large-scale problem into a set of smaller subproblems. That is, the functioning of AG in HLXDE is to enhance the exploitation ability of DE through group-wise crossovers, while DG is used for the divide-and-conquer strategy in CC. Third, although co-evolution with different subcomponents is similar to crossover in EAs, in HLXDE, three crossover operators (BinX, GbinX and GorthX) are employed and combined together to fully exploit

Table 3
Comparison the computational complexity of DE/rand/1 and HLXDE/rand/1 when both the algorithms were run for a fixed number of fitness evaluations.

Func.	Dimension	$T0$	$T1$	DE/rand/1 $\widehat{T2}$	DE/rand/1 $(\widehat{T2}-T1)/T0$	HLXDE/rand/1 $\widehat{T2}$	HLXDE/rand/1 $(\widehat{T2}-T1)/T0$
Step Function (f_6)	10		0.187	0.203	0.128	0.519	2.656
	30		0.516	0.559	0.344	1.263	5.976
	50		0.937	0.944	0.056	1.869	7.456
Generalized Penalized Function (f_{13})	10		0.518	0.559	0.328	0.894	3.008
	30		1.64	1.684	0.352	2.578	7.504
	50	0.125	2.718	2.747	0.232	3.988	10.16
Shifted Rotated Weierstrass Function (F_{11})	10		15.25	15.431	1.448	15.909	5.272
	30		46.562	47.135	4.584	49.169	20.856
	50		79.203	80.305	8.816	82.266	24.504
Shifted expanded Griewank's + Rosenbrock's function (F_{13})	10		0.61	0.791	1.448	1.15	4.32
	30		2.719	3.238	4.152	4.181	11.696
	50		6.266	7.1	6.672	8.65	19.072

The meaning of $T0, T1$ and $\widehat{T2}$ can be referred to [56].

Table 4
Comparison of absolute run-times of DE/rand/1 and HLXDE/rand/1 when both the algorithms were run until they attain a pre-defined objective function value.

Func.	Dimension	Threshold objective function value to reach	Mean computing time DE/rand/1	Mean computing time HLXDE/rand/1
Step Function (f_6)	10		0.019	0.025
	30	1.00E−08	0.184	0.169
	50		0.488	0.431
Generalized Penalized Function (f_{13})	10		0.094	0.112
	30	1.00E−08	0.912	0.791
	50		2.393	1.925
Shifted Rotated Weierstrass Function (F_{11})	10	1.00E−03	13.883	14.469
	30	4.10E+01	33.432	23.647
	50	7.50E+01	7.391	2.657
Shifted Expanded Griewank's + Rosenbrock's Function (F_{13})	10	1.00E+00	1.177	1.580
	30	5.00E+00	18.519	14.922
	50	1.00E+01	63.228	47.422

the linkage information. In a word, HLXDE is proposed for explicitly utilizing the linkage information to guide the multiple crossover operators, which makes it distinctively different from CCDG. What's more, HLXDE also provides some insights on how the idea of grouping variables can be extended beyond the CC framework.

3.3.4. Comparison with orthogonal crossover based DE (OXDE) [69]

Recently, Wang et al. used orthogonal crossover (OX) to enhance the search ability of DE and proposed OXDE. In OXDE, one vector is selected randomly for OX to generate its trial vector. Although employing a similar OX in DE, HLXDE differs from OXDE in the following aspects. First, the groups in HLXDE are constructed based on the linkage information between pairs of variables, while the groups in OXDE are randomly generated. That is, OXDE ignores the interaction between the variables. Second, the number of groups is automatically decided in HLXDE, and the number of groups is specified in OXDE to reduce the number of the orthogonal combinations. Third, HLXDE uses OED with both OA and FA, while OXDE only employs OX and is without FA. Due to these differences, HLXDE may be more effective than OXDE in enhance the performance of DE, which will be discussed in Section 4.5.

3.3.5. Comparison with EDA-based DE

Estimation of distribution algrotihm (EDA) is also incorporated into DE to enhance its performance, such as DE/EDA [57] and ED-DE [70]. In DE/EDA, the global information extracted by EDA is combined with the differential information obtained by DE to generate the solutions [57]. In ED-DE, EDA and DE are conducted in a serial cooperative way [70]. However, both DE/EDA and ED-DE did not explicitly employ EDA to detect the interaction between pairs of variables. That is, EDAs in both of them are only used to sample the promising solutions but not employed to guide the crossover process with the linkage information, which is significantly different from the motivations of HLXDE.

Table 5
Classical Benchmark functions [74].

Name	Characteristics	Test functions	S
Sphere	Separable, scalable	$f_1 = \sum_{i=1}^{D} x_i^2$	$[-100, 100]^D$
Schwefel 2.22	Separable, scalable	$f_2 = \sum_{i=1}^{D} \lvert x_i \rvert + \prod_{i=1}^{D} \lvert x_i \rvert$	$[-10, 10]^D$
Schwefel 1.2	Nonseparable, scalable	$f_3 = \sum_{i=1}^{D} \left(\sum_{j=1}^{i} x_j \right)^2$	$[-100, 100]^D$
Schwefel 2.21	Nonseparable, scalable	$f_4 = \max_i \{ \lvert x_i \rvert, 1 \leqslant i \leqslant D \}$	$[-100, 100]^D$
Rosenbrock	Nonseparable, scalable, narrow valley from local to global optimum	$f_5 = \sum_{i=1}^{D-1} [100(x_{i+1} - x_i^2)^2 + (x_i - 1)^2]$	$[-30, 30]^D$
Step	Separable, scalable	$f_6 = \sum_{i=1}^{D} (\lfloor x_i + 0.5 \rfloor)^2$	$[-100, 100]^D$
Quartic	Separable, scalable	$f_7 = \sum_{i=1}^{D} i x_i^4 + random[0, 1)$	$[-1.28, 1.28]^D$
Schwefel 2.26	Separable, scalable, numerous local optima	$f_8 = \sum_{i=1}^{D} (-x_i sin(\sqrt{\lvert x_i \rvert}))$	$[-500, 500]^D$
Rastrigin	Separable, scalable, numerous local optima	$f_9 = \sum_{i=1}^{D} [x_i^2 - 10cos(2\pi x_i) + 10]$	$[-5.12, 5.12]^D$
Ackley	Separable, scalable, numerous local optima	$f_{10} = -20exp\left(-0.2\sqrt{\frac{1}{D}\sum_{i=1}^{D} x_i^2}\right) - exp(\frac{1}{D}\sum_{i=1}^{D} cos 2\pi x_i) + 20 + e$	$[-32, 32]^D$
Griewank	Separable, scalable, numerous local optima	$f_{11} = \frac{1}{4000}\sum_{i=1}^{D} x_i^2 - \prod_{i=1}^{D} cos(\frac{x_i}{\sqrt{i}}) + 1$	$[-600, 600]^D$
Penalized 1	Separable, scalable, numerous local optima	$f_{12} = \frac{\pi}{D}\{10sin^2(\pi y_1) + \sum_{i=1}^{D-1} (y_i - 1)^2 [1 + 10sin^2(\pi y_{i+1})]$ $+ (y_D - 1)^2\} + \sum_{i=1}^{D} u(x_i, 10, 100, 4)$	$[-50, 50]^D$
Penalized 2	Separable, scalable, numerous local optima	$f_{13} = 0.1\{sin^2(3\pi x_1) + \sum_{i=1}^{D-1} (x_i - 1)^2 [1 + sin^2(3\pi x_{i+1})]$ $+ (x_D - 1)^2 [1 + sin^2(2\pi x_D)]\} + \sum_{i=1}^{D} u(x_i, 5, 100, 4)$ where $u(x_i, a, k, m) = \begin{cases} k(x_i - a)^m & x_i > a \\ 0 & -a \leqslant x_i \leqslant a \\ k(-x_i - a)^m & x_i < -a \end{cases}$ $y_i = 1 + 0.25(x_i + 1)$	$[-50, 50]^D$

4. Experimental study

In this section, comprehensive experiments are carried out to evaluate the effectiveness of HLXDE. Thirty-eight benchmark functions are selected as the test suite, including the classic functions [74] and the functions from the CEC 2005 special session on real-parameter optimization [56]. Here, the benchmark functions are presented first. Secondly, the experimental setup is shown. Finally, the comparisons between HLXDE and the corresponding DE algorithms are made.

4.1. Benchmark functions

Thirty-eight benchmark functions are used in this study. These functions are widely used in evaluating global numerical optimization algorithms. The first 13 functions (denoted as $f1 - f13$) are selected from the classical benchmark function suite in [74], which includes 6 unimodal functions and 7 multimodal functions. The next 25 functions (denoted as $F_1 - F_{25}$) are selected from the special session on real-parameter optimization of CEC 2005 [56]. These functions span a diverse set of problem characteristics, such as multimodality, ill conditioning, interdependence, and rotation. They can be categorized into four groups: unimodal functions ($F_1 - F_5$), basic multimodal functions ($F_6 - F_{12}$), expanded multimodal functions (F_{13} and F_{14}), and hybrid composition functions ($F_{15} - F_{25}$). The short descriptions of these 38 functions are shown in Tables 5 and 6, and more details of them can be found in [74,56], respectively.

4.2. Experimental setup

To make a fair comparison, the same initial random population is used to evaluate different algorithms, and the parameters for all the DE algorithms are set as follows unless a change is mentioned.

- Dimension of the function (D): 30 and 50.
- Population size (NP): 100 [4,43].
- Scaling Factor (F): 0.5 [55,33,4].
- Crossover Probability (Cr, Cr_G): 0.9 [55,4].
- Maximal number of fitness function evaluations ($MNFES$): If D = 30, 150,000 for f_1,f_6,f_{10},f_{12} and f_{13}; 500,000 for $f_3 - f_5$; 200,000 for f_2 and f_{11}; 300,000 for other functions. If $D = 50, D \times 10000$ for all the functions [56].
- Number of runs: 30.

In the experiments, comparisons between six original DE algorithms (i.e., DE/rand/1, DE/rand/2, DE/best/1, DE/best/2, DE/current-to-best/1 and DE/rand-to-best/1) and their corresponding HLXDE algorithms are made first. Then, the performance of several advanced DE variants with the corresponding HLXDE variants are compared, including the opposition

Table 6
Benchmark functions from the special session on real-parameter optimization of CEC2005 [56].

Name	Characteristics	Test Functions	S
F_1: Shifted Sphere Function	Shifted, separable, scalable		$[-100, 100]^D$
F_2: Shifted Schwefel's Problem 1.2	Shifted, nonseparable, scalable		$[-100, 100]^D$
F_3: Shifted Rotated High Conditioned Elliptic Function	Shifted, rotated, nonseparable, scalable		$[-100, 100]^D$
F_4: Shifted Schwefel's Problem 1.2 with Noise in Fitness	Shifted, nonseparable, scalable, noise in fitness		$[-100, 100]^D$
F_5: Schwefel's Problem 2.6 with Global Optimum on Bounds	Nonseparable, scalable		$[-100, 100]^D$
F_6: Shifted Rosenbrock's Function	Shifted, nonseparable, scalable, narrow valley from local to global optimum		$[-100, 100]^D$
F_7: Shifted Rotated Griewank's Function without Bounds	Rotated, shifted, nonseparable, scalable		$[0, 600]^D$
F_8: Shifted Rotated Ackley's Function with Global Optimum on Bounds	Rotated, shifted, nonseparable, scalable		$[-32, 32]^D$
F_9: Shifted Rastrigin's Function	Shifted, separable, scalable, numerous local optima		$[-5, 5]^D$
F_{10}: Shifted Rotated Rastrigin's Function	Shifted, rotated, noseparable, scalable, numerous local optima		$[-5, 5]^D$
F_{11}: Shifted Rotated Weierstrass Function	Shifted, rotated, noseparable, scalable		$[-0.5, 0.5]^D$
F_{12}: Schwefels Problem 2.13	Shifted, nonseparable, scalable		$[-\pi, \pi]^D$
F_{13}: Shifted Expanded Griewanks + Rosenbrocks Function	Shifted, nonseparable, scalable	Given in [56]$^\diamond$	$[-3, 1]^D$
F_{14}: Shifted Rotated Expanded Scaffers F6	Shifted, nonseparable, scalable		$[-100, 100]^D$
F_{15}: Hybrid Composition Function	Scalable, numerous local optima		$[-5, 5]^D$
F_{16}: Rotated Hybrid Composition Function	Rotated, nonseparable, scalable, numerous local optima		$[-5, 5]^D$
F_{17}: Rotated Hybrid Composition Function with Noise in Fitness	Scalable, rotated, nonseparable, numerous local optima		$[-5, 5]^D$
F_{18}: Rotated Hybrid Composition Function	Rotated, nonseparable, scalable, numerous local optima		$[-5, 5]^D$
F_{19}: Rotated Hybrid Composition Function with a Narrow Basin for the Global Optimum	Nonseparable, scalable, numerous local optima		$[-5, 5]^D$
F_{20}: Rotated Hybrid Composition Function with the Global Optimum on the Bounds	Nonseparable, scalable, numerous local optima		$[-5, 5]^D$
F_{21}: Rotated Hybrid Composition Function	Rotated, nonseparable, scalable, numerous local optima		$[-5, 5]^D$
F_{22}: Rotated Hybrid Composition Function with High Condition Number Matrix	Nonseparable, scalable, numerous local optima		$[-5, 5]^D$
F_{23}: Non-Continuous Rotated Hybrid Composition Function	Nonseparable, scalable, numerous local optima, non-continuous		$[-5, 5]^D$
F_{24}: Rotated Hybrid Composition Function	Rotated, nonseparable, scalable, numerous local optima		$[-5, 5]^D$
F_{25}: Rotated Hybrid Composition Function without Bounds	Nonseparable, scalable, numerous local optima		$[2, 5]^D$

$^\diamond$ The detail definitions of these 25 CEC'05 test functions can be found in [56], and the program codes for all of them can be available from http://www3.ntu.edu.sg/home/EPNSugan/.

based DE (ODE) [49], DE with strategy adaptation (SaDE) [48], the composite DE (CoDE) [68], the modified DE with *p*-best crossover (MDE_*p*BX) [30] and the modified DE (MoDE) [35]. All the parameters of these DE variants are set as their original papers. The simulations are carried out on an Intel Core 2 duo PC with 3.20 GHz CPU and 3 GB RAM. Due to space limitation, only mean and standard deviation of the best error values obtained by algorithms are shown in this paper. The best and worst values obtained by algorithms are presented in the supplemental file of this paper.[1]

Furthermore, in order to show the significant differences between HLXDE and the corresponding competitors, several nonparametric statistical tests [18] are also carried out by the KEEL software [1]. The results of the single-problem Wilcoxon signed-rank test [18] at $\alpha = 0.05$ are summarized in the last row of the tables as "*w*/*t*/*l*", which means that HLXDE wins, ties and loses on w, t and l functions, compared with its competitors.

4.3. Comparison with original DE algorithms

In this section, HLXDE is compared with the original DE algorithms to test the effectiveness of HLX for the original DE mutation strategies. The results for the functions at 30D are shown in Table 7 and the convergence graphs for some test

[1] The supplemental file can be obtained from the first author.

Table 7
Mean and standard deviation of the best error values obtained by the original DE algorithms and their corresponding HLXDE variants on all the functions at 30*D*.

Func.	DE/rand/1 Mean ± Std	HLXDE/rand/1 Mean ± Std	DE/rand/2 Mean ± Std	HLXDE-DE/rand/2 Mean ± Std	DE/rand-to-best/1 Mean ± Std	HLXDE/rand-to-best/1 Mean ± Std
f1	5.766e−014 ± 6.020e−014†	**5.212e−022 ± 4.596e−022**	1.383e+002 ± 3.820e+001†	**1.667e−006 ± 8.952e−007**	9.057e+001 ± 7.396e+001†	**6.635e−001 ± 1.601e+000**
f2	3.429e−010 ± 1.392e−010†	**7.247e−016 ± 3.993e−016**	1.490e+001 ± 2.575e+000†	**9.126e−004 ± 5.335e−004**	1.802e+000 ± 7.581e−001†	**1.054e−001 ± 2.320e−001**
f3	3.407e−011 ± 3.644e−011†	**1.142e−012 ± 3.857e−012**	1.393e+003 ± 3.243e+002†	**2.374e+001 ± 7.873e+000**	4.606e+002 ± 2.915e+002	3.963e+002 ± 2.407e+002
f4	1.796e−001 ± 3.715e−001†	**1.372e−002 ± 5.243e−002**	**7.337e+000 ± 1.172e+000**‡	8.072e+000 ± 8.584e−001	9.354e+000 ± 2.936e+000†	**8.162e+000 ± 2.211e+000**
f5	**2.722e−011 ± 1.310e−010**‡	4.699e−008 ± 1.555e−007	2.928e+001 ± 2.041e+000†	**8.428e+000 ± 6.659e−001**	5.897e+003 ± 8.355e+003†	**2.305e+002 ± 1.591e+002**
f6*	[39,090 ± 1914.977]	[**27,844 ± 1375.495**]	1.432e+002 ± 3.062e+001†	**0.000e+000 ± 0.000e+000**	1.037e+002 ± 6.904e+001†	**1.400e+000 ± 2.253e+000**
f7	4.407e−003 ± 1.438e−003	4.626e−003 ± 1.422e−003	7.312e−002 ± 1.810e−002†	**6.301e−002 ± 1.479e−002**	3.341e−003 ± 1.369e−003	3.724e−003 ± 1.687e−003
f8	6.397e+003 ± 9.289e+002†	**0.000e+000 ± 0.000e+000**	7.338e+003 ± 2.430e+002†	**1.380e−007 ± 1.235e−007**	4.272e+003 ± 4.099e+002†	**7.054e+002 ± 3.338e+002**
f9	1.386e+002 ± 2.361e+001†	**0.000e+000 ± 0.000e+000**	2.203e+002 ± 1.103e+001†	**3.423e−005 ± 2.738e−005**	2.806e+001 ± 4.901e+000†	**5.308e−001 ± 7.266e−001**
f10	6.925e−008 ± 2.610e−008†	**2.014e−011 ± 7.005e−012**	4.614e+000 ± 3.427e−001†	**1.254e−003 ± 2.524e−004**	2.796e+000 ± 8.540e−001†	**5.281e−001 ± 4.822e−001**
f11	0.000e+000 ± 0.000e+000	2.465e−004 ± 1.350e−003	1.221e+000 ± 5.099e−002†	**3.453e−003 ± 1.246e−002**	1.786e+000 ± 6.774e−001†	**6.574e−002 ± 1.143e−001**
f12	3.845e−015 ± 3.900e−015†	**1.010e−022 ± 1.535e−022**	6.198e+001 ± 1.672e+002†	**5.899e−006 ± 2.519e−006**	2.052e+000 ± 1.121e+000†	**9.681e−002 ± 1.399e−001**
f13	4.110e−014 ± 3.521e−014†	**6.082e−022 ± 5.767e−022**	5.158e+002 ± 5.376e+002†	**5.310e−006 ± 2.141e−006**	1.513e+001 ± 7.878e+000†	**2.252e−001 ± 3.656e−001**
F1*	[107,566 ± 2303.421]	[**74,409 ± 1351.813**]	8.781e−001 ± 2.833e−001†	**0.000e+000 ± 0.000e+000**	1.818e+003 ± 8.097e+002†	**6.776e+001 ± 1.300e+002**
F2	5.663e−005 ± 2.748e−005†	**8.644e−006 ± 1.299e−005**	7.881e+003 ± 1.576e+003†	**8.228e+002 ± 2.239e+002**	4.735e+003 ± 2.008e+003†	**3.663e+003 ± 1.819e+003**
F3	4.028e+005 ± 2.337e+005	3.320e+005 ± 2.167e+005	5.172e+007 ± 1.160e+007†	**1.051e+007 ± 4.461e+006**	7.836e+006 ± 8.074e+006	6.354e+006 ± 4.202e+006
F4	6.528e−002 ± 1.180e−001†	**3.868e−003 ± 7.070e−003**	1.478e+004 ± 3.062e+003†	**5.655e+003 ± 2.331e+003**	1.130e+003 ± 1.044e+003	7.396e+002 ± 5.595e+002
F5	5.264e+001 ± 7.048e+001	1.216e+002 ± 2.074e+002	8.033e+003 ± 8.267e+002†	**6.631e+003 ± 5.059e+002**	7.360e+003 ± 1.372e+003	6.976e+003 ± 1.507e+003
F6	2.467e+000 ± 1.684e+000†	**2.353e−001 ± 4.447e−001**	6.274e+003 ± 3.018e+003†	**2.922e+001 ± 9.320e+000**	1.700e+008 ± 1.507e+008†	**3.552e+007 ± 5.428e+007**
F7	4.696e+003 ± 1.278e−002†	**4.696e+003 ± 2.360e−002**	5.474e+003 ± 7.314e+001†	**4.733e+003 ± 1.434e−004**	5.962e+003 ± 1.957e+002†	**4.733e+003 ± 1.434e−004**
F8	2.094e+001 ± 5.080e−002	2.095e+001 ± 4.622e−002	2.096e+001 ± 4.365e−002	2.094e+001 ± 5.163e−002	2.095e+001 ± 3.128e−002	2.094e+001 ± 5.695e−002
F9	1.304e+002 ± 2.588e+001†	**0.000e+000 ± 0.000e+000**	2.104e+002 ± 1.557e+001†	**1.089e−005 ± 6.946e−006**	6.258e+001 ± 1.662e+001†	**6.561e+000 ± 4.533e+000**
F10	1.816e+002 ± 1.025e+001†	**1.561e+002 ± 4.725e+001**	2.360e+002 ± 1.364e+001†	**2.245e+002 ± 1.130e+001**	9.018e+001 ± 2.038e+001†	**8.087e+001 ± 2.040e+001**
F11	3.963e+001 ± 1.031e+000†	**3.829e+001 ± 3.135e+000**	3.981e+001 ± 9.298e−001†	**3.911e+001 ± 1.069e+000**	1.344e+001 ± 1.832e+000	1.276e+001 ± 1.954e+000
F12	1.805e+003 ± 3.024e+003	1.764e+003 ± 1.784e+003	5.247e+005 ± 5.156e+004†	**3.305e+005 ± 2.971e+004**	6.837e+004 ± 3.707e+004	5.266e+004 ± 2.375e+004
F13	1.479e+001 ± 1.014e+000†	**8.260e+000 ± 7.036e−001**	2.083e+001 ± 1.311e+000†	**1.117e+001 ± 1.289e+000**	**4.928e+000 ± 3.406e+000**‡	5.165e+000 ± 1.254e+000
F14	**1.328e+001 ± 1.697e−001**‡	1.338e+001 ± 1.915e−001	1.340e+001 ± 1.497e−001	1.343e+001 ± 1.358e−001	1.158e+001 ± 3.386e−001	**1.145e+001 ± 3.424e−001**
F15	4.067e+002 ± 2.537e+001	**4.033e+002 ± 1.826e+001**	4.097e+002 ± 1.939e+001†	**4.044e+002 ± 1.826e+001**	4.658e+002 ± 1.018e+002	**4.302e+002 ± 1.193e+002**
F16	2.023e+002 ± 1.355e+001	**1.944e+002 ± 3.373e+001**	2.645e+002 ± 1.125e+001†	**2.475e+002 ± 1.219e+001**	2.371e+002 ± 1.774e+002	**2.270e+002 ± 1.733e+002**
F17	2.308e+002 ± 2.165e+001†	**2.161e+002 ± 1.344e+001**	3.060e+002 ± 1.260e+001†	**2.790e+002 ± 1.466e+001**	2.730e+002 ± 1.776e+002	**2.009e+002 ± 1.465e+002**
F18	9.044e+002 ± 1.452e+000	9.044e+002 ± 1.190e+000	9.402e+002 ± 4.175e+000†	**9.277e+002 ± 2.605e+000**	9.725e+002 ± 3.854e+001	**9.711e+002 ± 2.864e+001**
F19	9.043e+002 ± 1.050e+000	**9.042e+002 ± 9.329e−001**	9.407e+002 ± 4.013e+000†	**9.280e+002 ± 1.699e+000**	9.798e+002 ± 2.297e+001	**9.719e+002 ± 3.201e+001**
F20	**9.013e+002 ± 1.919e+001**	9.042e+002 ± 8.509e−001	9.400e+002 ± 3.395e+000†	**9.283e+002 ± 2.277e+000**	9.777e+002 ± 2.798e+001	**9.745e+002 ± 3.197e+001**
F21	5.000e+002 ± 2.043e−005	5.000e+002 ± 1.880e−005	5.003e+002 ± 1.080e−001†	**5.000e+002 ± 2.318e−004**	1.021e+003 ± 1.954e+002	**1.005e+003 ± 2.122e+002**
F22	**9.020e+002 ± 9.139e+000**	9.021e+002 ± 1.176e+001	1.018e+003 ± 1.431e+001†	**1.004e+003 ± 8.314e+000**	1.005e+003 ± 3.086e+001	**1.001e+003 ± 2.632e+001**
F23	5.342e+002 ± 2.747e−004	5.342e+002 ± 3.059e−004	5.350e+002 ± 1.085e+000†	**5.342e+002 ± 8.969e−004**	1.073e+003 ± 1.439e+002	**1.017e+003 ± 1.915e+002**
F24	2.000e+002 ± 0.000e+000	2.000e+002 ± 0.000e+000	2.005e+002 ± 1.827e−001†	**2.000e+002 ± 1.085e−004**	8.649e+002 ± 2.384e+002	**7.668e+002 ± 2.709e+002**
F25	1.656e+003 ± 2.726e+000†	**1.653e+003 ± 2.567e+000**	1.691e+003 ± 3.705e+000†	**1.655e+003 ± 1.016e+000**	1.679e+003 ± 1.243e+001†	**1.655e+003 ± 2.800e+000**
w/t/l	19/17/2	–	35/2/1	–	18/19/1	–
Func.	DE/best/1 Mean ± Std	HLXDE/best/1 Mean ± Std	DE/best/2 Mean ± Std	HLXDE/best/2 Mean ± Std	DE/current-to-best/1 Mean ± Std	HLXDE/current-to-best/1 Mean ± Std
f1	1.500e+003 ± 7.769e+002†	**7.199e+001 ± 9.840e+001**	9.820e−032 ± 2.127e−031†	**4.666e−043 ± 8.832e−043**	2.458e+002 ± 2.536e+002†	**3.061e+001 ± 4.326e+001**
f2	1.123e+001 ± 3.266e+000†	**3.767e+000 ± 2.324e+000**	1.974e−021 ± 1.834e−021†	**1.565e−029 ± 1.440e−029**	3.570e+000 ± 1.278e+000†	**1.103e+000 ± 7.854e−001**
f3	1.839e+003 ± 7.844e+002	1.848e+003 ± 1.165e+003	1.694e−027 ± 3.319e−027†	**4.380e−032 ± 1.162e−031**	5.426e+002 ± 3.484e+002	5.456e+002 ± 4.001e+002
f4	2.633e+001 ± 4.816e+000†	**2.319e+001 ± 5.017e+000**	2.166e−016 ± 4.641e−016	2.997e−016 ± 4.233e−016	9.562e+000 ± 2.107e+000	9.093e+000 ± 2.527e+000
f5	3.030e+005 ± 2.226e+005†	**1.393e+004 ± 2.404e+004**	6.644e−001 ± 1.511e+000	6.644e−001 ± 1.511e+000	1.311e+004 ± 1.398e+004†	**2.013e+003 ± 2.172e+003**

(*continued on next page*)

Table 7 (*continued*)

Func.	DE/best/1 Mean ± Std	HLXDE/best/1 Mean ± Std	DE/best/2 Mean ± Std	HLXDE/best/2 Mean ± Std	DE/current-to-best/1 Mean ± Std	HLXDE/current-to-best/1 Mean ± Std
f6	1.696e+003 ± 7.724e+002†	**1.852e+002 ± 1.956e+002**	2.333e−001 ± 4.302e−001†	**0.000e+000 ± 0.000e+000**	2.414e+002 ± 1.492e+002†	**3.627e+001 ± 2.614e+001**
f7	1.030e−002 ± 7.500e−003	9.034e−003 ± 4.657e−003	4.244e−003 ± 2.045e−003	3.744e−003 ± 1.048e−003	5.920e−003 ± 2.138e−003	6.257e−003 ± 3.148e−003
f8	5.027e+003 ± 5.735e+002†	**2.750e+003 ± 7.825e+002**	7.245e+003 ± 3.200e+002†	**7.896e+000 ± 3.005e+001**	5.993e+003 ± 1.211e+003†	**2.848e+002 ± 1.493e+002**
f9	6.680e+001 ± 1.077e+001†	**3.475e+001 ± 1.078e+001**	1.770e+002 ± 1.377e+001†	**0.000e+000 ± 0.000e+000**	2.996e+001 ± 8.328e+000†	**1.007e−001 ± 3.033e−001**
f10	9.052e+000 ± 1.155e+000†	**3.877e+000 ± 1.261e+000**	1.018e−014 ± 2.664e−015†	**6.155e−015 ± 1.791e−015**	4.136e+000 ± 9.414e−001†	**2.668e+000 ± 9.609e−001**
f11	1.413e+001 ± 6.864e+000†	**1.886e+000 ± 1.058e+000**	8.366e−003 ± 1.204e−002†	**1.806e−003 ± 4.745e−003**	2.674e+000 ± 1.306e+000†	**1.117e+000 ± 3.925e−001**
f12	9.564e+003 ± 4.367e+004†	**3.755e+000 ± 2.429e+000**	1.198e−001 ± 5.797e−001†	**3.456e−003 ± 1.893e−002**	2.826e+000 ± 1.697e+000†	**4.433e−001 ± 4.625e−001**
f13	2.021e+005 ± 3.371e+005†	**4.232e+001 ± 1.376e+002**	7.325e−004 ± 2.788e−003†	**1.350e−032 ± 0.000e+000**	2.150e+002 ± 1.070e+003†	**1.379e+000 ± 1.428e+000**
F1	4.095e+003 ± 2.009e+003†	**2.167e+002 ± 3.106e+002**	6.063e−014 ± 1.442e−014†	**4.737e−014 ± 2.155e−014**	2.834e+003 ± 1.201e+003†	**6.834e+002 ± 6.252e+002**
F2	6.941e+003 ± 3.324e+003	5.729e+003 ± 2.946e+003	**1.251e−013 ± 4.814e−014**‡	3.126e−013 ± 1.592e−013	5.177e+003 ± 1.791e+003	5.099e+003 ± 2.039e+003
F3	1.821e+007 ± 1.343e+007	1.318e+007 ± 1.075e+007	1.384e+005 ± 7.072e+004†	**5.237e+004 ± 2.622e+004**	5.231e+006 ± 2.846e+006	6.153e+006 ± 4.401e+006
F4	3.381e+002 ± 4.878e+002	3.420e+002 ± 4.169e+002	1.139e−004 ± 1.829e−004†	**7.725e−006 ± 1.768e−005**	5.453e+002 ± 4.349e+002	5.586e+002 ± 4.938e+002
F5	8.699e+003 ± 2.174e+003	7.970e+003 ± 2.016e+003	4.777e+001 ± 8.288e+001	4.495e+001 ± 7.761e+001	7.903e+003 ± 2.031e+003	7.183e+003 ± 1.618e+003
F6	5.433e+008 ± 4.960e+008†	**6.955e+007 ± 9.728e+007**	1.196e+000 ± 1.858e+000†	**3.987e−001 ± 1.216e+000**	2.481e+008 ± 1.666e+008†	**7.847e+007 ± 9.735e+007**
F7	4.869e+003 ± 9.282e+001†	**4.728e+003 ± 9.926e+000**	**4.697e+003 ± 1.905e−001**‡	4.701e+003 ± 2.396e+000	6.285e+003 ± 3.369e+002†	**4.733e+003 ± 1.434e−004**
F8	2.094e+001 ± 5.609e−002	2.096e+001 ± 5.824e−002	2.096e+001 ± 4.988e−002	2.095e+001 ± 5.023e−002	2.097e+001 ± 4.223e−002	2.095e+001 ± 5.550e−002
F9	1.036e+002 ± 2.262e+001†	**5.437e+001 ± 2.242e+001**	1.829e+002 ± 1.574e+001†	**1.895e−014 ± 2.725e−014**	7.676e+001 ± 2.203e+001†	**1.594e+000 ± 2.018e+000**
F10	1.513e+002 ± 4.593e+001	1.444e+002 ± 3.433e+001	2.012e+002 ± 1.658e+001†	**1.871e+002 ± 1.153e+001**	1.092e+002 ± 2.475e+001†	**8.962e+001 ± 2.262e+001**
F11	2.258e+001 ± 3.471e+000	2.230e+001 ± 2.974e+000	3.921e+001 ± 9.983e−001†	**3.827e+001 ± 1.181e+000**	1.388e+001 ± 2.004e+000	1.446e+001 ± 2.497e+000
F12	9.718e+004 ± 4.695e+004	8.558e+004 ± 3.714e+004	1.135e+003 ± 1.805e+003	1.163e+003 ± 1.375e+003	4.087e+004 ± 2.697e+004	3.155e+004 ± 1.755e+004
F13	9.834e+000 ± 3.085e+000†	**6.071e+000 ± 1.776e+000**	1.513e+001 ± 1.762e+000†	**8.166e+000 ± 7.796e−001**	**4.923e+000 ± 3.076e+000**‡	6.066e+000 ± 8.151e−001
F14	1.191e+001 ± 4.804e−001	**1.181e+001 ± 6.150e−001**	1.333e+001 ± 1.659e−001	**1.328e+001 ± 1.604e−001**	**1.164e+001 ± 4.843e−001**‡	1.184e+001 ± 3.520e−001
F15	5.772e+002 ± 1.209e+002†	**5.052e+002 ± 1.047e+002**	**3.371e+002 ± 8.955e+001**	3.767e+002 ± 1.017e+002	**4.580e+002 ± 1.215e+002**	4.866e+002 ± 6.490e+001
F16	3.043e+002 ± 1.452e+002	**2.988e+002 ± 1.850e+002**	**2.730e+002 ± 9.158e+001**	2.839e+002 ± 9.749e+001	**1.867e+002 ± 1.353e+002**	2.197e+002 ± 1.583e+002
F17	2.920e+002 ± 1.471e+002	**2.554e+002 ± 1.159e+002**	3.190e+002 ± 9.158e+001	**3.085e+002 ± 1.103e+002**	2.730e+002 ± 1.623e+002	**1.978e+002 ± 1.397e+002**
F18	**9.711e+002 ± 2.999e+001**	9.734e+002 ± 2.556e+001	**8.976e+002 ± 3.317e+001**	9.037e+002 ± 1.973e+001	**9.829e+002 ± 1.724e+001**	9.851e+002 ± 2.927e+001
F19	9.844e+002 ± 2.726e+001	**9.772e+002 ± 2.798e+001**	9.042e+002 ± 1.976e+001	**9.034e+002 ± 1.969e+001**	9.809e+002 ± 2.516e+001	**9.792e+002 ± 2.183e+001**
F20	9.824e+002 ± 2.330e+001	**9.762e+002 ± 2.624e+001**	**8.967e+002 ± 3.284e+001**	9.060e+002 ± 1.479e+000	**9.820e+002 ± 2.493e+001**	9.842e+002 ± 1.970e+001
F21	1.104e+003 ± 1.332e+002	**1.051e+003 ± 1.838e+002**	**5.409e+002 ± 1.060e+002**	5.512e+002 ± 1.434e+002	1.065e+003 ± 1.563e+002	**1.019e+003 ± 1.681e+002**
F22	**1.006e+003 ± 4.865e+001**	1.013e+003 ± 5.523e+001	9.270e+002 ± 1.776e+001†	**9.184e+002 ± 1.468e+001**	**9.999e+002 ± 2.535e+001**	1.003e+003 ± 3.436e+001
F23	1.114e+003 ± 1.169e+002	**1.094e+003 ± 1.319e+002**	6.589e+002 ± 1.874e+002	**6.158e+002 ± 1.655e+002**	**1.043e+003 ± 1.437e+002**	1.086e+003 ± 1.453e+002
F24	**9.653e+002 ± 3.097e+002**	9.693e+002 ± 2.888e+002	2.000e+002 ± 0.000e+000	2.000e+002 ± 0.000e+000	**8.197e+002 ± 2.686e+002**	8.288e+002 ± 3.000e+002
F25	1.706e+003 ± 1.510e+001†	**1.655e+003 ± 1.056e+000**	1.659e+003 ± 6.682e+000†	**1.654e+003 ± 2.649e+000**	1.688e+003 ± 1.568e+001†	**1.655e+003 ± 1.124e+000**
w/t/l	18/20/0	–	20/16/2	–	16/20/2	–

* HLXDE and the competitor can obtain the equal optimum value within *MNFES* and *NFES* required to achieve the accuracy level is also shown in square brackets.
‡ HLXDE is significantly worse than its corresponding competitor by the Wilcoxon test at 5% significance level.
† HLXDE is significantly better than its corresponding competitor by the Wilcoxon test at 5% significance level.

functions are plotted in Fig. 1. The better values in terms of mean solution error compared between HLXDE and its corresponding DE algorithm are highlighted in ***boldface*** in the following tables of this paper.

From Table 7, we can find that HLXDE significantly outperforms the corresponding DE algorithm with respect to the overall performance. Specifically, according to the Wilcoxon's test, HLXDE/rand/1 significantly improves the performance of DE/rand/1 on 19 out of 38 functions and loses on only two functions. For DE/rand/2, HLXDE is significantly better on 35 functions and is worse on only one function. For DE with the exploitative strategies, HLXDE is significantly better than DE/best/1 and DE/best/2 on 18 and 20 functions, respectively. The significant improvements are also yielded for DE/current-to-best/1 and DE/rand-to-best/1. HLXDE is significantly better than DE/current-to-best/1 and DE/rand-to-best/1 on 16 and 18 functions, respectively.

For further investigating HLXDE on the functions at higher dimension, the comparisons are made on these functions at 50*D*. The results shown in Table 8 indicate that HLXDE is consistently superior to the corresponding DE algorithm. Specifically, for DE/rand/1 and DE/rand/2, HLXDE significantly outperforms them on 13 and 33 functions, respectively. HLXDE/best/1 is significantly better than DE/best/1 on 19 functions, while HLXDE/best/2 is significantly better than DE/best/2 on 22 functions. The significant improvements for DE/current-to-best/1 and DE/rand-to-best/1 are also obtained on 19 and 18 functions, respectively.

In terms of the best and worst values for the functions at 30*D* and 50*D* (presented in the supplemental file), HLXDE is consistently superior to the corresponding DE algorithm in most cases. Furthermore, the convergence graphs in Fig. 1 show that HLXDE is better than the corresponding DE algorithm in terms of the convergence rate for most of the selected functions.

To show the significant differences between HLXDE and its corresponding DE algorithm, the multi-problem Wilcoxon signed-rank tests [18] between pairs of algorithms on all the functions are also carried out. The results are shown in

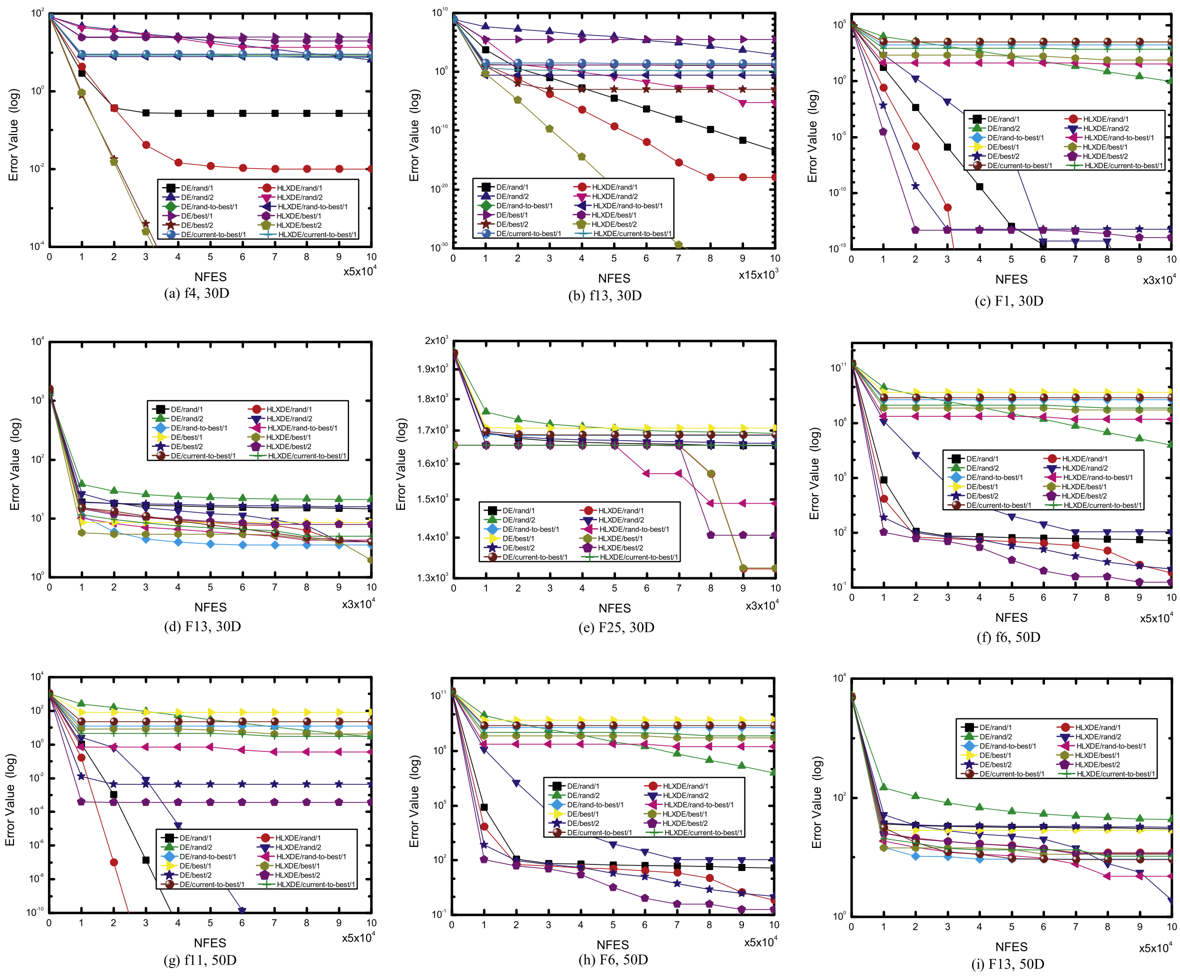

Fig. 1. Convergence graphs of the original DE algorithm and the corresponding HLXDE on some test functions. (a) $f4, 30D$, (b) $f13, 30D$, (c) $F1, 30D$, (d) $F13, 30D$, (e) $F25, 30D$, (f) $f6, 50D$, (g) $f11, 50D$, (h) $F6, 50D$, and (i) $F13, 50D$.

Table 8
Mean and standard deviation of the best error values obtained by the original DE algorithms and their corresponding HLXDE variants on all the functions at 50*D*.

Func.	DE/rand/1 Mean ± Std	HLXDE/rand/1 Mean ± Std	DE/rand/2 Mean ± Std	HLXDE-DE/rand/2 Mean ± Std	DE/rand-to-best/1 Mean ± Std	HLXDE/rand-to-best/1 Mean ± Std
f1	3.665e−035 ± 3.324e−035†	**1.614e−055 ± 1.172e−055**	1.925e+002 ± 5.969e+001†	**5.195e−019 ± 2.358e−019**	1.136e+003 ± 3.884e+002†	**1.947e+001 ± 3.414e+001**
f2	9.305e−018 ± 7.130e−018†	**3.767e−028 ± 2.421e−028**	9.796e+001 ± 9.186e+000†	**8.416e−005 ± 5.101e−005**	1.216e+001 ± 2.907e+000†	**1.451e+000 ± 1.172e+000**
f3	1.743e+000 ± 1.018e+000†	**1.206e+000 ± 9.661e−001**	5.046e+004 ± 4.506e+003†	**2.214e+004 ± 3.763e+003**	3.025e+003 ± 9.066e+002	2.672e+003 ± 9.144e+002
f4	6.067e+000 ± 2.920e+000†	**1.998e+000 ± 2.086e+000**	5.017e+001 ± 3.513e+000	4.934e+001 ± 1.963e+000	1.827e+001 ± 3.555e+000	1.676e+001 ± 3.047e+000
f5	2.340e+001 ± 1.006e+001	2.534e+001 ± 1.515e+001	5.716e+004 ± 2.840e+004†	**4.149e+001 ± 7.471e−001**	2.210e+005 ± 1.496e+005†	**1.145e+003 ± 1.479e+003**
f6*	[61,306 ± 2892.193]	[**42,288 ± 1811.439**]	1.961e+002 ± 4.978e+001†	**0.000e+000 ± 0.000e+000**	1.365e+003 ± 4.885e+002†	**2.503e+001 ± 3.443e+001**
f7	5.622e−003 ± 1.390e−003	5.675e−003 ± 1.377e−003	3.080e−001 ± 6.687e−002	3.311e−001 ± 4.498e−002	2.304e−002 ± 1.124e−002	2.624e−002 ± 8.932e−003
f8	1.186e+004 ± 1.464e+003†	**1.819e−011 ± 0.000e+000**	1.409e+004 ± 3.115e+002†	**4.620e−011 ± 2.227e−011**	9.203e+003 ± 5.777e+002†	**9.502e+002 ± 3.670e+002**
f9	2.137e+002 ± 4.488e+001†	**0.000e+000 ± 0.000e+000**	4.622e+002 ± 1.381e+001†	**1.583e−009 ± 1.148e−009**	6.760e+001 ± 8.288e+000†	**6.407e−001 ± 1.025e+000**
f10	7.457e−015 ± 9.014e−016†	**4.141e−015 ± 0.000e+000**	4.423e+000 ± 3.214e−001†	**1.468e−009 ± 4.342e−010**	6.423e+000 ± 7.714e−001†	**1.183e+000 ± 6.340e−001**
f11*	[163,493 ± 3205.807]	[**111,359 ± 2001.682**]	2.733e+000 ± 5.372e−001†	**0.000e+000 ± 0.000e+000**	1.123e+001 ± 3.496e+000†	**6.961e−001 ± 5.580e−001**
f12	9.423e−033 ± 0.000e+000	9.423e−033 ± 0.000e+000	3.776e+003 ± 5.406e+003†	**7.558e−019 ± 4.716e−019**	1.336e+001 ± 1.709e+001†	**3.455e−001 ± 4.046e−001**
f13	1.415e−032 ± 3.601e−033	1.350e−032 ± 0.000e+000	1.848e+004 ± 2.366e+004†	**1.374e−018 ± 7.376e−019**	2.951e+004 ± 5.841e+004†	**1.741e+000 ± 1.902e+000**
F1	4.358e−014 ± 2.445e−014†	**0.000e+000 ± 0.000e+000**	4.240e+002 ± 1.550e+002†	**1.895e−015 ± 1.038e−014**	1.528e+004 ± 4.102e+003†	**8.094e+002 ± 7.846e+002**
F2	4.908e+000 ± 4.067e+000	5.236e+000 ± 3.597e+000	7.491e+004 ± 8.669e+003†	**3.949e+004 ± 5.227e+003**	2.055e+004 ± 4.203e+003	1.864e+004 ± 3.925e+003
F3	2.605e+006 ± 9.083e+005†	**5.613e+005 ± 2.173e+005**	4.674e+008 ± 7.617e+007†	**2.685e+008 ± 6.007e+007**	8.649e+007 ± 3.960e+007	7.334e+007 ± 2.637e+007
F4	5.005e+002 ± 4.270e+002†	**1.911e+002 ± 1.535e+002**	9.331e+004 ± 8.926e+003†	**7.675e+004 ± 9.225e+003**	8.924e+003 ± 3.032e+003	8.983e+003 ± 3.549e+003
F5	1.822e+003 ± 3.827e+002	1.967e+003 ± 4.230e+002	2.200e+004 ± 1.420e+003†	**1.802e+004 ± 1.115e+003**	1.411e+004 ± 2.168e+003	1.321e+004 ± 1.978e+003
F6	3.700e+001 ± 2.442e+001†	**2.169e+001 ± 1.921e+001**	8.025e+006 ± 5.872e+006†	**5.620e+001 ± 2.406e+001**	1.696e+009 ± 5.795e+008†	**1.990e+008 ± 1.569e+008**
F7	**6.195e+003 ± 7.869e−003**‡	6.195e+003 ± 7.008e−002	8.683e+003 ± 1.927e+002†	**6.405e+003 ± 0.000e+000**	9.331e+003 ± 3.212e+002†	**6.405e+003 ± 0.000e+000**
F8	2.114e+001 ± 4.095e−002	2.113e+001 ± 3.617e−002	2.114e+001 ± 3.013e−002	2.113e+001 ± 3.418e−002	2.113e+001 ± 4.191e−002	2.112e+001 ± 3.663e−002
F9	2.073e+002 ± 4.153e+001†	**0.000e+000 ± 0.000e+000**	4.719e+002 ± 1.889e+001†	**7.126e−010 ± 3.754e−010**	1.728e+002 ± 2.730e+001†	**1.778e+001 ± 1.669e+001**
F10	3.513e+002 ± 2.002e+001	2.841e+002 ± 1.197e+002	5.191e+002 ± 2.222e+001†	**4.777e+002 ± 1.629e+001**	2.829e+002 ± 4.274e+001†	**2.469e+002 ± 4.609e+001**
F11	7.290e+001 ± 1.698e+000	7.159e+001 ± 3.541e+000	7.321e+001 ± 1.698e+000	7.251e+001 ± 1.265e+000	3.139e+001 ± 3.097e+000	3.182e+001 ± 3.210e+000
F12	9.668e+003 ± 1.072e+004	9.593e+003 ± 7.725e+003	2.638e+006 ± 1.762e+005†	**1.075e+006 ± 1.097e+005**	5.265e+005 ± 1.767e+005†	**2.639e+005 ± 9.144e+004**
F13	2.997e+001 ± 1.652e+000†	**1.538e+001 ± 1.111e+000**	4.282e+001 ± 2.537e+000†	**2.273e+001 ± 1.189e+000**	**8.581e+000 ± 1.494e+000**‡	1.055e+001 ± 1.378e+000
F14	2.308e+001 ± 1.275e−001	**2.305e+001 ± 1.716e−001**	**2.315e+001 ± 1.502e−001**	2.316e+001 ± 1.239e−001	**2.080e+001 ± 4.686e−001**	2.083e+001 ± 4.395e−001
F15	3.900e+002 ± 4.472e+001	**3.700e+002 ± 7.327e+001**	4.521e+002 ± 1.983e+000†	**3.938e+002 ± 3.699e+001**	5.355e+002 ± 4.882e+001†	**4.332e+002 ± 1.477e+002**
F16	2.537e+002 ± 1.006e+001	**2.237e+002 ± 6.983e+001**	3.648e+002 ± 1.528e+001†	**3.320e+002 ± 1.296e+001**	2.369e+002 ± 9.915e+001	**2.282e+002 ± 1.124e+002**
F17	**2.765e+002 ± 1.041e+001**	2.781e+002 ± 1.052e+001	4.104e+002 ± 1.729e+001†	**3.803e+002 ± 1.499e+001**	2.306e+002 ± 1.034e+002	**2.263e+002 ± 1.379e+002**
F18	**8.776e+002 ± 5.841e+001**	9.018e+002 ± 4.388e+001	1.035e+003 ± 9.889e+000†	**9.954e+002 ± 4.727e+000**	1.047e+003 ± 2.651e+001	**1.033e+003 ± 2.468e+001**
F19	**9.076e+002 ± 3.684e+001**	9.136e+002 ± 2.680e+001	1.036e+003 ± 1.210e+001†	**9.958e+002 ± 6.133e+000**	1.045e+003 ± 2.297e+001	**1.043e+003 ± 2.206e+001**
F20	**8.519e+002 ± 1.411e+002**‡	9.131e+002 ± 2.666e+001	1.030e+003 ± 1.262e+001†	**9.962e+002 ± 5.365e+000**	**1.043e+003 ± 2.268e+001**	1.044e+003 ± 1.982e+001
F21	5.000e+002 ± 0.000e+000	5.000e+002 ± 0.000e+000	6.450e+002 ± 4.948e+001†	**5.022e+002 ± 5.649e−001**	1.198e+003 ± 5.326e+001	**1.158e+003 ± 1.071e+002**
F22	9.574e+002 ± 1.126e+001	9.537e+002 ± 1.111e+001	1.134e+003 ± 2.560e+001†	**1.068e+003 ± 1.184e+001**	1.109e+003 ± 3.463e+001†	**1.083e+003 ± 2.668e+001**
F23	5.391e+002 ± 1.569e−002	5.391e+002 ± 1.597e−004	7.153e+002 ± 5.099e+001†	**5.464e+002 ± 2.660e+000**	1.199e+003 ± 5.533e+001	**1.157e+003 ± 9.244e+001**
F24	2.000e+002 ± 0.000e+000	2.000e+002 ± 2.475e−006	6.295e+002 ± 9.352e+001†	**2.682e+002 ± 2.227e+001**	1.219e+003 ± 8.423e+000	**1.213e+003 ± 1.845e+001**
F25	**1.681e+003 ± 7.838e+000**‡	1.694e+003 ± 4.209e+000	1.784e+003 ± 6.724e+000†	**1.715e+003 ± 2.461e+000**	1.782e+003 ± 1.445e+001†	**1.715e+003 ± 2.833e+000**

w/t//l	13/22/3	–	33/5/0	–	18/19/1	–
Func.	DE/best/1	HLXDE/best/1	DE/best/2	HLXDE/best/2	DE/current-to-best/1	HLXDE/current-to-best/1
	Mean ± Std	Mean ± Std	Mean ± Std	Mean ± Std	Mean ± Std	Mean ± Std
f1	8.362e+003 ± 2.660e+003†	**5.763e+002 ± 4.414e+002**	1.404e−065 ± 4.292e−065†	**1.273e−100 ± 3.693e−100**	2.175e+003 ± 6.924e+002†	**3.000e+002 ± 2.220e+002**
f2	4.125e+001 ± 7.078e+000†	**2.158e+001 ± 7.441e+000**	4.141e−034 ± 6.347e−034†	**2.649e−050 ± 2.672e−050**	1.875e+001 ± 3.124e+000†	**7.680e+000 ± 2.573e+000**
f3	9.261e+003 ± 2.607e+003	9.158e+003 ± 2.625e+003	4.144e−005 ± 4.727e−005	6.040e−005 ± 6.767e−005	3.290e+003 ± 1.153e+003	3.386e+003 ± 1.156e+003
f4	3.848e+001 ± 4.487e+000†	**3.528e+001 ± 4.243e+000**	1.311e+000 ± 8.330e−001†	**1.013e−001 ± 9.083e−002**	1.783e+001 ± 2.377e+000	1.728e+001 ± 3.083e+000
f5	5.835e+006 ± 2.858e+006†	**1.044e+005 ± 1.891e+005**	4.013e−001 ± 1.223e+000	1.063e+000 ± 1.793e+000	4.385e+005 ± 2.758e+005†	**3.099e+004 ± 2.873e+004**
f6	9.259e+003 ± 2.736e+003†	**8.118e+002 ± 7.062e+002**	2.733e+000 ± 3.695e+000†	**0.000e+000 ± 0.000e+000**	2.474e+003 ± 8.364e+002†	**4.533e+002 ± 3.057e+002**
f7	6.260e−002 ± 4.222e−002	7.711e−002 ± 7.586e−002	1.212e−002 ± 3.665e−003†	**9.062e−003 ± 2.771e−003**	3.402e−002 ± 1.410e−002	3.919e−002 ± 1.922e−002
f8	1.049e+004 ± 8.209e+002†	**5.501e+003 ± 1.681e+003**	1.406e+004 ± 4.820e+002†	**1.184e+001 ± 3.614e+001**	1.122e+004 ± 2.453e+003†	**4.263e+002 ± 1.774e+002**
f9	1.646e+002 ± 2.219e+001†	**7.711e+001 ± 1.946e+001**	3.502e+002 ± 2.274e+001†	**0.000e+000 ± 0.000e+000**	6.476e+001 ± 1.397e+001†	**1.658e−001 ± 3.771e−001**
f10	1.328e+001 ± 8.836e−001†	**6.042e+000 ± 1.339e+000**	4.634e−001 ± 6.822e−001†	**8.049e−015 ± 1.084e−015**	7.822e+000 ± 8.681e−001†	**4.681e+000 ± 1.016e+000**
f11	7.626e+001 ± 2.394e+001†	**6.173e+000 ± 3.986e+000**	6.895e−003 ± 8.388e−003†	**1.067e−003 ± 3.581e−003**	2.058e+001 ± 6.231e+000†	**3.700e+000 ± 1.998e+000**
f12	7.286e+005 ± 8.153e+005†	**3.680e+001 ± 1.622e+002**	1.852e−001 ± 3.568e−001†	**2.073e−003 ± 1.136e−002**	2.530e+001 ± 7.538e+001†	**2.679e+000 ± 2.072e+000**
f13	7.652e+006 ± 4.582e+006†	**9.514e+003 ± 2.787e+004**	2.427e−001 ± 9.120e−001†	**3.662e−004 ± 2.006e−003**	4.148e+004 ± 5.781e+004†	**1.946e+002 ± 5.773e+002**
F1	2.588e+004 ± 5.897e+003†	**1.292e+003 ± 1.177e+003**	1.232e−013 ± 3.973e−014†	**5.495e−014 ± 1.038e−014**	2.184e+004 ± 5.882e+003†	**5.537e+003 ± 2.503e+003**
F2	2.887e+004 ± 9.457e+003†	**2.320e+004 ± 7.924e+003**	8.874e−005 ± 9.002e−005	1.431e−004 ± 1.554e−004	2.322e+004 ± 5.615e+003†	**2.112e+004 ± 6.261e+003**
F3	1.529e+008 ± 6.755e+007	1.330e+008 ± 6.992e+007	6.470e+005 ± 2.869e+005†	**1.198e+005 ± 5.495e+004**	1.020e+008 ± 5.166e+007	8.985e+007 ± 4.542e+007
F4	6.199e+003 ± 3.589e+003	7.258e+003 ± 3.713e+003	4.019e+002 ± 3.550e+002†	**1.243e+002 ± 1.438e+002**	6.659e+003 ± 2.580e+003	7.385e+003 ± 2.715e+003
F5	1.801e+004 ± 2.991e+003	1.701e+004 ± 2.224e+003	2.748e+003 ± 5.588e+002	2.533e+003 ± 6.024e+002	1.464e+004 ± 1.697e+003	1.439e+004 ± 1.752e+003
F6	4.506e+009 ± 1.654e+009†	**5.372e+008 ± 5.632e+008**	1.484e+000 ± 1.974e+000†	**1.063e+000 ± 1.793e+000**	3.012e+009 ± 1.447e+009†	**1.300e+009 ± 6.504e+008**
F7	7.268e+003 ± 3.584e+002†	**6.405e+003 ± 0.000e+000**	**6.196e+003 ± 1.769e−001**‡	6.217e+003 ± 1.434e+001	9.845e+003 ± 3.750e+002†	**6.405e+003 ± 0.000e+000**
F8	2.114e+001 ± 4.037e−002	2.115e+001 ± 3.835e−002	**2.113e+001 ± 4.455e−002**‡	2.115e+001 ± 3.189e−002	2.113e+001 ± 3.652e−002	2.113e+001 ± 3.505e−002
F9	2.860e+002 ± 4.390e+001†	**1.181e+002 ± 2.730e+001**	3.895e+002 ± 2.795e+001†	**1.895e−014 ± 2.725e−014**	1.985e+002 ± 3.178e+001†	**5.777e+000 ± 4.219e+000**
F10	4.606e+002 ± 7.017e+001	4.375e+002 ± 6.673e+001	4.202e+002 ± 2.172e+001†	**3.824e+002 ± 2.384e+001**	2.838e+002 ± 5.224e+001	2.802e+002 ± 5.331e+001
F11	4.629e+001 ± 3.942e+000	4.785e+001 ± 3.390e+000	7.300e+001 ± 1.375e+000†	**7.198e+001 ± 1.212e+000**	3.594e+001 ± 3.057e+000	3.615e+001 ± 3.540e+000
F12	7.814e+005 ± 1.439e+005†	**3.639e+005 ± 1.482e+005**	6.324e+003 ± 6.566e+003	6.570e+003 ± 7.605e+003	3.148e+005 ± 1.388e+005†	**1.383e+005 ± 1.033e+005**
F13	2.959e+001 ± 7.342e+000†	**1.627e+001 ± 4.164e+000**	3.233e+001 ± 1.374e+000†	**1.551e+001 ± 1.275e+000**	**9.856e+000 ± 3.956e+000**‡	1.225e+001 ± 1.297e+000
F14	2.134e+001 ± 5.778e−001	**2.129e+001 ± 6.333e−001**	**2.306e+001 ± 1.393e−001**	2.307e+001 ± 1.882e−001	2.139e+001 ± 4.474e−001	**2.138e+001 ± 5.232e−001**
F15	5.797e+002 ± 5.227e+001	**5.641e+002 ± 9.178e+001**	3.027e+002 ± 9.534e+001	**2.751e+002 ± 9.150e+001**	5.773e+002 ± 6.644e+001	**5.535e+002 ± 6.519e+001**
F16	**3.482e+002 ± 9.904e+001**	3.776e+002 ± 1.183e+002	3.579e+002 ± 6.453e+001†	**2.923e+002 ± 5.514e+001**	**2.377e+002 ± 1.074e+002**	2.792e+002 ± 1.478e+002
F17	3.221e+002 ± 9.681e+001	**3.067e+002 ± 7.845e+001**	3.525e+002 ± 7.084e+001	**3.272e+002 ± 4.973e+001**	**2.294e+002 ± 1.003e+002**	2.385e+002 ± 9.985e+001
F18	1.097e+003 ± 3.092e+001	**1.079e+003 ± 2.897e+001**	9.221e+002 ± 3.018e+001	**9.197e+002 ± 2.832e+001**	1.064e+003 ± 1.818e+001†	**1.050e+003 ± 2.257e+001**
F19	1.086e+003 ± 2.076e+001	**1.080e+003 ± 2.738e+001**	**9.175e+002 ± 4.254e+001**	9.299e+002 ± 1.004e+001	1.061e+003 ± 1.817e+001	**1.056e+003 ± 2.339e+001**
F20	1.084e+003 ± 2.257e+001	**1.080e+003 ± 2.718e+001**	**9.102e+002 ± 4.797e+001**	9.231e+002 ± 2.964e+001	1.061e+003 ± 1.817e+001	**1.057e+003 ± 2.005e+001**
F21	1.230e+003 ± 5.590e+001	**1.214e+003 ± 6.744e+001**	5.150e+002 ± 6.708e+001	5.150e+002 ± 6.708e+001	**1.217e+003 ± 4.074e+001**	1.222e+003 ± 2.150e+001
F22	1.125e+003 ± 6.095e+001	**1.097e+003 ± 5.385e+001**	9.983e+002 ± 1.542e+001†	**9.696e+002 ± 1.101e+001**	1.125e+003 ± 3.338e+001†	**1.103e+003 ± 2.548e+001**
F23	1.244e+003 ± 4.350e+001	**1.237e+003 ± 4.457e+001**	6.331e+002 ± 2.052e+002†	**5.618e+002 ± 7.706e+001**	1.238e+003 ± 1.386e+001	**1.228e+003 ± 2.945e+001**
F24	**1.278e+003 ± 2.223e+001**	1.279e+003 ± 2.275e+001	2.000e+002 ± 0.000e+000	2.000e+002 ± 0.000e+000	**1.228e+003 ± 1.455e+001**	1.716e+003 ± 2.367e+000
F25	1.810e+003 ± 2.198e+001†	**1.716e+003 ± 2.326e+000**	**1.685e+003 ± 7.504e+000**‡	1.696e+003 ± 5.847e+000	1.797e+003 ± 1.601e+001†	**1.227e+003 ± 1.502e+001**
w/t/l	19/19/0	–	22/13/3	–	19/18/1	–

‡ HLXDE is significantly worse than its corresponding competitor by the Wilcoxon test at 5% significance level.

* HLXDE and the competitor can obtain the equal optimum value within *MNFES* and *NFES* required to achieve the accuracy level is also shown in square brackets.

† HLXDE is significantly better than its corresponding competitor by the Wilcoxon test at 5% significance level.

Table 9. It is clear that HLXDE obtains higher $R+$ values than $R-$ values in all the cases. Furthermore, the p values of all the cases are less than 0.05, which indicates that HLXDE is significantly better than its corresponding DE algorithm overall.

In summary, the overall results of Tables 7–9 and Fig. 1 clearly show that HLX can effectively improve the performance of most of the original DE algorithms studied.

With respect to the characteristics of the benchmark functions, a close inspection of Tables 7–9 suggests some interesting observations.

- For most of the separable functions (i.e., $f1 - f2, f6 - f13, F1$ and $F9$), HLXDE consistently obtains significantly better results than the corresponding DE algorithm. Specifically, in 127 out of 144 cases, HLXDE significantly outperforms the corresponding DE algorithm, and in the remaining 17 cases, there are no significant differences between pairs of competitors. In order to clearly explain this observation, the average number of groups decomposed by HLXDE for all the 38 functions is shown in Table 10. From Table 10, we can find that HLXDE correctly identifies the real number of groups for most of the separable functions. When solving these functions, GbinX is similar to BinX, and thus HLXDE differs from the original DE algorithm only in GorthX. Therefore, the significant improvements for these functions mainly contribute to GorthX.
- For the nonseparable functions, HLXDE significantly outperforms the corresponding DE algorithm in 121 out of 312 cases, while it is outperformed in only 16 cases. The reasons may be twofold. On the one hand, for these functions, the interaction between the pair of variables is not clear and rarely discussed. Although the grouping by HLX may be not accurate, HLX with group-wise crossovers is verified to be beneficial for solving these nonseparable functions from the results in Tables 7–9. On the other hand, the research by Chen et al. [7] has shown that the dynamically changed configuration of BBs provides a benefit to the optimizer and the decompositions may be changed with different search stages. In general, the results have demonstrated the advantages of utilizing linkage information for the nonseparable functions.

4.4. Comparison with advanced DE variants

In order to further evaluate the effectiveness of the proposed algorithm, HLX is incorporated into several advanced DE variants, namely, ODE [49], SaDE [48], CoDE [68], MDE_pBX [30] and MoDE [35]. The comparisons between HLXDE and

Table 9
Results of the multi-problem Wilcoxon's test for HLXDE *vs.* the corresponding DE algorithm for all the functions at 30D and 50D.

Algorithm at 30D	$R+$	$R-$	p-Value	$\alpha = 0.05$
HLXDE/rand/1 *vs.* DE/rand/1	531.5	171.5	5.76E−03	Yes
HLXDE/rand/2 *vs.* DE/rand/2	731	10	3.13E−10	Yes
HLXDE/best/1 *vs.* DE/best/1	686	55	4.12E−07	Yes
HLXDE/best/2 *vs.* DE/best/2	528.5	212.5	2.11E−02	Yes
HLXDE/current-to-best/1 *vs.* DE/curren-to-best/1	542.5	198.5	1.17E−02	Yes
HLXDE/rand-to-best/1 *vs.* DE/rand-to-best/1	736	5	7.27E−11	Yes
Algorithm at 50D	$R+$	$R-$	p-Value	$\alpha = 0.05$
HLXDE/rand/1 *vs.* DE/rand/1	495.5	207.5	2.92E−02	Yes
HLXDE/rand/2 *vs.* DE/rand/2	736.5	4.5	6.19E−11	Yes
HLXDE/best/1 *vs.* DE/best/1	683	58	5.80E−07	Yes
HLXDE/best/2 *vs.* DE/best/2	565.5	175.5	3.94E−03	Yes
HLXDE/current-to-best/1 *vs.* DE/curren-to-best/1	583.5	119.5	2.60E−04	Yes
HLXDE/rand-to-best/1 *vs.* DE/rand-to-best/1	700	41	7.24E−08	Yes

Table 10
Results of the average number of groups obtained by HLXDE for all the functions at 30D and 50D.

Func.	30D	50D	Func.	30D	50D	Func.	30D	50D
f1	30	50	F1	30	50	F14	14.4	9.3
f2	30	50	F2	11	17.6	F15	7.8	15
f3	11	17	F3	7.8	8.4	F16	7.9	6.8
f4	30	50	F4	5.6	6.6	F17	6.1	6.7
f5	30	50	F5	8.6	15.4	F18	6.9	8.1
f6	30	50	F6	13.7	24	F19	7.5	7.9
f7	5.1	5.4	F7	5.9	6.7	F20	7.3	8.7
f8	30	50	F8	6.7	7.1	F21	9.8	12.0
f9	30	50	F9	30	50	F22	11.2	19.7
f10	30	50	F10	5.8	6.9	F23	10.0	12.4
f11	30	50	F11	5.6	7	F24	10.9	8.2
f12	30	50	F12	7.1	50	F25	6.1	7.4
f13	30	50	F13	11.4	20.4			

Table 11
Mean and standard deviation of the best error values obtained by the advanced DE variants and their corresponding HLXDE variants on all the functions at 30*D*.

Func.	ODE Mean ± Std	HLXODE Mean ± Std	MDE_*p*BX Mean ± Std	HLXMDE_*p*BX Mean ± Std	MoDE Mean ± Std	HLXMoDE Mean ± Std
f1	2.236e−027 ± 2.719e−027†	**3.327e−030 ± 4.853e−030**	1.238e−003 ± 4.831e−003†	**4.769e−004 ± 2.350e−003**	6.505e−004 ± 2.812e−003†	**1.965e−032 ± 1.076e−031**
f2	1.519e−011 ± 1.060e−011†	**5.242e−017 ± 3.804e−017**	**4.169e−008 ± 1.847e−007**‡	3.140e−006 ± 1.720e−005	2.885e−003 ± 1.231e−002	**5.386e−014 ± 2.940e−013**
f3	2.939e−011 ± 6.026e−011†	**1.952e−012 ± 3.578e−012**	**5.966e−017 ± 1.633e−016**‡	4.182e−002 ± 1.309e−001	**1.106e−035 ± 4.798e−035**	8.042e−031 ± 3.718e−030
f4	4.282e−008 ± 1.759e−007	4.859e−004 ± 1.915e−003	5.166e+000 ± 1.956e+000	4.892e+000 ± 2.524e+000	1.807e−002 ± 1.585e−002	**4.823e−004 ± 5.574e−004**
f5	2.518e+001 ± 1.098e+000†	**2.465e+001 ± 8.037e−001**	4.698e+001 ± 3.145e+001	4.968e+001 ± 2.997e+001	4.511e+000 ± 5.297e+000	**1.595e+000 ± 1.986e+000**
f6*	[23,190 ± 1764.076]	[**20,972 ± 1129.064**]	[**8123 ± 11785.985**]	[10,649 ± 17624.343]	6.054e+002 ± 5.430e+002†	**2.070e+001 ± 2.886e+001**
f7	9.317e−004 ± 2.892e−004	9.001e−004 ± 3.338e−004	5.290e−004 ± 2.372e−004	5.578e−004 ± 3.194e−004	4.847e−003 ± 1.989e−003†	**4.137e−003 ± 1.711e−003**
f8	6.990e+003 ± 3.077e+002†	**0.000e+000 ± 0.000e+000**	1.216e+003 ± 4.337e+002†	**8.558e+002 ± 4.242e+002**	4.142e+003 ± 6.505e+002	**2.710e+003 ± 6.765e+002**
f9	3.598e+001 ± 1.913e+001†	**0.000e+000 ± 0.000e+000**	7.802e+000 ± 2.246e+000†	**5.398e+000 ± 2.096e+000**	6.009e+001 ± 1.407e+001†	**3.443e+001 ± 1.047e+001**
f10	3.529e−014 ± 2.039e−014†	**5.444e−015 ± 1.741e−015**	1.770e−002 ± 9.303e−002†	**1.577e−002 ± 8.542e−002**	7.700e+000 ± 1.822e+000†	**3.028e+000 ± 1.577e+000**
f11	2.465e−004 ± 1.350e−003	0.000e+000 ± 0.000e+000	4.921e−003 ± 1.241e−002†	**1.135e−003 ± 3.190e−003**	2.492e−001 ± 2.327e−001	**6.691e−002 ± 9.507e−002**
f12	3.490e−028 ± 5.109e−028†	**2.083e−031 ± 2.604e−031**	1.979e−002 ± 6.566e−002†	**1.743e−002 ± 7.737e−002**	5.000e+000 ± 6.302e+000†	**2.591e−001 ± 6.317e−001**
f13	2.491e−028 ± 3.618e−028†	**1.576e−030 ± 4.092e−030**	2.221e−002 ± 4.916e−002†	**1.431e−002 ± 7.335e−002**	5.566e+000 ± 6.701e+000†	**2.384e−001 ± 7.537e−001**
F1*	[66,706 ± 2350.339]	[**59,958 ± 1300.500**]	2.593e−001 ± 6.412e−001†	**1.420e−001 ± 6.586e−001**	1.190e−004 ± 5.492e−004†	**3.088e−013 ± 6.710e−013**
F2	1.795e−004 ± 1.713e−004†	**3.813e−005 ± 4.675e−005**	**1.913e−007 ± 5.556e−007**‡	1.142e+001 ± 1.750e+001	**5.135e−013 ± 3.928e−013**	6.594e−013 ± 9.208e−013
F3	6.483e+005 ± 3.758e+005†	**3.368e+005 ± 1.830e+005**	1.103e+006 ± 4.216e+005	1.263e+006 ± 4.526e+005	**4.742e+004 ± 2.434e+004**	7.036e+004 ± 5.047e+004
F4	1.068e−001 ± 1.272e−001†	**3.099e−002 ± 7.137e−002**	2.712e−004 ± 9.959e−004	5.691e−005 ± 1.921e−004	7.620e+000 ± 4.134e+001	**3.578e+000 ± 1.765e+001**
F5	1.194e+002 ± 9.176e+001	1.826e+002 ± 1.553e+002	3.522e+003 ± 4.900e+002	3.437e+003 ± 5.818e+002	**2.443e+003 ± 7.990e+002**	2.484e+003 ± 6.179e+002
F6	5.983e+001 ± 9.068e+001†	**2.425e+001 ± 1.898e+001**	4.265e+005 ± 1.024e+006	1.429e+005 ± 2.392e+005	3.227e+001 ± 2.902e+001†	**2.214e+000 ± 3.257e+000**
F7	4.697e+003 ± 1.478e−001	4.697e+003 ± 1.432e−001	4.741e+003 ± 3.052e+001†	**4.726e+003 ± 8.423e+000**	4.702e+003 ± 2.051e+001†	**4.696e+003 ± 8.436e−001**
F8	2.094e+001 ± 6.122e−002	2.092e+001 ± 1.104e−001	**2.096e+001 ± 5.771e−002**‡	2.102e+001 ± 5.178e−002	2.095e+001 ± 6.850e−002	2.095e+001 ± 6.019e−002
F9	7.318e+001 ± 2.054e+001†	**0.000e+000 ± 0.000e+000**	1.584e+001 ± 4.847e+000†	**1.226e+001 ± 3.250e+000**	8.351e+001 ± 2.302e+001†	**4.868e+001 ± 1.680e+001**
F10	4.629e+001 ± 3.544e+001	4.037e+001 ± 1.296e+001	**2.846e+001 ± 1.146e+001**‡	3.506e+001 ± 1.071e+001	1.246e+002 ± 4.320e+001†	**8.367e+001 ± 3.401e+001**
F11	9.247e+000 ± 1.114e+001	**7.216e+000 ± 4.459e+000**	2.429e+001 ± 5.454e+000	**2.244e+001 ± 5.070e+000**	2.854e+001 ± 3.953e+000	**2.704e+001 ± 4.979e+000**
F12	**2.191e+003 ± 2.577e+003**	2.765e+003 ± 3.705e+003	**1.054e+004 ± 6.014e+003**	1.159e+004 ± 7.608e+003	9.984e+003 ± 5.263e+003†	**3.273e+003 ± 3.254e+003**
F13	**6.734e+000 ± 2.281e+000**	7.230e+000 ± 7.441e−001	**2.945e+000 ± 5.018e−001**	2.951e+000 ± 4.621e−001	6.343e+000 ± 2.061e+000†	**4.606e+000 ± 1.628e+000**
F14	1.301e+001 ± 4.026e−001†	**1.273e+001 ± 4.463e−001**	**1.162e+001 ± 4.957e−001**‡	1.216e+001 ± 5.093e−001	1.190e+001 ± 6.850e−001	1.227e+001 ± 7.095e−001
F15	**4.233e+002 ± 4.302e+001**	4.267e+002 ± 4.494e+001	**3.211e+002 ± 6.097e+001**	3.304e+002 ± 5.398e+001	4.637e+002 ± 8.929e+001†	**3.808e+002 ± 9.343e+001**
F16	1.068e+002 ± 7.704e+001	**7.036e+001 ± 4.892e+001**	**9.903e+001 ± 1.239e+002**	1.091e+002 ± 1.197e+002	2.604e+002 ± 1.350e+002†	**1.838e+002 ± 1.182e+002**
F17	1.407e+002 ± 7.165e+001	**9.965e+001 ± 7.240e+001**	**1.212e+002 ± 1.585e+002**	1.711e+002 ± 1.725e+002	2.533e+002 ± 1.435e+002	**1.908e+002 ± 1.520e+002**
F18	9.015e+002 ± 1.920e+001	**8.944e+002 ± 3.203e+001**	**8.996e+002 ± 5.540e+001**	9.043e+002 ± 5.309e+001	9.529e+002 ± 3.499e+001†	**9.268e+002 ± 3.835e+001**
F19	**9.010e+002 ± 1.912e+001**	9.050e+002 ± 1.586e+000	8.906e+002 ± 5.934e+001	**8.864e+002 ± 5.957e+001**	9.673e+002 ± 2.870e+001†	**9.313e+002 ± 2.744e+001**
F20	**9.010e+002 ± 1.911e+001**	9.014e+002 ± 1.922e+001	8.968e+002 ± 5.571e+001	**8.960e+002 ± 5.786e+001**	9.750e+002 ± 2.709e+001†	**9.285e+002 ± 3.778e+001**
F21	5.000e+002 ± 1.388e−005	5.000e+002 ± 1.603e−005	5.890e+002 ± 2.212e+002	**5.247e+002 ± 1.169e+002**	9.311e+002 ± 3.192e+002†	**6.359e+002 ± 2.684e+002**
F22	**9.104e+002 ± 1.065e+001**	9.122e+002 ± 7.810e+000	9.357e+002 ± 1.163e+001	**9.310e+002 ± 1.547e+001**	9.431e+002 ± 2.875e+001	**9.364e+002 ± 2.936e+001**
F23	5.477e+002 ± 7.424e+001	**5.342e+002 ± 3.190e−004**	**5.380e+002 ± 9.195e+000**	5.425e+002 ± 1.881e+001	1.045e+003 ± 1.606e+002†	**8.005e+002 ± 2.449e+002**
F24	2.000e+002 ± 0.000e+000	2.000e+002 ± 0.000e+000	2.000e+002 ± 0.000e+000	2.000e+002 ± 1.048e−004	4.176e+002 ± 3.684e+002†	**2.100e+002 ± 5.477e+001**
F25	1.657e+003 ± 3.287e+000	**1.656e+003 ± 2.998e+000**	**1.622e+003 ± 5.218e+000**	1.623e+003 ± 5.750e+000	1.685e+003 ± 1.524e+001†	**1.660e+003 ± 6.720e+000**
w/t/l	15/33/0	–	10/22/6	–	23/15/0	–
Func.	CoDE Mean ± Std	HLXCoDE Mean ± Std	SaDE Mean ± Std	HLXSaDE Mean ± Std		
f1	2.281e−007 ± 8.285e−008†	**2.207e−008 ± 1.324e−008**	1.623e−048 ± 4.460e−048†	**5.084e−065 ± 1.499e−064**		
f2	1.160e−007 ± 3.792e−008†	**8.846e−008 ± 3.455e−008**	6.106e−045 ± 1.536e−044†	**9.109e−048 ± 7.939e−048**		
f3	4.384e+003 ± 1.415e+003†	**5.958e+002 ± 3.108e+002**	**1.555e−019 ± 5.900e−019**‡	1.949e−014 ± 5.133e−014		
f4	**3.214e−002 ± 6.224e−003**‡	1.139e−001 ± 2.143e−002	1.370e+000 ± 2.434e+000	1.268e+000 ± 2.098e+000		
f5	3.332e+000 ± 1.959e+000	3.969e+000 ± 2.086e+000	1.281e+001 ± 5.863e+000†	**4.249e+000 ± 3.959e+000**		

(*continued on next page*)

Table 11 (*continued*)

Func.	CoDE Mean ± Std	HLXCoDE Mean ± Std	SaDE Mean ± Std	HLXSaDE Mean ± Std
f6*	[62,487 ± 1907.356]	[**57,646** ± **3057.055**]	[**10,028** ± **1648.494**]	[11,336 ± 446.561]
f7	2.547e−002 ± 6.241e−003	2.646e−002 ± 5.517e−003	1.562e−003 ± 7.960e−004	1.450e−003 ± 4.611e−004
f8	1.213e−012 ± 8.721e−013†	**0.000e+000** ± **0.000e+000**	3.553e+001 ± 6.336e+001†	**0.000e+000** ± **0.000e+000**
f9	1.022e−011 ± 1.729e−011†	**0.000e+000** ± **0.000e+000**	1.426e+000 ± 1.129e+000†	**0.000e+000** ± **0.000e+000**
f10	1.314e−004 ± 3.737e−005†	**6.274e**−**005** ± **1.782e**−**005**	4.023e−015 ± 6.486e−016	4.023e−015 ± 6.486e−016
f11	4.192e−009 ± 3.721e−009†	**2.319e**−**009** ± **5.766e**−**009**	2.789e−003 ± 6.607e−003†	**0.000e+000** ± **0.000e+000**
f12	8.211e−008 ± 3.763e−008†	**4.033e**−**009** ± **3.353e**−**009**	1.382e−002 ± 7.571e−002	1.570e−032 ± 4.726e−040
f13	1.916e−007 ± 7.825e−008†	**1.228e**−**008** ± **1.227e**−**008**	1.099e−003 ± 3.353e−003	1.350e−032 ± 0.000e+000
F1*	5.684e−014 ± 0.000e+000†	**3.221e**−**014** ± **2.865e**−**014**	[31,030 ± 1755.366]	[**29,701** ± **723.774**]
F2	3.187e+003 ± 7.146e+002†	**1.697e+003** ± **5.918e+002**	**1.728e**−**009** ± **3.348e**−**009**‡	4.345e−006 ± 1.413e−005
F3	3.401e+007 ± 6.080e+006†	**2.487e+007** ± **8.727e+006**	**4.020e+005** ± **1.853e+005**‡	5.335e+005 ± 2.853e+005
F4	**8.166e+003** ± **1.718e+003**‡	9.733e+003 ± 2.280e+003	8.429e−001 ± 2.595e+000	1.442e+000 ± 2.902e+000
F5	3.791e+003 ± 4.632e+002	3.871e+003 ± 5.887e+002	1.743e+003 ± 5.370e+002	2.004e+003 ± 5.252e+002
F6	2.071e+001 ± 2.477e+000†	**1.563e+001** ± **1.766e+000**	3.191e+001 ± 2.764e+001†	**5.916e+000** ± **4.942e+000**
F7	4.696e+003 ± 0.000e+000	4.696e+003 ± 0.000e+000	4.696e+003 ± 0.000e+000	4.696e+003 ± 0.000e+000
F8	2.095e+001 ± 5.367e−002	2.094e+001 ± 1.040e−001	2.095e+001 ± 5.097e−002	2.094e+001 ± 5.565e−002
F9	3.430e−013 ± 2.181e−013†	**2.653e**−**014** ± **2.884e**−**014**	3.084e+000 ± 1.798e+000†	**6.633e**−**002** ± **2.524e**−**001**
F10	1.783002 ± 1.269e+001†	**1.649e+002** ± **1.258e+001**	1.005e+002 ± 1.026e+001†	**4.990e+001** ± **9.850e+000**
F11	3.267e+001 ± 1.645e+000	3.236e+001 ± 1.487e+000	3.262e+001 ± 1.328e+000†	**2.728e+001** ± **1.472e+000**
F12	9.448e+004 ± 1.098e+004†	**7.127e+004** ± **1.351e+004**	4.197e+003 ± 8.799e+003	3.811e+003 ± 3.111e+003
F13	6.571e+000 ± 5.357e−001†	**4.554e+000** ± **4.721e**−**001**	7.871e+000 ± 9.458e−001†	**2.514e+000** ± **2.038e**−**001**
F14	1.323e+001 ± 1.789e−001†	**1.307e+001** ± **1.541e**−**001**	1.303e+001 ± 2.030e−001†	**1.287e+001** ± **1.611e**−**001**
F15	4.100e+002 ± 5.477e+001	**4.000e+002** ± **4.549e+001**	**3.469e+002** ± **6.306e+001**‡	3.803e+002 ± 7.594e+001
F16	2.015e+002 ± 1.186e+001†	**1.854e+002** ± **1.846e+001**	1.370e+002 ± 2.353e+001†	**9.782e+001** ± **1.997e+001**
F17	2.382e+002 ± 2.080e+001	**2.359e+002** ± **2.634e+001**	1.710e+002 ± 1.324e+001†	**1.513e+002** ± **1.605e+001**
F18	9.065e+002 ± 3.516e−001	9.065e+002 ± 4.889e−001	8.752e+002 ± 5.414e+001	**8.554e+002** ±**e+ 5.639e+001**
F19	9.065e+002 ± 3.423e−001	9.065e+002 ± 5.797e−001	**8.629e+002** ± **5.600e+001**	8.671e+002 ± 5.576e+001
F20	**9.064e+002** ± **3.595e**−**001**	9.065e+002 ± 3.963e−001	8.818e+002 ± 5.026e+001	**8.597e+002** ± **5.686e+001**
F21	5.000e+002 ± 1.963e−005	5.000e+002 ± 8.014e−006	5.000e+002 ± 1.388e−005	5.000e+002 ± 1.267e−005
F22	**9.248e+002** ± **1.071e+001**	9.262e+002 ± 8.963e+000	**9.215e+002** ± **1.017e+001**	9.217e+002 ± 9.391e+000
F23	5.342e+002 ± 3.321e−004	5.342e+002 ± 3.577e−004	5.342e+002 ± 5.494e−005	5.342e+002 ± 2.084e−004
F24	2.000e+002 ± 0.000e+000	2.000e+002 ± 4.767e−005	2.000e+002 ± 0.000e+000	2.000e+002 ± 0.000e+000
F25	**1.645e+003** ± **2.449e+000**‡	1.657e+003 ± 3.421e+000	1.648e+003 ± 2.707e+000†	**1.645e+003** ± **3.750e+000**
w/t/l	19/16/3	–	15/19/4	–

* HLXDE and the competitor can obtain the equal optimum value within *MNFES* and *NFES* required to achieve the accuracy level are is shown in square brackets.
‡ HLXDE is significantly worse than its corresponding competitor by the Wilcoxon test at 5% significance level respectively.
† HLXDE is significantly better than its corresponding competitor by the Wilcoxon test at 5% significance level respectively.

Table 12
Mean and standard deviation of the best error values obtained by the advanced DE variants and their corresponding HLXDE variants on all the functions at 50*D*.

Func.	ODE Mean ± Std	HLXODE Mean ± Std	MDE_*p*BX Mean ± Std	HLXMDE_*p*BX Mean ± Std	MoDE Mean ± Std	HLXMoDE Mean ± Std
f1	6.193e−057 ± 3.310e−056†	**4.128e−076 ± 8.069e−076**	2.231e+000 ± 4.139e+000†	**2.746e−001 ± 6.716e−001**	4.151e+001 ± 1.848e+002†	**5.734e−064 ± 2.564e−063**
f2	1.956e−021 ± 1.926e−021†	**1.502e−032 ± 1.071e−032**	9.162e−002 ± 9.973e−002†	**6.836e−003 ± 1.203e−002**	4.447e−001 ± 9.097e−001†	**3.754e−010 ± 1.679e−009**
f3	3.529e−001 ± 4.866e−001	4.164e−001 ± 3.278e−001	**3.926e−005 ± 8.464e−005**‡	2.291e+001 ± 2.320e+001	**9.022e−012 ± 1.529e−011**‡	4.986e+000 ± 8.343e+000
f4	2.544e−001 ± 5.534e−001	2.172e−001 ± 4.107e−001	1.194e+001 ± 2.947e+000	1.173e+001 ± 3.233e+000	2.425e+001 ± 4.304e+000†	**1.017e+001 ± 4.282e+000**
f5	4.594e+001 ± 8.261e−001†	**4.477e+001 ± 1.195e+000**	4.635e+002 ± 8.180e+002	1.648e+002 ± 1.254e+002	2.278e+003 ± 8.945e+003	**1.719e+001 ± 2.713e+001**
f6*	[40,083 ± 6505.175]	[**32,234 ± 1831.125**]	4.333e−001 ± 1.654e+000	3.333e−001 ± 8.023e−001	4.206e+003 ± 1.921e+003†	**1.223e+002 ± 1.501e+002**
f7	1.191e−003 ± 4.023e−004	1.172e−003 ± 5.853e−004	1.927e−003 ± 7.636e−004	2.596e−003 ± 1.542e−003	4.218e−002 ± 5.065e−002	**2.368e−002 ± 2.740e−002**
f8	1.274e+004 ± 1.029e+003†	**1.819e−011 ± 0.000e+000**	4.296e+003 ± 6.730e+002†	**2.671e+003 ± 5.840e+002**	8.559e+003 ± 8.847e+002†	**4.891e+003 ± 1.020e+003**
f9	6.617e+001 ± 4.469e+001†	**0.000e+000 ± 0.000e+000**	1.945e+001 ± 3.204e+000†	**1.521e+001 ± 6.226e+000**	1.074e+002 ± 1.949e+001†	**6.926e+001 ± 1.757e+001**
f10	4.141e−015 ± 0.000e+000	4.141e−015 ± 0.000e+000	6.518e−001 ± 4.139e−001†	**2.153e−001 ± 3.246e−001**	1.104e+001 ± 1.311e+000	**3.694e+000 ± 1.477e+000**
f11	3.366e−003 ± 6.080e−003†	**0.000e+000 ± 0.000e+000**	2.358e−001 ± 2.424e−001†	**6.524e−002 ± 1.012e−001**	1.715e+000 ± 3.530e+000	**1.218e−001 ± 1.705e−001**
f12	9.655e−033 ± 4.143e−034†	**9.423e−033 ± 0.000e+000**	1.220e−001 ± 8.290e−002†	**5.027e−002 ± 6.693e−002**	3.289e+000 ± 2.315e+000†	**1.089e−001 ± 1.353e−001**
f13	7.325e−004 ± 2.788e−003†	**1.350e−032 ± 0.000e+000**	1.831e+000 ± 2.089e+000†	**2.820e−001 ± 4.572e−001**	8.489e+000 ± 8.787e+000†	**2.251e−001 ± 4.752e−001**
F1	1.895e−015 ± 1.038e−014	0.000e+000 ± 0.000e+000	5.927e+001 ± 9.162e+001†	**1.394e+001 ± 2.236e+001**	4.561e+001 ± 1.511e+002†	**6.168e−012 ± 2.316e−011**
F2	**6.347e+000 ± 5.394e+000**‡	1.053e+001 ± 9.315e+000	**2.312e−004 ± 3.351e−004**‡	1.870e+002 ± 2.123e+002	**9.991e−010 ± 2.719e−009**‡	2.715e+001 ± 4.819e+001
F3	3.684e+006 ± 1.329e+006†	**7.618e+005 ± 2.967e+005**	**2.113e+006 ± 5.962e+005**‡	2.737e+006 ± 7.856e+005	**3.164e+005 ± 1.429e+005**‡	1.543e+006 ± 5.309e+005
F4	6.138e+002 ± 3.610e+002†	**4.529e+002 ± 3.041e+002**	1.484e+002 ± 2.135e+002	4.316e+002 ± 6.916e+002	**2.792e+002 ± 2.831e+002**‡	1.130e+003 ± 6.689e+002
F5	2.305e+003 ± 3.224e+002	2.247e+003 ± 3.225e+002	8.035e+003 ± 8.333e+002	7.899e+003 ± 8.008e+002	**6.328e+003 ± 1.164e+003**	7.434e+003 ± 1.401e+003
F6	1.424e+004 ± 4.120e+004†	**6.408e+001 ± 2.666e+001**	8.454e+006 ± 1.137e+007	5.009e+006 ± 7.914e+006	1.123e+005 ± 3.755e+005†	**5.978e+001 ± 7.098e+001**
F7	6.196e+003 ± 1.144e−001†	**6.196e+003 ± 3.474e−001**	6.325e+003 ± 5.794e+001	6.335e+003 ± 4.729e+001	6.213e+003 ± 4.964e+001	**6.205e+003 ± 2.017e+001**
F8	2.114e+001 ± 2.593e−002†	**2.105e+001 ± 1.397e−001**	**2.114e+001 ± 2.853e−002**‡	2.116e+001 ± 1.030e−001	**2.112e+001 ± 3.065e−002**‡	2.119e+001 ± 4.335e−002
F9	1.711e+002 ± 7.566e+001†	**0.000e+000 ± 0.000e+000**	5.435e+001 ± 1.039e+001†	**3.539e+001 ± 8.740e+000**	1.942e+002 ± 3.580e+001†	**8.323e+001 ± 1.953e+001**
F10	8.353e+001 ± 7.249e+001	7.619e+001 ± 2.390e+001	**7.110e+001 ± 1.475e+001**‡	8.309e+001 ± 1.643e+001	**2.732e+002 ± 6.627e+001**	2.933e+002 ± 8.045e+001
F11	1.726e+001 ± 6.185e+000	1.670e+001 ± 5.097e+000	5.559e+001 ± 6.564e+000†	**4.794e+001 ± 8.273e+000**	**5.647e+001 ± 7.068e+000**	5.720e+001 ± 6.003e+000
F12	1.357e+004 ± 8.039e+003	1.255e+004 ± 1.085e+004	3.543e+004 ± 1.719e+004	4.040e+004 ± 2.726e+004	7.149e+004 ± 3.131e+004†	**2.415e+004 ± 1.678e+004**
F13	1.310e+001 ± 6.388e+000	1.409e+001 ± 1.698e+000	**5.326e+000 ± 8.962e−001**‡	6.139e+000 ± 1.081e+000	2.143e+001 ± 8.887e+000†	**1.194e+001 ± 3.185e+000**
F14	2.300e+001 ± 2.065e−001†	**2.231e+001 ± 4.662e−001**	**2.000e+001 ± 9.143e−001**‡	2.145e+001 ± 5.548e−001	**2.247e+001 ± 5.269e−001**	2.249e+001 ± 7.416e−001
F15	3.900e+002 ± 4.472e+001	**3.801e+002 ± 6.158e+001**	3.393e+002 ± 9.861e+001	**3.304e+002 ± 5.398e+001**	4.458e+002 ± 9.166e+001	**4.168e+002 ± 1.257e+002**
F16	**5.908e+001 ± 4.613e+001**‡	7.235e+001 ± 5.087e+001	**5.063e+001 ± 2.343e+001**	1.091e+002 ± 1.197e+002	2.572e+002 ± 1.415e+002	**2.259e+002 ± 1.364e+002**
F17	1.632e+002 ± 9.714e+001	**1.207e+002 ± 9.409e+001**	**1.204e+002 ± 1.317e+002**	1.711e+002 ± 1.725e+002	2.889e+002 ± 1.531e+002	**2.113e+002 ± 1.149e+002**
F18	**9.034e+002 ± 4.464e+001**	9.068e+002 ± 3.671e+001	9.675e+002 ± 1.080e+001	**9.043e+002 ± 5.309e+001**	**9.575e+002 ± 1.983e+001**	9.611e+002 ± 2.176e+001
F19	**8.753e+002 ± 5.835e+001**	9.080e+002 ± 3.696e+001	9.674e+002 ± 1.021e+001	**8.864e+002 ± 5.957e+001**	9.737e+002 ± 2.623e+001†	**9.561e+002 ± 2.797e+001**
F20	9.154e+002 ± 2.727e+001	**9.082e+002 ± 3.705e+001**	9.686e+002 ± 8.119e+000	**8.960e+002 ± 5.786e+001**	9.762e+002 ± 2.972e+001†	**9.561e+002 ± 2.797e+001**
F21	5.000e+002 ± 0.000e+000	5.000e+002 ± 0.000e+000	5.957e+002 ± 2.031e+002	**5.247e+002 ± 1.169e+002**	9.825e+002 ± 3.232e+002	**7.587e+002 ± 3.261e+002**
F22	**9.525e+002 ± 9.553e+000**	9.553e+002 ± 1.137e+001	9.834e+002 ± 1.521e+001	**9.310e+002 ± 1.547e+001**	**9.478e+002 ± 2.220e+001**	9.484e+002 ± 3.105e+001
F23	5.391e+002 ± 2.375e−002	5.391e+002 ± 1.896e−002	6.770e+002 ± 2.258e+002	**5.425e+002 ± 1.881e+001**	1.028e+003 ± 1.651e+002	**9.650e+002 ± 2.506e+002**
F24	2.000e+002 ± 4.287e−006	2.000e+002 ± 4.287e−006	5.311e+002 ± 4.630e+002	**2.000e+002 ± 1.048e−004**	3.852e+002 ± 3.549e+002	**2.887e+002 ± 2.705e+002**
F25	**1.687e+003 ± 7.217e+000**‡	1.695e+003 ± 6.433e+000	1.683e+003 ± 6.057e+000	**1.623e+003 ± 5.750e+000**	1.685e+003 ± 1.461e+001†	**1.665e+003 ± 2.803e+000**
w/t/l	15/21/2	–	11/20/7	–	16/17/5	–

Func.	CoDE Mean ± Std	HLXCoDE Mean ± Std	SaDE Mean ± Std	HLXSaDE Mean ± Std
f1	2.439e−010 ± 1.392e−010†	**1.726e−014 ± 1.897e−014**	1.956e−079 ± 8.808e−079†	**2.620e−138 ± 9.996e−138**
f2	1.038e−007 ± 2.361e−008†	**1.258e−008 ± 4.012e−009**	4.560e−056 ± 2.362e−055†	**1.186e−076 ± 2.436e−076**
f3	3.936e+004 ± 4.108e+003†	**3.088e+004 ± 3.256e+003**	**1.827e−004 ± 2.085e−004**‡	2.458e−001 ± 3.421e−001
f4	**1.098e+001 ± 7.234e−001**‡	1.770e+001 ± 1.236e+000	7.468e+000 ± 6.789e+000	8.686e+000 ± 4.352e+000
f5	1.233e+002 ± 3.533e+001	1.132e+002 ± 3.438e+001	5.310e+001 ± 2.948e+001†	**2.567e+001 ± 3.510e+001**

(*continued on next page*)

Table 12 (*continued*)

Func.	CoDE Mean ± Std	HLXCoDE Mean ± Std	SaDE Mean ± Std	HLXSaDE Mean ± Std
f6*	[167,194 ± 4712.450]	[**135,454 ± 5274.014**]	[30,666 ± 11590.806]	[**19,972 ± 824.174**]
f7	7.353e−002 ± 1.143e−002	7.167e−002 ± 1.332e−002	5.598e−003 ± 1.795e−003	4.756e−003 ± 1.335e−003
f8	4.608e−008 ± 2.731e−008†	**1.819e−011 ± 0.000e−000**	1.342e+002 ± 1.065e+002†	**1.819e−011 ± 0.000e+000**
f9	4.558e−001 ± 3.798e−001†	**3.231e−011 ± 2.413e−011**	9.419e+000 ± 3.044e+000†	**3.317e−002 ± 1.817e−001**
f10	2.822e−006 ± 6.598e−007†	**6.485e−008 ± 2.502e−008**	7.516e−001 ± 5.845e−001†	**4.141e−015 ± 0.000e+000**
f11	1.029e−009 ± 8.098e−010†	**6.769e−013 ± 1.091e−012**	8.767e−003 ± 1.330e−002†	**3.288e−004 ± 1.801e−003**
f12	9.589e−010 ± 8.959e−010†	**1.458e−015 ± 1.109e−015**	1.451e−002 ± 4.813e−002†	**9.423e−033 ± 0.000e+000**
f13	7.357e−010 ± 3.671e−010†	**5.608e−015 ± 4.501e−015**	3.445e−001 ± 9.960e−001†	**3.662e−004 ± 2.006e−003**
F1*	6.989e−011 ± 4.473e−011†	**6.063e−014 ± 1.442e−014**	[63,821 ± 5348.005]	[**49,550 ± 1128.039**]
F2	3.758e+004 ± 6.320e+003†	**2.594e+004 ± 4.193e+003**	**1.315e−003 ± 1.579e−003**‡	1.377e+000 ± 1.277e+000
F3	1.615e+008 ± 3.457e+007†	**1.113e+008 ± 3.049e+007**	**4.809e+005 ± 1.575e+005**‡	6.676e+005 ± 2.720e+005
F4	5.679e+004 ± 8.572e+003	5.658e+004 ± 9.547e+003	1.887e+003 ± 1.396e+003	1.532e+003 ± 8.596e+002
F5	1.244e+004 ± 1.057e+003	1.218e+004 ± 8.990e+002	**4.258e+003 ± 6.437e+002**‡	4.635e+003 ± 5.752e+002
F6	1.893e+002 ± 4.709e+001†	**4.474e+001 ± 1.250e+001**	7.239e+001 ± 3.973e+001†	**2.950e+001 ± 2.746e+001**
F7	6.195e+003 ± 0.000e+000	6.195e+003 ± 0.000e+000	6.195e+003 ± 1.539e−001	6.196e+003 ± 1.170e+000
F8	2.113e+001 ± 4.504e−002	2.113e+001 ± 4.283e−002	2.112e+001 ± 5.361e−002	2.114e+001 ± 3.586e−002
F9	2.827e−003 ± 2.143e−003†	**6.133e−012 ± 4.694e−012**	1.416e+001 ± 4.211e+000†	**0.000e+000 ± 0.000e+000**
F10	4.055e+002 ± 1.753e+001†	**3.489e+002 ± 2.049e+001**	2.280e+002 ± 1.788e+001†	**1.015e+002 ± 2.041e+001**
F11	6.564e+001 ± 1.470e+000†	**6.195e+001 ± 1.932e+000**	6.253e+001 ± 1.855e+000†	**5.047e+001 ± 6.472e+000**
F12	5.603e+005 ± 5.561e+004†	**2.930e+005 ± 3.884e+004**	1.043e+004 ± 8.261e+003	1.259e+004 ± 9.417e+003
F13	1.896e+001 ± 1.042e+000†	**9.765e+000 ± 7.541e−001**	1.728e+001 ± 1.692e+000†	**7.289e+000 ± 1.284e+000**
F14	2.306e+001 ± 1.762e−001†	**2.284e+001 ± 2.082e−001**	2.273e+001 ± 1.420e−001†	**2.216e+001 ± 3.714e−001**
F15	**3.850e+002 ± 6.708e+001**	3.900e+002 ± 4.472e+001	**3.103e+002 ± 9.570e+001**	3.409e+002 ± 9.278e+001
F16	2.913e+002 ± 1.004e+001†	**2.532e+002 ± 1.072e+001**	1.623e+002 ± 3.456e+001†	**7.596e+001 ± 1.597e+001**
F17	3.264e+002 ± 1.108e+001†	**3.101e+002 ± 1.536e+001**	2.520e+002 ± 7.521e+001†	**1.108e+002 ± 1.081e+002**
F18	**9.228e+002 ± 1.404e+000**	9.240e+002 ± 3.201e+000	9.542e+002 ± 3.831e+001	**9.499e+002 ± 3.566e+001**
F19	9.233e+002 ± 1.530e+000†	**9.225e+002 ± 1.322e+000**	9.556e+002 ± 1.136e+001	**9.385e+002 ± 4.814e+001**
F20	9.235e+002 ± 1.582e+000	**9.227e+002 ± 1.563e+000**	9.584e+002 ± 1.154e+001†	**9.504e+002 ± 6.522e+000**
F21	9.939e+002 ± 1.163e+002	**9.157e+002 ± 2.133e+002**	**6.019e+002 ± 2.488e+002**	6.696e+002 ± 3.013e+002
F22	**9.415e+002 ± 5.348e+000**	9.455e+002 ± 1.334e+001	9.776e+002 ± 9.241e+000	**9.705e+002 ± 1.042e+001**
F23	9.937e+002 ± 1.070e+002	**9.452e+002 ± 1.750e+002**	5.892e+002 ± 1.615e+002	**5.715e+002 ± 1.448e+002**
F24	2.000e+002 ± 0.000e+000	2.000e+002 ± 0.000e+000	**2.000e+002 ± 4.287e−006**	2.496e+002 ± 2.216e+002
F25	1.687e+003 ± 2.239e+000	1.687e+003 ± 3.300e+000	1.676e+003 ± 4.553e+000	**1.672e+003 ± 7.206e+000**
w/t/l	22/15/1	–	18/16/4	–

* HLXDE and the competitor can obtain the equal optimum value within *MNFES* and *NFES* required to achieve the accuracy level is also shown in square brackets.
‡ HLXDE is significantly worse than its corresponding competitor by the Wilcoxon test at 5% significance level.
† HLXDE is significantly better than its corresponding competitor by the Wilcoxon test at 5% significance level.

the corresponding DE variants are made on all the functions at 30D and 50D. The results are shown in Tables 11 and 12. The convergence graphs for some test functions are plotted in Fig. 2.

From the results of functions at 30D in Table 11, it is clear that HLX exhibits substantial improvement for most of the DE variants. For ODE, HLXDE is significantly better on 15 out of 38 functions, without losing on any functions. For MDE_pBX, HLXDE significantly outperforms it on 10 functions and is outperformed by it on six functions. Although HLX does not lead to great benefits for MDE_pBX, HLXDE can significantly outperform MDE_pBX on nine out of the 12 separable functions. For MoDE, HLXDE can significantly outperform it on 23 functions. For SaDE and CoDE, HLXDE is significantly better on 15 and 19 functions, respectively, and is worse on four and three functions, respectively. These results clearly indicate that HLX is effective not only for the DE variants with single mutation strategy, but also for the DE variants with multiple mutation strategies.

From the results of functions at 50D in Table 12, HLXDE is consistently superior to most of the advanced DE variants. Specifically, for ODE, HLXDE is significantly better on 15 functions and is worse on two functions. For MDE_pBX, HLXDE significantly outperforms it on 11 functions and is outperformed by it on seven functions. For MoDE, HLXDE is significantly better on 16 functions and is worse on five functions. For SaDE and CoDE, HLXDE is significantly better on 18 and 22 functions, respectively, and is worse on four and one function, respectively. Therefore, as the results indicate, HLXDE is able to enhance the performance of the advanced DE variants for the functions with higher dimension.

The results of the best and worst values presented in the supplemental file also show that HLXDE is consistently superior to the corresponding advanced DE variant for most functions. Fig. 2 also shows that HLXDE is better than the corresponding advanced DE variant in terms of the convergence rate for most of the selected functions.

Additionally, the multi-problem Wilcoxon signed-rank tests at $\alpha = 0.05$ and $\alpha = 0.1$ are also conducted between HLXDE and its corresponding DE variant, and the results are shown in Table 13. It is clear that HLXDE obtains higher $R+$ values than $R-$ values in all the cases. It indicates that HLXDE is better than its corresponding DE variant overall. Additionally, in four cases for functions at 30D (HLXODE *vs.* ODE, HLXSaDE *vs.* SaDE, HLXMoDE *vs.* MoDE and HLXCoDE *vs.* CoDE), the p values are less than 0.05. For functions at 50D, the p values of three cases (HLXODE *vs.* ODE, HLXMoDE *vs.* MoDE and HLXCoDE

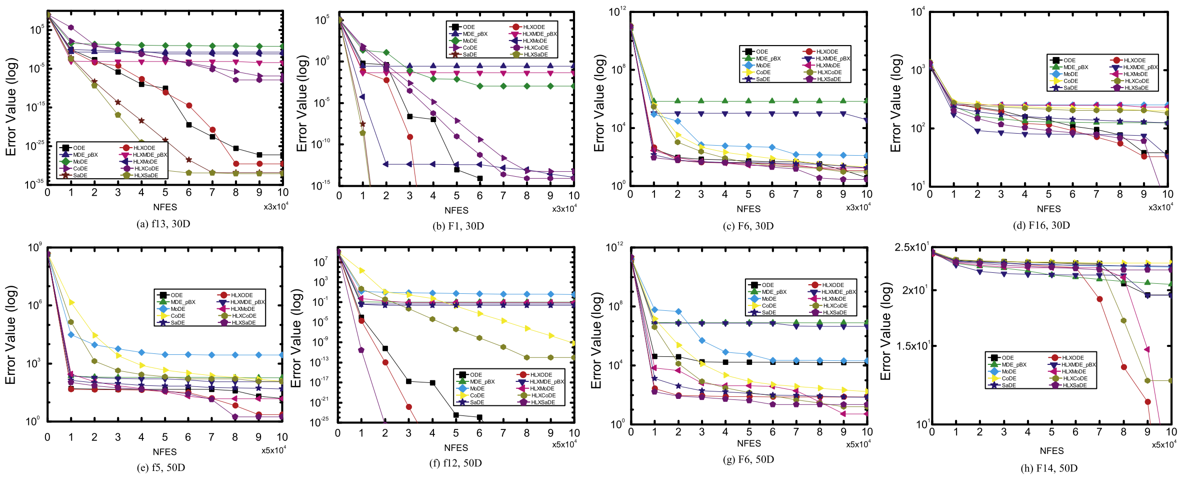

Fig. 2. Convergence graphs of the advanced DE variant and the corresponding HLXDE on some test functions. (a) $f13, 30D$, (b) $F1, 30D$, (c) $F6, 30D$, (d) $F16, 30D$, (e) $f5, 50D$, (f) $f12, 50D$, (g) $F6, 50D$, and (h) $F14, 50D$.

Table 13
Results of the multi-problem Wilcoxon's test for HLXDE *vs.* the corresponding DE variant for all the functions at 30D and 50D.

Algorithm at 30D	$R+$	$R-$	p-Value	$\alpha = 0.05$	$\alpha = 0.1$
HLXODE *vs.* ODE	508	195	1.73E−02	Yes	Yes
HLXSaDE *vs.* SaDE	510.5	192.5	1.55E−02	Yes	Yes
HLXMoDE *vs.* MoDE	628	75	6.74E−06	Yes	Yes
HLXCoDE *vs.* CoDE	494.5	208.5	3.04E−02	Yes	Yes
HLXMDE_pBX *vs.* MDE_pBX	374.5	366.5	4.70E−01	No	No
Algorithm at 50D	$R+$	$R-$	p-Value	$\alpha = 0.05$	$\alpha = 0.1$
HLXODE *vs.* ODE	547.5	193.5	9.35E−03	Yes	Yes
HLXSaDE *vs.* SaDE	483.5	257.5	1.03E−01	No	No
HLXMoDE *vs.* MoDE	566.5	174.5	3.75E−03	Yes	Yes
HLXCoDE *vs.* CoDE	613	90	2.64E−05	Yes	Yes
HLXMDE_pBX *vs.* MDE_pBX	487	254	9.27E−02	No	Yes

Table 14
Mean and standard deviation of the best error values obtained by DE/rand/1, DE/best/2, ODE and their corresponding HLXDE variants with different crossover operators on functions at 30*D*.

Func.	DE/rand/1			DE/best/2		
	UFX	TPX	HLX	UFX	TPX	HLX
f1	2.158e−016 ± 8.834e−01†	1.383e−013 ± 5.480e−014†	5.212e−022 ± 4.596e−022	3.339e−022 ± 2.779e−022†	1.016e−022 ± 1.339e−022†	4.666e−043 ± 8.832e−043
f2	7.753e−014 ± 1.561e−014†	6.073e−011 ± 1.737e−011†	7.247e−016 ± 3.993e−016	1.293e−016 ± 7.750e−017†	8.323e−016 ± 5.910e−016†	1.565e−029 ± 1.440e−029
f3	4.235e+003 ± 9.891e+002†	2.951e−009 ± 1.694e−009†	1.142e−012 ± 3.857e−012	1.053e+003 ± 4.891e+002†	7.635e−020 ± 1.340e−019†	4.380e−032 ± 1.162e−031
f4	3.785e−007 ± 1.422e−007	8.515e−007 ± 3.611e−007	1.372e−002 ± 5.243e−002	1.367e−015 ± 1.295e−015†	4.801e−016 ± 8.972e−016	2.997e−016 ± 4.233e−016
f5	1.568e+001 ± 1.881e+000†	5.709e−023 ± 1.153e−022‡	4.699e−008 ± 1.555e−007	3.083e+000 ± 1.467e+000†	2.658e−001 ± 1.011e+000‡	6.644e−001 ± 1.511e+000
f6*	[34,623 ± 1010.184]	[41,066 ± 1208.114]	[27,844 ± 1375.495]	[27,586 ± 1277.048]	[28,156 ± 3471.031]	[16,259 ± 1226.863]
f7	7.386e−003 ± 1.522e−003†	7.348e−003 ± 2.123e−003†	4.626e−003 ± 1.422e−003	5.007e−003 ± 1.021e−003†	4.748e−003 ± 1.375e−003†	3.744e−003 ± 1.048e−003
f8	1.058e+003 ± 1.018e+003†	3.282e−007 ± 1.698e−006†	0.000e+000 ± 0.000e+000	4.257e+003 ± 9.451e+002†	2.458e+003 ± 1.506e+003†	7.896e+000 ± 3.005e+001
f9	1.022e+002 ± 7.621e+000†	9.869e+001 ± 8.595e+000†	0.000e+000 ± 0.000e+000	1.140e+002 ± 6.679e+000†	1.183e+002 ± 1.042e+001†	0.000e+000 ± 0.000e+000
f10	3.875e−009 ± 1.132e−009†	1.128e−007 ± 3.058e−008†	2.014e−011 ± 7.005e−012	6.337e−012 ± 3.896e−012†	3.236e−012 ± 1.931e−012†	6.155e−015 ± 1.791e−015
f11	0.000e+000 ± 0.000e+000	0.000e+000 ± 0.000e+000	2.465e−004 ± 1.350e−003	1.971e−003 ± 4.682e−003	9.604e−003 ± 9.415e−003†	1.806e−003 ± 4.745e−003
f12	3.157e−016 ± 1.423e−016†	1.213e−013 ± 5.850e−014†	1.010e−022 ± 1.535e−022	1.430e−021 ± 2.172e−021†	3.110e−002 ± 9.871e−002‡	3.456e−003 ± 1.893e−002
f13	1.016e−015 ± 4.635e−016†	3.339e−013 ± 1.699e−013†	6.082e−022 ± 5.767e−022	1.105e−021 ± 1.668e−021†	2.197e−003 ± 4.470e−003†	1.350e−032 ± 0.000e+000
F1	5.684e−015 ± 1.734e−014	5.684e−015 ± 1.734e−014	0.000e+000 ± 0.000e+000	5.495e−014 ± 1.038e−014	5.684e−014 ± 0.000e+000	4.737e−014 ± 2.155e−014
F2	4.451e+003 ± 7.934e+002†	5.881e−004 ± 2.738e−004†	8.644e−006 ± 1.299e−005	1.566e+003 ± 5.804e+002†	3.791e−010 ± 4.807e−010†	3.126e−013 ± 1.592e−013
F3	7.595e+007 ± 1.551e+007†	1.899e+007 ± 4.466e+006†	3.320e+005 ± 2.167e+005	4.650e+007 ± 1.329e+007†	4.414e+006 ± 1.724e+006†	5.237e+004 ± 2.622e+004
F4	9.298e+003 ± 1.650e+003†	4.608e−001 ± 1.969e−001†	3.868e−003 ± 7.070e−003	4.407e+003 ± 1.533e+003†	4.807e−005 ± 4.457e−005†	7.725e−006 ± 1.768e−005
F5	2.222e+003 ± 2.340e+002†	1.506e+003 ± 2.243e+002†	1.216e+002 ± 2.074e+002	1.434e+003 ± 4.164e+002†	7.476e+002 ± 3.752e+002†	4.495e+001 ± 7.761e+001
F6	1.950e+001 ± 1.580e+000†	5.441e−006 ± 9.669e−006†	2.353e−001 ± 4.447e−001	2.127e+001 ± 2.228e+001‡	6.644e−001 ± 1.511e+000	3.987e−001 ± 1.216e+000
F7	4.696e+003 ± 1.570e−004	4.696e+003 ± 6.486e−003	4.696e+003 ± 2.360e−002	4.696e+003 ± 5.872e−002‡	4.697e+003 ± 1.461e−001‡	4.701e+003 ± 2.396e+000
F8	2.095e+001 ± 3.844e−002	2.094e+001 ± 6.070e−002	2.095e+001 ± 4.622e−002	2.095e+001 ± 3.648e−002	2.096e+001 ± 4.826e−002	2.095e+001 ± 5.023e−002
F9	1.001e+002 ± 8.347e+000†	9.321e+001 ± 9.794e+000†	0.000e+000 ± 0.000e+000	1.130e+002 ± 8.634e+000†	1.092e+002 ± 1.053e+001†	1.895e−014 ± 2.725e−014
F10	1.879e+002 ± 9.576e+000†	1.837e+002 ± 8.891e+000†	1.561e+002 ± 4.725e+001	1.954e+002 ± 9.892e+000†	1.813e+002 ± 1.015e+001	1.871e+002 ± 1.153e+001
F11	3.977e+001 ± 8.926e−001†	3.781e+001 ± 1.275e+000‡	3.829e+001 ± 3.135e+000	3.935e+001 ± 1.188e+000†	3.731e+001 ± 1.512e+000‡	3.827e+001 ± 1.181e+000
F12	2.392e+005 ± 2.842e+004†	1.744e+005 ± 4.554e+004†	1.764e+003 ± 1.784e+003	5.140e+004 ± 7.194e+004†	2.420e+004 ± 5.028e+004†	1.163e+003 ± 1.375e+003
F13	1.313e+001 ± 8.050e−001†	9.929e+000 ± 7.220e−001†	8.260e+000 ± 7.036e−001	1.316e+001 ± 1.038e+000†	1.025e+001 ± 8.333e−001†	8.166e+000 ± 7.796e−001
F14	1.336e+001 ± 1.411e−001	1.335e+001 ± 1.162e−001	1.338e+001 ± 1.915e−001	1.332e+001 ± 1.633e−001	1.326e+001 ± 1.502e−001	1.328e+001 ± 1.604e−001
F15	3.275e+002 ± 4.467e+001‡	3.933e+002 ± 2.537e+001	4.033e+002 ± 1.826e+001	3.333e+002 ± 9.223e+001‡	3.527e+002 ± 8.694e+001	3.767e+002 ± 1.017e+002
F16	2.160e+002 ± 1.319e+001†	2.030e+002 ± 9.758e+000	1.944e+002 ± 3.373e+001	2.574e+002 ± 7.941e+001	2.717e+002 ± 1.013e+002	2.839e+002 ± 9.749e+001
F17	2.359e+002 ± 1.402e+001†	2.248e+002 ± 2.928e+001	2.161e+002 ± 1.344e+001	3.007e+002 ± 9.717e+001	2.752e+002 ± 9.237e+001	3.085e+002 ± 1.103e+002
F18	9.068e+002 ± 5.145e−001†	9.074e+002 ± 1.310e+000†	9.044e+002 ± 1.190e+000	9.037e+002 ± 1.962e+001	9.040e+002 ± 1.968e+001	9.037e+002 ± 1.973e+001
F19	9.069e+002 ± 6.201e−001†	9.072e+002 ± 1.041e+000†	9.042e+002 ± 9.329e−001	9.034e+002 ± 1.956e+001	8.972e+002 ± 3.300e+001	9.034e+002 ± 1.969e+001
F20	9.069e+002 ± 6.799e−001†	9.070e+002 ± 1.043e+000†	9.042e+002 ± 8.509e−001	9.069e+002 ± 1.207e+000†	9.046e+002 ± 1.985e+001‡	9.060e+002 ± 1.479e+000
F21	5.000e+002 ± 1.700e−005	5.000e+002 ± 1.880e−005	5.000e+002 ± 1.880e−005	5.000e+002 ± 1.700e−005	5.433e+002 ± 1.135e+002	5.512e+002 ± 1.434e+002
F22	9.419e+002 ± 7.208e+000†	9.307e+002 ± 4.283e+000†	9.021e+002 ± 1.176e+001	9.341e+002 ± 1.125e+001†	9.204e+002 ± 1.041e+001	9.184e+002 ± 1.468e+001
F23	5.342e+002 ± 1.675e−004	5.342e+002 ± 2.091e−004	5.342e+002 ± 3.059e−004	5.476e+002 ± 7.355e+001‡	5.610e+002 ± 1.022e+002	6.158e+002 ± 1.655e+002
F24	2.000e+002 ± 0.000e+000	2.000e+002 ± 0.000e+000	2.000e+002 ± 0.000e+000	2.000e+002 ± 0.000e+000	2.000e+002 ± 0.000e+000	2.000e+002 ± 0.000e+000
F25	1.653e+003 ± 2.184e+000	1.655e+003 ± 1.934e+000†	1.653e+003 ± 2.567e+000	1.655e+003 ± 3.067e+000†	1.655e+003 ± 3.234e+000†	1.654e+003 ± 2.649e+000

w/t/l	26/11/1	23/13/2	–	23/11/4	17/16/5	–

Func.	ODE		
	UFX	TPX	HLX
f1	1.354e−023 ± 1.007e−023†	8.499e−024 ± 7.706e−024†	3.327e−030 ± 4.853e−030
f2	4.014e−013 ± 2.054e−013†	3.074e−011 ± 1.173e−011†	5.242e−017 ± 3.804e−017
f3	2.411e+002 ± 2.209e+002†	3.665e−008 ± 5.240e−008†	1.952e−012 ± 3.578e−012
f4	2.165e−034 ± 3.556e−034‡	2.189e−027 ± 1.130e−026‡	4.859e−004 ± 1.915e−003
f5	2.549e+001 ± 4.724e−001†	2.161e+001 ± 1.239e+000‡	2.465e+001 ± 8.037e−001
f6*	[26,003 ± 1346.127]	[25,990 ± 1369.206]	[20,972 ± 1129.064]
f7	1.976e−003 ± 4.809e−004†	1.279e−003 ± 4.060e−004†	9.001e−004 ± 3.338e−004
f8	3.204e+003 ± 4.409e+002†	9.971e+000 ± 3.951e+001†	0.000e+000 ± 0.000e+000
f9	6.894e+001 ± 1.569e+001†	4.045e+001 ± 1.886e+001†	0.000e+000 ± 0.000e+000
f10	1.266e−012 ± 4.741e−013†	1.731e−012 ± 1.064e−012†	5.444e−015 ± 1.741e−015
f11*	[83,970 ± 9680.665]	[74,423 ± 6515.694]	[61,757/4506.738]
f12	2.426e−024 ± 2.867e−024†	5.734e−024 ± 1.314e−023†	2.083e−031 ± 2.604e−031
f13	3.093e−024 ± 3.224e−024†	8.027e−025 ± 1.143e−024†	1.576e−030 ± 4.092e−030
F1*	[72,636 ± 1586.469]	[73,200 ± 1894.457]	[59,958 ± 1300.500]
F2	4.892e+003 ± 2.285e+003†	9.451e−003 ± 5.091e−003†	3.813e−005 ± 4.675e−005
F3	7.882e+007 ± 1.466e+007†	2.589e+007 ± 5.085e+006†	3.368e+005 ± 1.830e+005
F4	1.166e+004 ± 2.197e+003†	2.815e+000 ± 1.853e+000†	3.099e−002 ± 7.137e−002
F5	2.342e+003 ± 5.499e+002†	1.539e+003 ± 4.017e+002†	1.826e+002 ± 1.553e+002
F6	3.964e+001 ± 2.378e+001†	1.742e+001 ± 8.895e+000‡	2.425e+001 ± 1.898e+001
F7	4.696e+003 ± 3.410e−003‡	4.697e+003 ± 6.331e−002	4.697e+003 ± 1.432e−001
F8	2.096e+001 ± 5.979e−002	2.094e+001 ± 4.696e−002	2.092e+001 ± 1.104e−001
F9	1.032e+002 ± 1.146e+001†	8.307e+001 ± 2.861e+001†	0.000e+000 ± 0.000e+000
F10	1.844e+002 ± 1.032e+001†	1.639e+002 ± 2.773e+001†	4.037e+001 ± 1.296e+001
F11	3.296e+001 ± 6.330e+000†	1.950e+001 ± 1.409e+001†	7.216e+000 ± 4.459e+000
F12	2.299e+005 ± 8.120e+004†	1.435e+005 ± 9.722e+004†	2.765e+003 ± 3.705e+003
F13	1.226e+001 ± 1.076e+000†	8.882e+000 ± 1.122e+000†	7.230e+000 ± 7.441e−001
F14	1.340e+001 ± 1.780e−001†	1.333e+001 ± 1.397e−001†	1.273e+001 ± 4.463e−001
F15	3.967e+002 ± 5.561e+001‡	4.267e+002 ± 4.498e+001	4.267e+002 ± 4.494e+001
F16	2.134e+002 ± 8.784e+000†	2.078e+002 ± 1.383e+001†	7.036e+001 ± 4.892e+001
F17	2.366e+002 ± 9.688e+000†	2.278e+002 ± 1.600e+001†	9.965e+001 ± 7.240e+001
F18	9.071e+002 ± 4.552e−001†	9.074e+002 ± 1.366e+000†	8.944e+002 ± 3.203e+001
F19	9.070e+002 ± 4.382e−001†	9.075e+002 ± 1.221e+000†	9.050e+002 ± 1.586e+000
F20	9.071e+002 ± 4.261e−001†	9.078e+002 ± 1.835e+000†	9.014e+002 ± 1.922e+001
F21	5.000e+002 ± 1.880e−005	5.000e+002 ± 1.880e−005	5.000e+002 ± 1.603e−005
F22	9.520e+002 ± 5.296e+000†	9.359e+002 ± 6.251e+000†	9.122e+002 ± 7.810e+000
F23	5.342e+002 ± 2.287e−004	5.342e+002 ± 2.991e−004	5.342e+002 ± 3.190e−004
F24	2.000e+002 ± 0.000e+000	2.000e+002 ± 0.000e+000	2.000e+002 ± 0.000e+000
F25	1.655e+003 ± 1.692e+000‡	1.657e+003 ± 2.472e+000	1.656e+003 ± 2.998e+000
w/t/l	27/7/4	26/9/3	–

* HLXDE and the competitor can obtain the equal optimum value within *MNFES* and *NFES* required to achieve the accuracy level is also shown in square brackets.
‡ HLXDE is significantly worse than its corresponding competitor by the Wilcoxon test at 5% significance level.
† HLXDE is significantly better than its corresponding competitor by the Wilcoxon test at 5% significance level respectively.

Table 15
Results of the multi-problem Wilcoxon's test for HLXDE with HLX *vs.* DE with different crossover operators (i.e., UFX and TPX) on functions at 30*D*.

Algorithm		$R+$	$R-$	p-Value	$\alpha = 0.05$	$\alpha = 0.1$
DE/rand/1	UFX	620.5	82.5	1.36E−05	Yes	Yes
	TPX	547	156	2.54E−03	Yes	Yes
DE/best/2	UFX	538	165	4.12E−03	Yes	Yes
	TPX	435.5	305.5	3.42E−01	No	No
ODE	UFX	658.5	82.5	6.92E−06	Yes	Yes
	TPX	657	84	7.92E−06	Yes	Yes

vs. CoDE) are less than 0.05. These results indicate that HLXDE is significantly better than the corresponding DE variants in most cases based on multiple-problem statistical analysis.

In general, the overall results of Tables 11–13 and Fig. 2 clearly show that HLX is also able to improve the performance of most DE variants studied.

4.5. Comparison with DE with other crossover operator

As mentioned above, the crossover operator plays an important role in the performance of DE. In this section, two typical crossover operators, two-point crossover (TPX) [15] and uniform crossover (UFX) [59], are used in DE to compare with HLXDE. Then, the comparisons between HLXDE and two DE variants with the advanced crossover operator, DEahcSPX [43] and OXDE [69], are also made.

4.5.1. Comparison against DE with UFX and TPX

In this subsection, two prominent alternatives for crossover in GA, UFX and TPX, are used in DE. Here, DE with TPX is denoted as TPXDE, and DE with UFX is denoted as UFXDE. Three DE algorithms, DE/rand/1, DE/best/2 and ODE, are selected for comparison. The results for all the functions at 30*D* are shown in Table 14. In addition, the results of the multi-problem Wilcoxon's test are also reported in Table 15.

From Table 14, it is interesting to find that HLXDE is significantly better than UFXDE and TPXDE in all cases. Specifically, for DE/rand/1, HLXDE significantly outperforms UFXDE and TPXDE on 26 and 23 functions, respectively, and is outperformed by them on only one and two functions, respectively. For DE/best/2, HLXDE is significantly better than UFXDE and TPXDE on 23 and 17 functions, respectively and is worse on four and five functions, respectively. For ODE, HLXDE can obtain significant improvements on 27 and 26 functions, when compared with UFXDE and TPXDE, respectively. In addition, based on the best and worst values for the test functions (presented in the supplemental file), HLXDE is consistently superior to both UFXDE and TPXDE in most cases.

According to the multi-problem Wilcoxon signed-rank test, the results in Table 15 clear show that HLXDE obtains higher $R+$ values than $R-$ values in all the cases. For the Wilcoxon's test at $\alpha = 0.05$, there are significant differences in all the cases between HLXDE and UFXDE and in two cases between HLXDE and TPXDE. For the Wilcoxon's test at $\alpha = 0.1$, significant differences are observed in three cases between HLXDE and UFXDE and in two cases between HLXDE and TPXDE.

The results of Tables 14 and 15 clearly indicate that HLX is more effectively than UFX and TPX in enhancing the performance of DE.

Furthermore, in order to evaluate the effectiveness of HLX when combining with other crossover operators, UFX and TPX are also employed in HLX to replace BinX. That is, BinX is replaced by UFX or TPX in *Step 8* of Algorithm 5. HLX with UFX and TPX are denoted as HLUFX and HLTPX, respectively. The results of the comparisons between HLUFXDE and UFXDE (HLTPXDE and TPXDE) are shown in Table 16. From Table 16, we can find that HLUFXDE and HLTPXDE can obtain the better results overall, when compared with UFXDE and TPXDE respectively. Specifically, for DE/rand/1, HLUFXDE is significantly better than UFXDE on 22 functions and is worse on three functions, while HLTPXDE is significantly better than TPXDE on 15 functions and is worse on seven functions. For DE/best/2 and ODE, HLUFXDE is significantly better than UFXDE on 20 and 19 functions, respectively, while HLTPXDE is significantly better than TPXDE on 15 and 15 functions, respectively. The overall results of Table 16 show that HLX is also an effective approach when combining with other crossover operators.

4.5.2. Comparison against DEahcSPX and OXDE

In DEahcSPX, the simplex crossover (SPX) is incorporated into DE to carry out the adaptive local search [43]. In OXDE, the orthogonal crossover (OX) on a pair of the mutant and target vectors is employed to combine the advantages of both OX and DE [69]. Here, HLXDE is compared with DEahcSPX and OXDE on the first 27 benchmark functions at 30*D* to test the effectiveness of group-wise crossover.[2] Four DE mutation strategies (i.e., DE/rand/1, DE/rand/2, DE/best/2 and DE/rand-to-best/1) are used. The results are shown in Table 17. The convergence graphs for some typical functions are plotted in Fig. 3.

[2] Due to that no significant differences can be found among HLXDE, OXDE and DEahcSPX on $F15 - F25$, the detailed results for these functions are not provided in this paper.

Table 16
Mean and standard deviation of the best error values obtained by HLUX (HLXDE with UFX) and HLPX (HLXDE with TPX) on functions at 30*D*.

Func.	DE/rand/1				DE/best/2				ODE			
	HLUFX		HLTPX		HLUFX		HLTPX		HLUFX		HLTPX	
f1	2.502e−020 ± 8.532e−021	+	5.345e−020 ± 3.440e−020	+	2.113e−032 ± 2.568e−032	+	5.071e−033 ± 9.059e−033	+	5.489e−028 ± 8.237e−028	+	1.027e−027 ± 1.025e−027	+
f2	4.047e−016 ± 1.359e−016	+	1.532e−015 ± 4.599e−016	+	1.786e−023 ± 1.130e−023	+	1.894e−023 ± 1.511e−023	+	4.787e−016 ± 2.106e−016	+	1.069e−015 ± 7.125e−016	+
f3	1.258e−004 ± 1.029e−004	+	5.998e−009 ± 5.273e−009	−	3.883e−009 ± 3.506e−009	+	5.674e−018 ± 7.169e−018	−	2.747e−004 ± 2.054e−004	+	4.766e−008 ± 4.540e−008	=
f4	6.468e−006 ± 1.399e−006	−	1.363e−005 ± 4.563e−006	−	1.027e−012 ± 7.131e−013	−	1.269e−012 ± 1.019e−012	−	5.340e−028 ± 1.118e−027	−	9.409e−033 ± 1.708e−032	+
f5	1.838e+001 ± 1.601e+000	−	3.534e−005 ± 4.601e−005	−	5.842e−001 ± 1.369e+000	+	7.973e−001 ± 1.622e+000	−	2.566e+001 ± 3.416e−001	=	2.237e+001 ± 7.574e−001	−
f6*	[28,979 ± 1444.110]	=	[29,745 ± 1421.972]	=	[20,386 ± 1164.108]	=	[20,082 ± 880.845]	=	[22,952 ± 1130.834]	=	[22,284 ± 1184.964]	=
f7	6.773e−003 ± 1.164e−003	=	7.586e−003 ± 1.901e−003	=	4.973e−003 ± 1.302e−003	=	5.281e−003 ± 1.564e−003	=	1.980e−003 ± 4.762e−004	=	1.491e−003 ± 5.379e−004	=
f8	0.000e+000 ± 0.000e+000	+	0.000e+000 ± 0.000e+000	+	3.948e+000 ± 2.162e+001	+	7.896e+000 ± 4.325e+001	+	0.000e+000 ± 0.000e+000	+	0.000e+000 ± 0.000e+000	+
f9	0.000e+000 ± 0.000e+000	+	0.000e+000 ± 0.000e+000	+	0.000e+000 ± 0.000e+000	+	0.000e+000 ± 0.000e+000	+	0.000e+000 ± 0.000e+000	+	0.000e+000 ± 0.000e+000	+
f10	7.765e−011 ± 2.050e−011	+	1.179e−010 ± 3.158e−011	+	6.510e−015 ± 1.703e−015	+	6.391e−015 ± 1.741e−015	+	2.368e−014 ± 1.205e−014	+	2.297e−014 ± 1.027e−014	+
f11	0.000e+000 ± 0.000e+000	+	0.000e+000 ± 0.000e+000	=	9.036e−004 ± 2.856e−003	=	2.465e−004 ± 1.350e−003	+	68,753 ± 5295.217	=	66,257 ± 4203.990	=
f12	8.677e−021 ± 5.025e−021	+	1.027e−020 ± 6.369e−021	+	2.887e−032 ± 2.028e−032	+	1.751e−032 ± 4.896e−033	+	1.379e−028 ± 1.443e−028	+	1.009e−028 ± 1.164e−028	+
f13	2.603e−020 ± 1.192e−020	+	4.257e−020 ± 3.803e−020	+	2.755e−032 ± 2.481e−032	+	3.662e−004 ± 2.006e−003	+	1.859e−028 ± 2.084e−028	+	1.862e−028 ± 2.752e−028	+
F1	0.000e+000 ± 0.000e+000	=	0.000e+000 ± 0.000e+000	=	3.411e−014 ± 2.832e−014	+	3.979e−014 ± 2.649e−014	+	63,809 ± 1376.232	=	63,962 ± 1462.630	=
F2	3.479e−001 ± 2.601e−001	+	8.305e−004 ± 4.769e−004	=	1.266e−003 ± 9.934e−004	+	7.073e−009 ± 7.990e−009	−	3.416e+000 ± 2.428e+000	+	1.059e−002 ± 8.017e−003	=
F3	7.736e+006 ± 2.805e+006	+	4.092e+006 ± 1.382e+006	+	1.722e+006 ± 7.356e+005	+	1.158e+006 ± 5.512e+005	+	1.398e+007 ± 5.071e+006	+	8.591e+006 ± 2.717e+006	+
F4	2.312e+003 ± 6.868e+002	+	4.586e+001 ± 2.043e+001	−	2.750e+002 ± 1.861e+002	+	1.845e−001 ± 1.401e−001	−	4.582e+003 ± 2.023e+003	+	5.618e+001 ± 3.915e+001	−
F5	2.238e+003 ± 2.034e+002	=	1.882e+003 ± 2.856e+002	−	1.325e+003 ± 3.509e+002	=	1.032e+003 ± 4.173e+002	−	2.444e+003 ± 2.988e+002	=	2.284e+003 ± 3.615e+002	−
F6	1.379e+001 ± 2.737e+000	+	1.305e+000 ± 1.085e+000	−	3.516e−005 ± 6.689e−005	+	2.658e−001 ± 1.011e+000	=	3.801e+001 ± 2.215e+001	+	2.125e+001 ± 8.009e+000	−
F7	4.696e+003 ± 0.000e+000	=	4.696e+003 ± 2.565e−004	=	4.696e+003 ± 2.660e−002	=	4.696e+003 ± 3.239e−002	=	4.696e+003 ± 1.792e−003	=	4.696e+003 ± 3.349e−003	=
F8	2.095e+001 ± 4.110e−002	=	2.094e+001 ± 4.685e−002	=	2.096e+001 ± 4.630e−002	=	2.095e+001 ± 4.455e−002	=	2.095e+001 ± 5.591e−002	=	2.094e+001 ± 6.857e−002	=
F9	0.000e+000 ± 0.000e+000	+	0.000e+000 ± 0.000e+000	+	3.790e−015 ± 1.442e−014	+	3.790e−015 ± 1.442e−014	+	0.000e+000 ± 0.000e+000	+	0.000e+000 ± 0.000e+000	+
F10	1.650e+002 ± 1.233e+001	+	1.592e+002 ± 1.084e+001	+	1.621e+002 ± 1.473e+001	+	1.595e+002 ± 1.431e+001	+	1.615e+002 ± 1.383e+001	+	1.446e+002 ± 3.351e+001	+
F11	3.592e+001 ± 1.288e+000	+	3.531e+001 ± 1.231e+000	+	3.501e+001 ± 1.868e+000	+	3.473e+001 ± 1.653e+000	+	1.896e+001 ± 1.144e+001	+	1.573e+001 ± 1.064e+001	=
F12	1.997e+005 ± 2.434e+004	+	1.971e+005 ± 2.836e+004	−	7.031e+004 ± 6.181e+004	=	3.762e+004 ± 5.506e+004	=	2.134e+005 ± 5.090e+004	=	1.727e+005 ± 7.186e+004	=
F13	7.162e+000 ± 6.736e−001	+	6.783e+000 ± 6.045e−001	+	7.085e+000 ± 6.550e−001	+	6.925e+000 ± 6.453e−001	+	7.273e+000 ± 5.448e−001	+	6.951e+000 ± 5.455e−001	+
F14	1.333e+001 ± 1.588e−001	=	1.328e+001 ± 1.523e−001	=	1.330e+001 ± 1.953e−001	=	1.325e+001 ± 1.834e−001	=	1.334e+001 ± 1.992e−001	=	1.328e+001 ± 1.385e−001	=
F15	3.633e+002 ± 4.901e+001	−	3.833e+002 ± 5.307e+001	=	3.092e+002 ± 1.257e+002	=	3.294e+002 ± 9.720e+001	=	4.000e+002 ± 5.252e+001	=	4.133e+002 ± 3.457e+001	=
F16	1.857e+002 ± 1.083e+001	+	1.858e+002 ± 1.221e+001	+	2.273e+002 ± 8.786e+001	=	2.435e+002 ± 1.140e+002	=	1.931e+002 ± 1.397e+001	+	1.903e+002 ± 1.230e+001	+
F17	2.095e+002 ± 1.321e+001	+	2.115e+002 ± 1.165e+001	+	2.776e+002 ± 8.173e+001	=	2.791e+002 ± 9.628e+001	=	2.171e+002 ± 1.142e+001	=	2.198e+002 ± 1.365e+001	+
F18	9.066e+002 ± 4.012e−001	+	9.068e+002 ± 4.327e−001	=	9.038e+002 ± 1.967e+001	=	9.075e+002 ± 1.492e+000	=	9.072e+002 ± 8.402e−001	=	9.037e+002 ± 1.961e+001	=
F19	9.068e+002 ± 4.302e−001	=	9.068e+002 ± 4.449e−001	=	9.072e+002 ± 1.597e+000	=	9.076e+002 ± 1.707e+000	=	9.068e+002 ± 3.411e−001	=	9.073e+002 ± 8.616e−001	=
F20	9.067e+002 ± 5.504e−001	=	9.070e+002 ± 1.037e+000	=	9.073e+002 ± 1.548e+000	=	9.073e+002 ± 1.633e+000	=	9.070e+002 ± 5.190e−001	=	9.072e+002 ± 4.655e−001	=
F21	5.000e+002 ± 1.700e−005	=	5.000e+002 ± 1.880e−005	=	5.200e+002 ± 7.611e+001	=	5.406e+002 ± 1.053e+002	=	5.000e+002 ± 1.880e−005	=	5.000e+002 ± 1.880e−005	=
F22	9.369e+002 ± 5.402e+000	+	9.301e+002 ± 6.631e+000	=	9.287e+002 ± 8.064e+000	+	9.223e+002 ± 1.296e+001	=	9.430e+002 ± 6.389e+000	+	9.356e+002 ± 6.146e+000	=
F23	5.342e+002 ± 1.965e−004	=	5.342e+002 ± 2.240e−004	=	5.595e+002 ± 9.657e+001	=	5.732e+002 ± 1.191e+002	=	5.342e+002 ± 2.162e−004	=	5.342e+002 ± 2.738e−004	=
F24	2.000e+002 ± 0.000e+000	=	2.000e+002 ± 0.000e+000	=	2.000e+002 ± 0.000e+000	=	2.000e+002 ± 0.000e+000	=	2.000e+002 ± 0.000e+000	=	2.000e+002 ± 0.000e+000	=
F25	1.650e+003 ± 2.094e+000	+	1.651e+003 ± 2.510e+000	+	1.651e+003 ± 2.410e+000	+	1.651e+003 ± 3.418e+000	+	1.651e+003 ± 2.616e+000	+	1.652e+003 ± 2.842e+000	+
+/=/−	22/13/3		15/15/7		20/17/1		15/17/6		19/18/1		15/19/4	

+, = and − The HLXDE variant is significantly better than, equal to and worse than DE with the corresponding crossover operator by the Wilcoxon test at 5% significance level respectively.
* The HLXDE variant can obtain the equal optimum value within *MNFES* and *NFES* required to achieve the accuracy level is also shown in square brackets.

Table 17
Mean and standard deviation of the best error values obtained by DEahcSPX, OXDE and HLXDE with different mutation strategies on functions $f1-f13$ and $F1-F14$ at 30D.

Func.	DE/rand/1			DE/best/2		
	DEahcSPX	OXDE	HLXDE	DEahcSPX	OXDE	HLXDE
f1	1.972e−019 ± 1.816e−019†	5.448e−017 ± 4.063e−017†	**5.212e−022 ± 4.596e−022**	6.727e−043 ± 7.196e−043	4.495e−033 ± 7.342e−033†	**4.666e−043 ± 8.832e−043**
f2	8.476e−014 ± 4.482e−014†	4.608e−012 ± 1.947e−012†	**7.247e−016 ± 3.993e−016**	**3.016e−030 ± 3.625e−030**‡	2.403e−022 ± 1.371e−022†	1.565e−029 ± 1.440e−029
f3	**1.064e−014 ± 1.360e−014**‡	2.071e−011 ± 2.974e−011†	1.142e−012 ± 3.857e−012	**3.264e−038 ± 4.031e−038**‡	3.441e−026 ± 7.729e−026†	4.380e−032 ± 1.162e−031
f4	4.949e−001 ± 5.253e−001†	2.418e−001 ± 4.087e−001†	**1.372e−002 ± 5.243e−002**	**2.995e−017 ± 9.025e−017**‡	1.917e−015 ± 6.772e−015	2.997e−016 ± 4.233e−016
f5	2.651e−007 ± 1.433e−006†	**1.141e−014 ± 3.272e−014**‡	4.699e−008 ± 1.555e−007	9.302e−001 ± 1.715e+000†	1.196e+000 ± 1.858e+000	**6.644e−001 ± 1.511e+000**
f6*	[28,627 ± 1838.828]	[32,874 ± 1376.584]	[**27,844 ± 1375.495**]	1.067e+000 ± 1.202e+000†	3.000e−001 ± 5.350e−001†	0.000e+000 ± 0.000e+000
f7	**2.394e−003 ± 1.053e−003**‡	**2.694e−003 ± 7.082e−004**‡	4.626e−003 ± 1.422e−003	4.025e−003 ± 1.268e−003	3.825e−003 ± 1.373e−003	**3.744e−003 ± 1.048e−003**
f8	6.491e+003 ± 6.273e+002†	6.063e−014 ± 3.321e−013	**0.000e+000 ± 0.000e+000**	7.094e+003 ± 4.037e+002†	1.184e+001 ± 3.614e+001	**7.896e+000 ± 3.005e+001**
f9	1.271e+002 ± 2.656e+001†	1.250e+002 ± 1.275e+001†	**0.000e+000 ± 0.000e+000**	1.547e+002 ± 1.672e+001†	1.411e+002 ± 1.196e+001†	0.000e+000 ± 0.000e+000
f10	1.103e−010 ± 4.266e−011†	2.216e−009 ± 5.910e−010†	**2.014e−011 ± 7.005e−012**	4.997e−001 ± 6.360e−001†	7.694e−015 ± 1.616e−015†	**6.155e−015 ± 1.791e−015**
f11	5.751e−004 ± 2.212e−003	2.465e−004 ± 1.350e−003	2.465e−004 ± 1.350e−003	6.895e−003 ± 9.219e−003†	1.205e−002 ± 1.419e−002†	**1.806e−003 ± 4.745e−003**
f12	9.977e−021 ± 9.115e−021†	4.830e−018 ± 4.442e−018†	**1.010e−022 ± 1.535e−022**	1.627e−001 ± 3.890e−001†	4.492e−002 ± 9.305e−002†	**3.456e−003 ± 1.893e−002**
f13	1.056e−019 ± 1.366e−019†	2.648e−017 ± 1.829e−017†	**6.082e−022 ± 5.767e−022**	2.197e−003 ± 4.470e−003†	5.398e−002 ± 2.915e−001†	**1.350e−032 ± 0.000e+000**
F1*	[83,481 ± 1971.064]	[92,908 ± 1948.822]	[**74,409 ± 1351.813**]	5.495e−014 ± 2.352e−014	**3.032e−014 ± 2.884e−014**‡	4.737e−014 ± 2.155e−014
F2	**6.133e−007 ± 4.576e−007**‡	7.030e−005 ± 7.751e−005†	8.644e−006 ± 1.299e−005	**1.724e−013 ± 7.536e−014**‡	**1.743e−013 ± 6.830e−014**‡	3.126e−013 ± 1.592e−013
F3	3.609e+005 ± 2.113e+005	4.611e+005 ± 3.139e+005	**3.320e+005 ± 2.167e+005**	8.322e+004 ± 5.080e+004†	1.503e+005 ± 9.724e+004†	**5.237e+004 ± 2.622e+004**
F4	**1.631e−003 ± 1.993e−003**	5.396e−002 ± 7.264e−002†	3.868e−003 ± 7.070e−003	3.914e−005 ± 9.908e−005†	1.987e−004 ± 3.284e−004†	**7.725e−006 ± 1.768e−005**
F5	**2.896e+001 ± 3.049e+001**‡	**3.538e+001 ± 3.411e+001**‡	1.216e+002 ± 2.074e+002	1.301e+002 ± 1.749e+002†	2.555e+001 ± 3.729e+001	4.495e+001 ± 7.761e+001
F6	4.176e+000 ± 2.792e+000†	2.498e+000 ± 1.347e+000†	**2.353e−001 ± 4.447e−001**	1.063e+000 ± 1.793e+000†	1.063e+000 ± 1.793e+000	**3.987e−001 ± 1.216e+000**
F7	**4.696e+003 ± 8.563e−003**‡	**4.696e+003 ± 6.411e−005**‡	4.696e+003 ± 2.360e−002	**4.697e+003 ± 1.941e−001**‡	**4.696e+003 ± 2.519e−003**‡	4.701e+003 ± 2.396e+000
F8	2.096e+001 ± 4.948e−002	2.094e+001 ± 5.816e−002	2.095e+001 ± 4.622e−002	2.095e+001 ± 5.515e−002	2.095e+001 ± 3.285e−002	2.095e+001 ± 5.023e−002
F9	1.234e+002 ± 2.789e+001†	1.267e+002 ± 1.325e+001†	**0.000e+000 ± 0.000e+000**	1.590e+002 ± 2.507e+001†	1.480e+002 ± 1.264e+001†	**1.895e−014 ± 2.725e−014**
F10	**1.639e+002 ± 1.410e+001**	1.759e+002 ± 8.009e+000	**1.561e+002 ± 4.725e+001**	1.833e+002 ± 2.710e+001	1.925e+002 ± 1.638e+001	1.871e+002 ± 1.153e+001
F11	3.862e+001 ± 1.424e+000	3.901e+001 ± 1.273e+000	**3.829e+001 ± 3.135e+000**	**3.790e+001 ± 1.416e+000**	3.949e+001 ± 1.186e+000†	3.827e+001 ± 1.181e+000
F12	1.929e+003 ± 2.647e+003	**1.539e+003 ± 1.479e+003**	1.764e+003 ± 1.784e+003	1.926e+003 ± 2.445e+003	1.387e+003 ± 2.797e+003	**1.163e+003 ± 1.375e+003**
F13	1.468e+001 ± 1.320e+000†	1.266e+001 ± 8.987e−001†	**8.260e+000 ± 7.036e−001**	1.429e+001 ± 1.564e+000†	1.336e+001 ± 1.200e+000†	**8.166e+000 ± 7.796e−001**
F14	**1.328e+001 ± 1.599e−001**‡	**1.326e+001 ± 1.598e−001**‡	1.338e+001 ± 1.915e−001	**1.317e+001 ± 2.450e−001**‡	1.323e+001 ± 2.552e−001	1.328e+001 ± 1.604e−001

w/t/l	12/9/6	13/9/5	–	14/7/6	14/10/3	–
Func.	DE/rand/2			DE/rand-to-best/1		
	DEahcSPX	OXDE	HLXDE	DEahcSPX	OXDE	HLXDE
f1	1.042e+000 ± 3.500e−001†	3.671e−001 ± 1.312e−001†	**1.667e−006 ± 8.952e−007**	1.394e+002 ± 9.868e+001†	5.164e+001 ± 4.250e+001†	**6.635e−001 ± 1.601e+000**
f2	7.647e−001 ± 1.779e−001†	1.354e−001 ± 2.057e−002†	**9.126e−004 ± 5.335e−004**	2.660e+000 ± 1.608e+000†	1.557e+000 ± 8.344e−001†	**1.054e−001 ± 2.320e−001**
f3	**8.523e+000 ± 2.718e+000**‡	2.130e+002 ± 5.659e+001†	2.374e+001 ± 7.873e+000	6.258e+002 ± 3.162e+002†	4.122e+002 ± 1.949e+002	**3.963e+002 ± 2.407e+002**
f4	**2.791e−001 ± 6.383e−002**‡	**4.381e−002 ± 1.266e−002**‡	8.072e+000 ± 8.584e−001	8.761e+000 ± 2.138e+000	**7.996e+000 ± 1.778e+000**	8.162e+000 ± 2.211e+000
f5	1.281e+001 ± 6.291e−001†	**6.338e+000 ± 7.283e−001**‡	8.428e+000 ± 6.659e−001	8.987e+003 ± 9.793e+003†	3.691e+003 ± 4.259e+003†	**2.305e+002 ± 1.591e+002**
f6	1.367e+000 ± 1.033e+000†	2.667e−001 ± 4.498e−001†	**0.000e+000 ± 0.000e+000**	1.729e+002 ± 9.283e+001†	5.947e+001 ± 3.437e+001†	**1.400e+000 ± 2.253e+000**
f7	**6.696e−003 ± 2.805e−003**‡	**1.301e−002 ± 3.484e−003**‡	6.301e−002 ± 1.479e−002	**3.464e−003 ± 1.863e−003**	3.690e−003 ± 1.866e−003	3.724e−003 ± 1.687e−003
f8	7.366e+003 ± 2.227e+002†	2.560e+003 ± 2.815e+002†	**1.380e−007 ± 1.235e−007**	4.032e+003 ± 5.018e+002†	2.784e+003 ± 8.248e+002†	**7.054e+002 ± 3.338e+002**
f9	1.717e+002 ± 1.808e+001†	1.614e+002 ± 9.274e+000†	**3.423e−005 ± 2.738e−005**	3.069e+001 ± 9.120e+000†	2.568e+001 ± 8.606e+000†	**5.308e−001 ± 7.266e−001**
f10	7.414e−001 ± 2.082e−001†	4.040e−001 ± 1.018e−001†	**1.254e−003 ± 2.524e−004**	3.875e+000 ± 7.265e−001†	2.987e+000 ± 8.206e−001†	**5.281e−001 ± 4.822e−001**
f11	1.914e−001 ± 7.569e−002†	2.693e−001 ± 2.320e−001†	**3.453e−003 ± 1.246e−002**	2.932e+000 ± 1.345e+000†	1.609e+000 ± 4.885e−001†	**6.574e−002 ± 1.143e−001**
f12	7.036e−001 ± 4.410e−001†	3.117e−001 ± 1.634e−001†	**5.899e−006 ± 2.519e−006**	2.759e+000 ± 1.738e+000†	1.662e+000 ± 1.205e+000†	**9.681e−002 ± 1.399e−001**
f13	2.191e+000 ± 1.232e+000†	3.796e−001 ± 1.705e−001†	**5.310e−006 ± 2.141e−006**	3.569e+001 ± 3.636e+001†	1.117e+001 ± 1.056e+001†	**2.252e−001 ± 3.656e−001**
F1	4.352e−004 ± 2.905e−004†	1.390e−005 ± 5.291e−006†	**0.000e+000 ± 0.000e+000**	3.157e+003 ± 1.477e+003†	1.779e+003 ± 9.892e+002†	**6.776e+001 ± 1.300e+002**
F2	**5.180e+002 ± 2.124e+002**‡	3.098e+003 ± 7.599e+002†	8.228e+002 ± 2.239e+002	5.861e+003 ± 1.798e+003†	4.458e+003 ± 1.913e+003	**3.663e+003 ± 1.819e+003**
F3	**4.021e+006 ± 1.221e+006**‡	3.290e+007 ± 8.821e+006†	1.051e+007 ± 4.461e+006	7.058e+006 ± 4.343e+006	**5.205e+006 ± 2.993e+006**	6.354e+006 ± 4.202e+006
F4	**2.239e+003 ± 7.065e+002**‡	7.570e+003 ± 1.273e+003†	5.655e+003 ± 2.331e+003	9.321e+002 ± 6.836e+002	1.068e+003 ± 7.783e+002	**7.396e+002 ± 5.595e+002**
F5	**4.207e+003 ± 3.940e+002**‡	**3.265e+003 ± 2.759e+002**‡	6.631e+003 ± 5.059e+002	7.233e+003 ± 1.241e+003	**6.054e+003 ± 1.714e+003**	6.976e+003 ± 1.507e+003
F6	5.128e+001 ± 3.089e+001†	**2.591e+001 ± 9.552e−001**‡	2.922e+001 ± 9.320e+000	3.074e+008 ± 3.246e+008†	1.212e+008 ± 9.903e+007†	**3.552e+007 ± 5.428e+007**
F7	5.241e+003 ± 5.464e+001†	**4.698e+003 ± 2.220e−001**‡	4.733e+003 ± 1.434e−004	5.978e+003 ± 2.258e+002†	4.843e+003 ± 6.111e+001†	**4.733e+003 ± 1.434e−004**
F8	2.095e+001 ± 6.071e−002	2.094e+001 ± 4.424e−002	2.094e+001 ± 5.163e−002	**2.093e+001 ± 6.362e−002**	2.095e+001 ± 5.074e−002	2.094e+001 ± 5.695e−002
F9	1.928e+002 ± 1.598e+001†	1.776e+002 ± 8.741e+000†	**1.089e−005 ± 6.946e−006**	6.889e+001 ± 1.396e+001†	6.135e+001 ± 1.288e+001†	**6.561e+000 ± 4.533e+000**
F10	**1.898e+002 ± 1.680e+001**‡	2.144e+002 ± 1.117e+001‡	2.245e+002 ± 1.130e+001	9.158e+001 ± 2.478e+001	8.515e+001 ± 1.972e+001	**8.087e+001 ± 2.040e+001**
F11	**3.901e+001 ± 1.251e+000**	3.976e+001 ± 1.050e+000	3.911e+001 ± 1.069e+000	1.448e+001 ± 2.367e+000†	**1.255e+001 ± 2.474e+000**	1.276e+001 ± 1.954e+000
F12	**2.461e+005 ± 6.964e+004**‡	3.559e+005 ± 3.777e+004†	3.305e+005 ± 2.971e+004	6.944e+004 ± 3.304e+004†	**5.185e+004 ± 2.006e+004**	5.266e+004 ± 2.375e+004
F13	1.686e+001 ± 1.052e+000†	1.534e+001 ± 9.927e−001†	**1.117e+001 ± 1.289e+000**	3.681e+000 ± 8.001e−001‡	**3.549e+000 ± 1.306e+000**‡	5.165e+000 ± 1.254e+000
F14	**1.339e+001 ± 1.502e−001**	1.340e+001 ± 1.586e−001	1.343e+001 ± 1.358e−001	1.137e+001 ± 4.275e−001	**1.136e+001 ± 3.920e−001**	1.145e+001 ± 3.424e−001
w/t/l	15/3/9	17/3/7	–	18/8/1	14/12/1	–

* HLXDE and the competitor can obtain the equal optimum value within *MNFES* and *NFES* required to achieve the accuracy level is also shown in square brackets.

‡ HLXDE is significantly worse than its corresponding competitor by the Wilcoxon test at 5% significance level.

† HLXDE is significantly better than its corresponding competitor by the Wilcoxon test at 5% significance level.

From Table 17, it is clear that HLXDE obtains significantly better results than DEahcSPX and OXDE in most of the cases. Specifically, with DE/rand/1, HLXDE significantly outperforms DEahcSPX and OXDE on 12 and 13 functions, respectively, and is outperformed by them on six and five functions, respectively. With DE/rand/2, HLXDE is significantly better than DEahcSPX on 15 functions and is worse on nine functions, while HLXDE is significantly better than OXDE on 17 functions and is worse on seven functions. With DE/best/2 and DE/rand-to-best/1, HLXDE is consistently superior to DEahcSPX and OXDE. HLXDE with DE/best/2 is significantly better than DEahcSPX and OXDE on 14 and 14 functions, respectively, while HLXDE with DE/rand-to-best/1 is significantly better than DEahcSPX and OXDE on 18 and 14 functions, respectively. In addition, the best and worst values presented in the supplemental file also show that HLXDE is consistently superior to DEahcSPX and OXDE overall.

In order to further show the significant differences between HLXDE and the two DE variants, the Friedman test and Wilcoxon's test are also carried out and the results are shown in Tables 18 and 19. According to the average ranking values by Friedman test, Table 18 clearly shows that HLXDE consistently obtains best ranking values among the three competitors in all the cases. Based on the multi-problem Wilcoxon signed-rank test, the results in Table 19 also show that HLXDE obtains higher $R+$ values than $R-$ values in all the cases. For the Wilcoxon's test at $\alpha = 0.05$, there are significant differences in three cases between HLXDE and DEahcSPX and in two cases between HLXDE and OXDE. For the Wilcoxon's test at $\alpha = 0.1$, significant differences are observed in three cases between HLXDE and DEahcSPX and in all four cases between HLXDE and OXDE. The results of Tables 18 and 19 indicate that HLXDE is significantly better than DEahcSPX and OXDE in most of the cases based on multiple-problem statistical analysis.

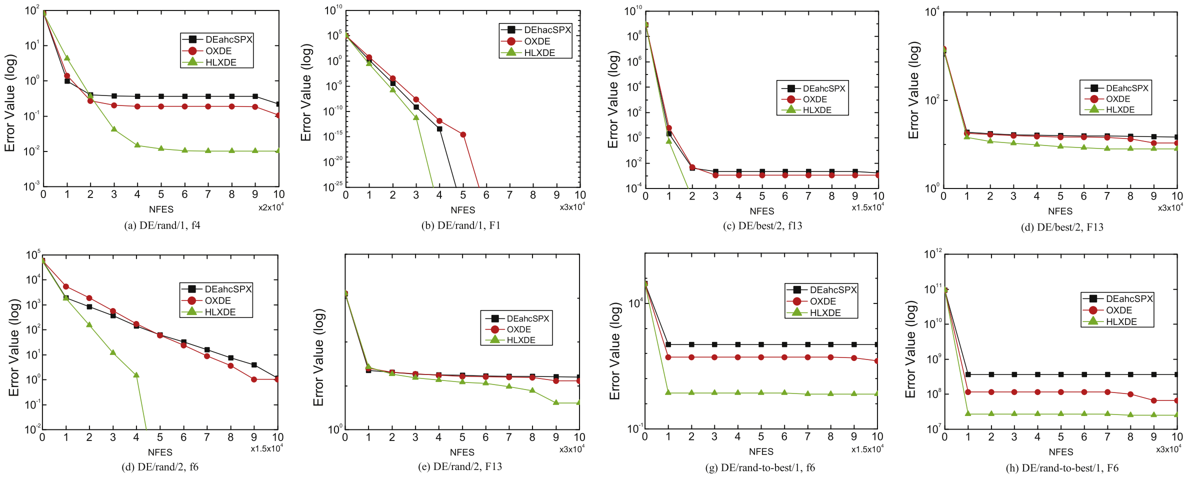

Fig. 3. Convergence graphs of HLXDE, DEahcSPX and OXDE on some test functions at 30*D*.

Table 18
Average ranking values of the DE variants with advanced crossover operator for functions $f1 - f13$ and $F1 - F14$ at 30D.

Algorithm	Mutation			
	DE/rand/1	DE/rand/2	DE/best/2	DE/rand-to-best/1
DEahcSPX	2.15	2.26	2.30	2.74
OXDE	2.09	2.06	2.20	1.83
HLXDE	**1.76**	**1.69**	**1.50**	**1.43**

Table 19
Results of the multi-problem Wilcoxon's test for HLXDE *vs.* DEahcSPX and OXDE, respectively, for functions $f1 - f13$ and $F1 - F14$ at 30D.

Mutation	Algorithm	$R+$	$R-$	p-Value	$\alpha = 0.05$	$\alpha = 0.1$
DE/rand/1	DEahcSPX	285	93	2.04E−02	Yes	Yes
	OXDE	265	113	6.61E−02	No	Yes
DE/rand/2	DEahcSPX	183.5	167.5	8.29E−01	No	No
	OXDE	269.5	108.5	5.17E−02	No	Yes
DE/best/2	DEahcSPX	304.5	73.5	5.32E−03	Yes	Yes
	OXDE	321.5	56.5	1.40E−03	Yes	Yes
DE/rand-to-best/1	DEahcSPX	344	7	1.80E−05	Yes	Yes
	OXDE	288.5	89.5	1.60E−02	Yes	Yes

Table 20
Mean and standard deviation of the best error values obtained by HLXDE1, HLXDE2 and HLXDE on the selected nonseparable functions at 30*D*.

Func.	DE/rand/1			DE/best/2		
	HLXDE1	HLXDE2	HLXDE	HLXDE1	HLXDE2	HLXDE
f3	1.265e−009 ± 1.040e−009†	1.851e−007 ± 1.793e−007†	**1.142e−012 ± 3.857e−012**	1.090e−023 ± 4.385e−023†	1.204e−020 ± 2.441e−020†	**4.380e−032 ± 1.162e−031**
f4	5.284e−004 ± 1.999e−003	1.372e−002 ± 5.243e−002	1.372e−002 ± 5.243e−002	3.034e−016 ± 3.317e−016	2.997e−016 ± 4.233e−016	2.997e−016 ± 4.233e−016
f5	1.368e−007 ± 7.128e−007	4.699e−008 ± 1.555e−007	4.699e−008 ± 1.555e−007	1.595e+000 ± 1.986e+000†	6.644e−001 ± 1.511e+000	**6.644e−001 ± 1.511e+000**
F2	6.563e−004 ± 3.450e−004†	1.608e−002 ± 1.289e−002†	**8.644e−006 ± 1.299e−005**	1.696e−012 ± 4.229e−012†	1.580e−010 ± 1.817e−010†	**3.126e−013 ± 1.592e−013**
F3	4.568e+005 ± 2.792e+005	4.942e+005 ± 2.578e+005†	**3.320e+005 ± 2.167e+005**	1.634e+005 ± 9.049e+004†	2.267e+005 ± 1.334e+005†	**5.237e+004 ± 2.622e+004**
F4	4.193e−002 ± 4.091e−002†	1.016e+000 ± 7.969e−001†	**3.868e−003 ± 7.070e−003**	1.082e−004 ± 2.998e−004†	4.367e−004 ± 5.310e−004†	**7.725e−006 ± 1.768e−005**
F5	7.214e+001 ± 4.708e+001	1.698e+002 ± 8.642e+001†	**1.216e+002 ± 2.074e+002**	5.111e+001 ± 6.480e+001	5.523e+001 ± 8.968e+001	**4.495e+001 ± 7.761e+001**
F6	1.404e+000 ± 9.531e−001†	3.942e+000 ± 2.194e+000†	**2.353e−001 ± 4.447e−001**	2.658e−001 ± 1.011e+000	5.315e−001 ± 1.378e+000	3.987e−001 ± 1.216e+000
F7	4.696e+003 ± 1.779e−002	**4.696e+003 ± 9.660e−004**‡	4.696e+003 ± 2.360e−002	4.699e+003 ± 1.341e+000‡	**4.698e+003 ± 3.352e−001**‡	4.701e+003 ± 2.396e+000
F8	2.095e+001 ± 5.139e−002	2.094e+001 ± 5.386e−002	2.095e+001 ± 4.622e−002	2.096e+001 ± 5.019e−002	2.095e+001 ± 3.658e−002	2.095e+001 ± 5.023e−002
F10	1.809e+002 ± 1.178e+001†	1.852e+002 ± 1.137e+001†	**1.561e+002 ± 4.725e+001**	1.871e+002 ± 1.752e+001	1.901e+002 ± 1.286e+001	1.871e+002 ± 1.153e+001
F11	3.858e+001 ± 1.238e+000	3.957e+001 ± 8.022e−001†	**3.829e+001 ± 3.135e+000**	3.921e+001 ± 1.057e+000†	3.968e+001 ± 1.235e+000†	**3.827e+001 ± 1.181e+000**
F12	1.534e+003 ± 1.545e+003	2.246e+003 ± 1.902e+003	1.764e+003 ± 1.784e+003	8.956e+002 ± 1.367e+003	1.199e+003 ± 2.039e+003	1.163e+003 ± 1.375e+003
F13	8.333e+000 ± 8.387e−001	**7.753e+000 ± 8.338e−001**‡	8.260e+000 ± 7.036e−001	8.129e+000 ± 8.320e−001	**7.621e+000 ± 7.225e−001**‡	8.166e+000 ± 7.796e−001
F14	1.330e+001 ± 2.454e−001	1.336e+001 ± 1.175e−001	1.338e+001 ± 1.915e−001	1.333e+001 ± 1.629e−001	1.331e+001 ± 1.841e−001	**1.328e+001 ± 1.604e−001**
w/t/l	6/9/0	8/5/2	–	6/8/1	5/8/2	–
Func.	ODE			SaDE		
	HLXDE1	HLXDE2	HLXDE	HLXDE1	HLXDE2	HLXDE
f3	4.964e−010 ± 1.032e−009†	5.415e−009 ± 4.896e−009†	**1.952e−012 ± 3.578e−012**	7.077e−015 ± 2.330e−014	1.899e−012 ± 4.206e−012†	1.949e−014 ± 5.133e−014
f4	9.782e−003 ± 5.358e−002	4.859e−004 ± 1.915e−003	4.859e−004 ± 1.915e−003	1.787e+000 ± 2.070e+000	1.268e+000 ± 2.098e+000	1.268e+000 ± 2.098e+000
f5	2.469e+001 ± 9.368e−001	2.465e+001 ± 8.037e−001	2.465e+001 ± 8.037e−001	2.548e+000 ± 3.276e+000	4.249e+000 ± 3.959e+000	4.249e+000 ± 3.959e+000
F2	1.570e−003 ± 1.200e−003†	1.002e−002 ± 1.184e−002†	**3.813e−005 ± 4.675e−005**	**6.392e−007 ± 1.193e−006**‡	2.490e−005 ± 4.060e−005†	4.345e−006 ± 1.413e−005
F3	4.943e+005 ± 2.601e+005†	7.053e+005 ± 4.148e+005†	**3.368e+005 ± 1.830e+005**	5.080e+005 ± 2.660e+005	6.473e+005 ± 2.807e+005	5.335e+005 ± 2.853e+005
F4	1.833e−001 ± 2.397e−001†	7.388e−001 ± 5.195e−001†	**3.099e−002 ± 7.137e−002**	1.311e+000 ± 2.518e+000	8.149e+000 ± 1.657e+001†	1.442e+000 ± 2.902e+000
F5	1.796e+002 ± 6.383e+001	2.573e+002 ± 1.924e+002	1.826e+002 ± 1.553e+002	**1.667e+003 ± 4.590e+002**‡	1.737e+003 ± 5.521e+002	2.004e+003 ± 5.252e+002
F6	3.962e+001 ± 2.152e+001†	4.309e+001 ± 2.362e+001†	**2.425e+001 ± 1.898e+001**	1.295e+001 ± 1.473e+001†	2.345e+001 ± 2.974e+001†	**5.916e+000 ± 4.942e+000**
F7	4.697e+003 ± 1.440e−001	**4.696e+003 ± 5.945e−003**‡	4.697e+003 ± 1.432e−001	4.696e+003 ± 0.000e+000	4.696e+003 ± 0.000e+000	4.696e+003 ± 0.000e+000
F8	2.094e+001 ± 5.800e−002	2.095e+001 ± 5.830e−002	2.092e+001 ± 1.104e−001	2.093e+001 ± 5.762e−002	2.095e+001 ± 5.154e−002	2.094e+001 ± 5.565e−002
F10	6.688e+001 ± 5.688e+001	9.133e+001 ± 6.613e+001†	**4.037e+001 ± 1.296e+001**	7.323e+001 ± 1.605e+001†	8.009e+001 ± 1.329e+001†	**4.990e+001 ± 9.850e+000**
F11	9.485e+000 ± 1.076e+001	1.033e+001 ± 1.346e+001	**7.216e+000 ± 4.459e+000**	2.977e+001 ± 4.117e+000†	3.135e+001 ± 1.378e+000†	**2.728e+001 ± 1.472e+000**
F12	3.115e+003 ± 2.217e+003	1.733e+003 ± 1.684e+003	2.765e+003 ± 3.705e+003	2.694e+003 ± 2.132e+003	4.506e+003 ± 6.246e+003	3.811e+003 ± 3.111e+003
F13	7.228e+000 ± 9.034e−001	7.291e+000 ± 1.114e+000	7.230e+000 ± 7.441e−001	4.550e+000 ± 3.109e−001†	4.884e+000 ± 6.707e−001†	**2.514e+000 ± 2.038e−001**
F14	1.320e+001 ± 2.197e−001†	1.325e+001 ± 1.922e−001†	**1.273e+001 ± 4.463e−001**	1.304e+001 ± 1.710e−001†	1.302e+001 ± 1.918e−001†	**1.287e+001 ± 1.611e−001**
w/t/l	6/9/0	7/7/1	–	5/8/2	8/7/0	–

‡ HLXDE is significantly worse than its corresponding competitor by the Wilcoxon test at 5% significance level respectively.
† HLXDE is significantly better than its corresponding competitor by the Wilcoxon test at 5% significance level respectively.

In general, from the results in Tables 17–19, we can conclude that DE with HLX is able to bring more benefits for improving the performance of DE than DEahcSPX and OXDE.

4.6. Effectiveness of AG in HLXDE

In order to study the effectiveness of AG in HLX, we consider the following two variants of HLXDE. First, to evaluate the influence of AG for GbinX, HLXDE1 is proposed, where GbinX is removed from HLXDE. Second, to test the effectiveness of AG for GorthX, HLXDE2 is introduced, where AG is removed from HLXDE and each variable is regarded as a factor in OX, as that in [82]. In addition, as Table 10 shows, HLX can identify most of the separable functions. For those separable functions, HLXDE1 and HLXDE2 are similar to HLXDE. Therefore, 15 nonseparable functions (i.e., $f3 - f5, F2 - F8$ and $F10 - F14$) are selected for comparison. The results are shown in Table 20, where four DE algorithms (i.e., DE/rand/1, DE/best/2, ODE and SaDE) are used.

From Table 20, it is clear that HLXDE is significantly better than HLXDE1 and HLXDE2 in most cases. HLXDE significantly outperforms HLXDE1 on six functions in the case of DE/rand/1, while HLXDE is significantly better than HLXDE1 on six functions in the case of DE/best/2. In the cases of ODE and SaDE, HLXDE is significantly better than HLXDE1 on six and five functions, respectively. For HLXDE2, HLXDE is significantly better than it on eight, five, seven and eight functions in the cases of DE/rand/1, DE/best/2, ODE and SaDE, respectively. These results indicate that AG is effective for both GbinX and GorthX.

The Friedman test and Wilcoxon's test are also conducted to show the significant differences between the HLXDE variants, and the results are shown in Tables 21 and 22. As Table 21 shows, HLXDE can obtain the best average ranking value by Friedman test in most of the cases except for SaDE. Furthermore, based on the results in Table 22, the significant differences in all the cases between HLXDE and HLXDE2 are observed. It demonstrates that AG is effective for enhancing the performance of OX in HLX. For the comparison between HLXDE and HLXDE1, HLXDE obtains higher $R+$ values than $R-$ values in most cases, which also indicates that AG is useful for GbinX to enhance the search ability of HLXDE.

4.7. Sensitivity to ϵ value

As mentioned in Section 3.2, the threshold value (ϵ) is used to determine the interaction between pairs of variables. If the value of ϵ is large, most pairs of variables would be regarded to be independent of each other. On the contrary, if the value of ϵ is small, most of them would be regarded as being nonseparable. In order to investigate the sensitivity of HLXDE to the ϵ value, the comparisons of HLXDE with the pre-set ϵ value with DE are made. The ϵ value is set as 0.1, 0.5, 0.7 and 0.9 respectively. Then, the Wilcoxon's test is also conducted to show the differences between the HLXDE variants. In this study, the adaptive ϵ value is set as the mean value of all the elements in LM for different functions. According to our preliminary tests, HLXDE with different ϵ values can obtain the similar results for most of the separable functions, therefore 15 nonseparable functions ($f3 - f5, F2 - F8$ and $F10 - F14$) are used for comparison. The results are reported in Table 23 and the average ranking values of the HLXDE variants are also shown in Table 24.

From Table 23, the performance of HLXDE/rand/1 becomes worse with the increase of the ϵ value. Specifically, HLXDE/rand/1 with $\epsilon = 0.1$, 0.5, 0.7 and 0.9 is significantly better than DE/rand/1 on 11, five, two and two functions, respectively, and is worse on one, two, four and seven functions, respectively. On the other hand, HLXDE with adaptive ϵ value is significantly better than HLXDE with $\epsilon = 0.1$, 0.5, 0.7 and 0.9 on five, seven, seven and seven functions, respectively, and is

Table 21
Average ranking values of the HLXDE variants for the nonseparable functions at 30D.

Algorithm	DE/rand/1	DE/best/2	ODE	SaDE
HLXDE1	1.90	1.87	2.00	**1.67**
HLXDE2	2.50	2.43	2.63	2.63
HLXDE	**1.60**	**1.70**	**1.37**	1.70

Table 22
Results of the multi-problem Wilcoxon's test for HLXDE *vs.* the two variants HLXDE1 and HLXDE2 for the nonseparable functions at 30D.

Algorithm		$R+$	$R-$	p-Value	$\alpha = 0.05$	$\alpha = 0.1$
DE/rand/1	HLXDE1	67.5	43.5	3.34E−01	No	No
	HLXDE2	100	20	2.14E−02	Yes	Yes
DE/best/1	HLXDE1	82	38	2.01E−01	No	No
	HLXDE2	91	14	1.40E+01	Yes	Yes
ODE	HLXDE1	104	16	1.15E−02	Yes	Yes
	HLXDE2	90.5	14.5	1.57E−02	Yes	Yes
SaDE	HLXDE1	55.5	64.5	1.00E+00	No	No
	HLXDE2	91.5	13.5	1.32E−02	Yes	Yes

Table 23
Mean and standard deviation of the best error values obtained HLXDE on the selected nonseparable functions at 30*D* with different ϵ values. The ϵ value that is set adaptively for the tested functions are also shown in the last column.

Func.	HLXDE/rand/1								
	$\epsilon = 0.1$		$\epsilon = 0.5$		$\epsilon = 0.7$		$\epsilon = 0.9$		Adaptive ϵ
Yf3	**4.588e−014 ± 1.128e−013**†	–	5.174e−012 ± 2.457e−011†	+	3.503e−011 ± 3.913e−011	+	3.717e−009 ± 3.675e−009‡	+	1.142e−012 ± 3.857e−012 (0.36)†
Yf4	1.484e−003 ± 5.501e−003†	=	1.484e−003 ± 5.501e−003†	=	1.484e−003 ± 5.501e−003†	=	1.484e−003 ± 5.501e−003†	=	1.372e−002 ± 5.243e−002 (0.00)†
Yf5	1.200e−007 ± 3.355e−007‡	+	1.200e−007 ± 3.355e−007‡	+	1.200e−007 ± 3.355e−007‡	+	1.200e−007 ± 3.355e−007‡	+	4.699e−008 ± 1.555e−007 (0.00)‡
F2	**2.134e−006 ± 2.682e−006**†	–	1.063e−005 ± 1.939e−005†	+	1.024e−004 ± 8.839e−005‡	+	1.426e−003 ± 1.211e−003‡	+	8.644e−006 ± 1.299e−005 (0.36)†
F3	**2.763e+005 ± 1.695e+005**†	–	3.586e+005 ± 2.187e+005	=	3.562e+005 ± 1.664e+005	=	6.328e+005 ± 3.774e+005‡	=	3.320e+005 ± 2.167e+005 (0.23)
F4	5.540e−003 ± 9.875e−003†	+	3.913e−002 ± 5.940e−002	=	2.466e−001 ± 4.108e−001‡	+	5.184e−001 ± 5.190e−001‡	+	3.868e−003 ± 7.070e−003 (0.23)†
F5	1.597e+002 ± 1.860e+002†	+	1.451e+002 ± 1.895e+002‡	+	1.109e+002 ± 7.675e+001‡	=	1.415e+002 ± 7.887e+001‡	+	1.216e+002 ± 2.074e+002 (0.27)
F6	3.319e−001 ± 6.334e−001†	+	2.688e+000 ± 2.011e+000	+	3.198e+000 ± 1.704e+000	+	4.533e+000 ± 2.377e+000‡	+	2.353e−001 ± 4.447e−001 (0.036)†
F7	4.696e+003 ± 2.120e−002†	=	4.696e+003 ± 1.751e−002†	=	**4.696e+003 ± 6.665e−003**	–	**4.696e+003 ± 1.298e−003**	–	4.696e+003 ± 2.360e−002 (0.24)†
F8	2.092e+001 ± 6.107e−002	=	2.094e+001 ± 6.397e−002	=	2.094e+001 ± 5.706e−002	=	2.094e+001 ± 5.580e−002	=	2.095e+001 ± 4.622e−002 (0.36)
F10	**1.260e+002 ± 5.208e+001**†	–	1.845e+002 ± 9.235e+000	=	1.838e+002 ± 1.063e+001	=	1.848e+002 ± 1.167e+001	=	1.561e+002 ± 4.725e+001 (0.24)†
F11	**3.498e+001 ± 5.350e+000**†	–	3.940e+001 ± 1.154e+000	+	3.936e+001 ± 1.037e+000	+	3.939e+001 ± 1.132e+000	+	3.829e+001 ± 3.135e+000 (0.22)†
F12	1.331e+003 ± 1.848e+003	=	1.331e+003 ± 1.848e+003	=	1.404e+003 ± 1.895e+003	=	1.368e+003 ± 1.543e+003	=	1.331e+003 ± 1.848e+003 (0.06)
F13	7.552e+000 ± 6.314e−001†	+	7.467e+000 ± 5.839e−001†	+	7.601e+000 ± 6.853e−001†	+	7.850e+000 ± 8.099e−001†	=	7.166e+000 ± 6.639e−001 (0.03)†
F14	1.329e+001 ± 1.463e−001	=	1.326e+001 ± 2.210e−001	=	1.335e+001 ± 1.428e−001	=	1.329e+001 ± 2.100e−001	=	1.332e+001 ± 1.708e−001 (0.05)‡
+/=/−[1]	11/3/1		5/8/2		2/9/4		2/6/7		9/4/2
+/=/−[2]	5/5/5		7/8/0		7/7/1		7/7/1		–
Func.	HLXCoDE								
	$\epsilon = 0.1$		$\epsilon = 0.5$		$\epsilon = 0.7$		$\epsilon = 0.9$		Adaptive ϵ
Yf3	1.612e+002 ± 1.370e+002†	=	1.460e+003 ± 5.748e+002†	+	3.495e+003 ± 8.494e+002†	+	4.529e+003 ± 9.669e+002	+	5.958e+002 ± 3.108e+002(0.36)†
Yf4	**1.027e−001 ± 1.585e−002**‡	–	**1.027e−001 ± 1.585e−002**‡	–	**1.027e−001 ± 1.585e−002**‡	–	**1.027e−001 ± 1.585e−002**‡	–	1.139e−001 ± 2.143e−002 (0.00)‡
Yf5	9.722e+000 ± 4.768e+000‡	+	9.722e+000 ± 4.768e+000‡	+	9.722e+000 ± 4.768e+000‡	+	9.722e+000 ± 4.768e+000‡	+	3.969e+000 ± 2.086e+000 (0.00)
F2	**1.384e+003 ± 8.274e+002**†	–	1.904e+003 ± 5.605e+002†	+	3.096e+003 ± 6.622e+002	+	3.557e+003 ± 9.988e+002	+	1.697e+003 ± 5.918e+002 (0.36)†
F3	**2.148e+007 ± 9.525e+006**†	–	2.640e+007 ± 7.384e+006†	+	2.826e+007 ± 7.530e+006†	=	3.112e+007 ± 7.256e+006	=	2.487e+007 ± 8.727e+006 (0.23)†
F4	**9.229e+003 ± 2.337e+003**	–	9.782e+003 ± 2.482e+003‡	+	1.028e+004 ± 2.397e+003‡	+	**8.862e+003 ± 2.426e+003**	–	9.733e+003 ± 2.280e+003 (0.23)‡
F5	**4.084e+003 ± 6.638e+002**	–	4.159e+003 ± 5.347e+002‡	+	3.926e+003 ± 5.517e+002	+	3.964e+003 ± 5.577e+002	+	3.871e+003 ± 5.887e+002 (0.27)
F6	1.783e+001 ± 1.208e+001†	+	2.154e+001 ± 2.897e+000	+	2.679e+001 ± 1.786e+001‡	+	2.731e+001 ± 1.593e+001‡	+	1.563e+001 ± 1.766e+000 (0.036)†
F7	4.696e+003 ± 0.000e+000	=	4.696e+003 ± 0.000e+000	=	4.696e+003 ± 0.000e+000	=	4.696e+003 ± 0.000e+000	=	4.696e+003 ± 0.000e+000 (0.24)
F8	2.094e+001 ± 1.025e−001	=	2.094e+001 ± 5.629e−002	=	2.097e+001 ± 3.926e−002	=	2.094e+001 ± 4.861e−002	=	2.094e+001 ± 1.040e−001 (0.36)
F10	1.660e+002 ± 1.469e+001†	=	**1.574e+002 ± 1.298e+001**†	–	**1.575e+002 ± 1.394e+001**†	–	**1.564e+002 ± 1.680e+001**†	–	1.649e+002 ± 1.258e+001 (0.24)†
F11	3.255e+001 ± 1.529e+000	=	**3.193e+001 ± 1.291e+000**†	–	**3.194e+001 ± 1.519e+000**†	–	**3.175e+001 ± 1.195e+000**†	–	3.236e+001 ± 1.487e+000 (0.22)
F12	**7.053e+004 ± 1.167e+004**†	–	**7.053e+004 ± 1.167e+004**†	–	**6.865e+004 ± 1.271e+004**†	–	**6.949e+004 ± 1.462e+004**†	–	7.127e+004 ± 1.351e+004 (0.06)†
F13	**4.476e+000 ± 4.464e−001**†	–	**4.505e+000 ± 4.761e−001**†	–	**4.455e+000 ± 3.980e−001**†	–	4.585e+000 ± 3.791e−001†	+	4.554e+000 ± 4.721e−001 (0.03)†
F14	1.315e+001 ± 1.562e−001†	=	1.314e+001 ± 2.223e−001	=	1.308e+001 ± 2.007e−001†	+	1.318e+001 ± 1.468e−001	=	1.307e+001 ± 1.541e−001 (0.05)†
+/=/−[1]	8/5/2		7/4/4		7/4/4		4/8/3		8/5/2
+/=/−[2]	2/6/7		7/3/5		7/3/5		6/4/5		–

+, = and − indicate HLXDE with adaptive ϵ value is significantly better than, equal to and worse than its corresponding competitor by the Wilcoxon test at 5% significance level respectively.
+/=/−[1] indicates the Wilcoxon test results between HLXDE with the preset ϵ value and the corresponding original DE algorithm.
+/=/−[2] indicates the Wilcoxon test results between HLXDE with adaptive ϵ value and HLXDE with the corresponding ϵ value.
‡ The HLXDE variant with different ϵ value is significantly worse than its corresponding DE algorithm by the Wilcoxon test at 5% significance level respectively.
† The HLXDE variant with different ϵ value is significantly better than its corresponding DE algorithm by the Wilcoxon test at 5% significance level respectively.

Table 24
Average ranking values of HLXDE with different ϵ values for the nonseparable functions at 30*D*.

ϵ	HLXDE/rand/1	HLXCoDE
0.1	**2.20**	2.73
0.5	3.03	3.00
0.7	3.37	3.20
0.9	4.03	3.36
Adaptive ϵ	2.36	**2.70**

worse on five, zero, one and one function, respectively. For CoDE, HLXCoDE with $\epsilon = 0.1, 0.5, 0.7$ and 0.9 is significantly better on eight, seven, seven and four functions, respectively, and is worse on two, four, four and three functions, respectively. When compared with HLXCoDE with adaptive ϵ value, HLXCoDE with $\epsilon = 0.1, 0.5, 0.7$ and 0.9 is significantly better on seven, five, five and five functions, respectively, but is worse on two, seven, seven and six functions, respectively. In addition, as Table 24 shows, HLXDE with adaptive ϵ value can obtain the best average ranking value for CoDE and the second best average ranking value for DE/rand/1.

In summary, we can obtain some interesting observations from Tables 23 and 24. First, HLXDE with adaptive ϵ value is significantly better than, or at least comparable to, the HLXDE variant with a pre-set ϵ value for all the test functions. Furthermore, HLXDE with a fixed ϵ value is not always effective for different functions. The adaptive control of ϵ in this study can provide an effective method to alleviate this drawback. Second, due to the fact that each element of *LM* is normalized in [0, 1], the value of ϵ can be set within the range [0, 1]. In contrast, the appropriate ϵ values for different functions in DG may vary greatly [44]. In this sense, the appropriate ϵ value for different functions in HLXDE is easier to be obtained than DG.

4.8. Benefit of randomness in AG

In AG, randomness is introduced to improve the performance of HLXDE. In order to study the effectiveness of randomness in AG, the HLXDE variant without randomness, denoted as HLXDEwoR, is considered. Three DE algorithms, DE/rand/1, DE/best/1 and CoDE, are used for comparison. The comparison results between HLXDE and HLXDEwoR on 15 nonseparable functions are shown in Table 25. In addition, the Wilcoxon's test is also conducted to show the significant differences between them, and the results are reported in Table 26.

From Table 25, it is clear that HLXDE is significantly better than HLXDEwoR in all the cases. Specifically, for DE/rand/1, HLXDE is better than HLXDEwoR on six functions and is worse on five functions. For DE/best/1 and CoDE, HLXDE is better than HLXDEwoR on six and seven functions, respectively, and is worse on one and four functions, respectively. Furthermore, as Table 26 shows, HLXDE obtains higher $R+$ values than $R-$ values in all the cases. These results indicate that the randomness in AG can bring benefit to HLXDE for these test functions. The reason may lie in the fact that AG with different order of components will identify different grouping structures at different search stages. As stated in [7], the configuration of BBs may dynamically change along with the search stages. In addition, HLXDE with an improper ϵ value will generate an inappropriate fixed grouping. The randomness in AG can alleviate this drawback by generating dynamical grouping structures.

Overall, the randomness introduced in AG is beneficial for HLXDE when solving the nonseparable functions.

4.9. Scalability study

To better understand the scalability of HLX, HLXDE is tested on the functions $f1 - f13$ at 100*D* and 200*D* first. Then, a suite of 11 benchmark functions at 1000*D* from the CEC 2012 special session on large-scale global optimization [60] is used to further study the performance of HLXDE for the higher-dimensional problems.

4.9.1. Performance on $f1 - f13$ at 100D and 200D

In this subsection, the first 13 benchmark functions $f1 - f13$ are scalable and thus are selected for the scalability study. The dimensions are scaled to 100*D* and 200*D*. Here, four DE algorithms, DE/rand/2, DE/best/1, ODE and SaDE are used for comparison. For all the compared algorithms, *NP* is set to $4 \times D$ and *MNFES* is set to $D \times 50000$. All the other parameters are kept unchanged as described in Section 4.1. The results for these functions at 100*D* and 200*D* are shown in Tables 27 and 28, respectively. Furthermore, the results of the multi-problem Wilcoxon signed-rank tests at $\alpha = 0.05$ and $\alpha = 0.1$ are also shown in Table 29.

From Tables 27 and 28, it is clear that HLXDE can obtain significantly better results than the corresponding DE algorithm on most test functions at 100*D* and 200*D*. Specifically, HLXDE is significantly better than the corresponding DE/rand/2, DE/best/1 and SaDE on 12, 11 and 8 functions at 100*D*, respectively. For functions at 200*D*, HLXDE significantly outperforms the corresponding DE/rand/2, DE/best/1 and SaDE on 12, 11 and 11 functions, respectively. In the case of ODE, HLXDE is significantly outperformed by ODE on 10 functions at 100*D*, while significantly outperforming it on 11 functions at 200*D*. The results of the multi-problem Wilcoxon's test in Table 29 also show HLXDE can obtain higher $R+$ values than $R-$ values in most cases. In addition, the significant differences in most cases between HLXDE and the corresponding DE algorithm are also observed. Therefore, these results of Tables 27–29 indicate that HLX is effective for DE in solving the high-dimensional problems.

Table 25
Mean and standard deviation of the best error values obtained by HLXDE and the corresponding variants without introducing random in the grouping operator (denoted as HLXDEwoR) on the selected nonseparable functions at 30*D*.

Func.	HLXDEwoR/rand/1	HLXDE/rand/1	HLXDEwoR/best/1	HLXDE/best/1	HLXCoDEwoR	HLXCoDE
Yf3	**4.111e−013 ± 6.428e−013**[‡]	1.142e−012 ± 3.857e−012	2.130e+003 ± 1.144e+003[†]	**1.848e+003 ± 1.165e+003**	**7.180e+000 ± 2.684e+000**[‡]	5.958e+002 ± 3.108e+002
Yf4	2.216e−003 ± 6.631e−003	1.372e−002 ± 5.243e−002	2.253e+001 ± 4.626e+000	2.319e+001 ± 5.017e+000	**1.061e−001 ± 1.832e−002**[‡]	1.139e−001 ± 2.143e−002
Yf5	1.241e−007 ± 6.363e−007	4.699e−008 ± 1.555e−007	8.391e+005 ± 1.322e+006[†]	**1.393e+004 ± 2.404e+004**	6.836e+002 ± 3.915e+002[†]	**3.969e+000 ± 2.086e+000**
F2	2.533e−005 ± 4.547e−005[†]	**8.644e−006 ± 1.299e−005**	6.971e+003 ± 3.347e+003[†]	**5.729e+003 ± 2.946e+003**	1.826e+003 ± 6.291e+002[†]	**1.697e+003 ± 5.918e+002**
F3	**2.942e+005 ± 1.582e+005**[‡]	3.320e+005 ± 2.167e+005	**1.108e+007 ± 7.449e+006**[‡]	1.318e+007 ± 1.075e+007	2.761e+007 ± 8.258e+006	2.487e+007 ± 8.727e+006
F4	6.493e−002 ± 2.309e−001[†]	**3.868e−003 ± 7.070e−003**	5.394e+002 ± 5.802e+002[†]	**3.420e+002 ± 4.169e+002**	**9.155e+003 ± 2.782e+003**[‡]	9.733e+003 ± 2.280e+003
F5	2.334e+002 ± 2.069e+002[†]	**1.216e+002 ± 2.074e+002**	8.744e+003 ± 2.187e+003	7.970e+003 ± 2.016e+003	4.264e+003 ± 7.316e+002[†]	**3.871e+003 ± 5.887e+002**
F6	2.809e+000 ± 1.579e+000[†]	**2.353e−001 ± 4.447e−001**	8.965e+007 ± 1.432e+008	6.955e+007 ± 9.728e+007	1.962e+001 ± 1.726e+000[†]	**1.563e+001 ± 1.766e+000**
F7	4.696e+003 ± 1.413e−002[†]	**4.696e+003 ± 2.360e−002**	4.731e+003 ± 6.416e+000	4.728e+003 ± 9.926e+000	4.696e+003 ± 0.000e+000	4.696e+003 ± 0.000e+000
F8	**2.093e+001 ± 5.387e−002**[‡]	2.095e+001 ± 4.622e−002	2.100e+001 ± 5.595e−002[†]	**2.096e+001 ± 5.824e−002**	2.093e+001 ± 5.604e−002	2.094e+001 ± 1.040e−001
F10	**1.377e+002 ± 4.961e+001**[‡]	1.561e+002 ± 4.725e+001	1.529e+002 ± 3.230e+001	1.444e+002 ± 3.433e+001	1.828e+002 ± 1.397e+001[†]	**1.649e+002 ± 1.258e+001**
F11	3.837e+001 ± 3.630e+000	3.829e+001 ± 3.135e+000	2.198e+001 ± 2.917e+000	2.230e+001 ± 2.974e+000	3.250e+001 ± 1.249e+000[†]	**3.236e+001 ± 1.487e+000**
F12	1.925e+003 ± 2.303e+003[†]	**1.331e+003 ± 1.848e+003**	9.774e+004 ± 5.064e+004[†]	**8.558e+004 ± 3.714e+004**	7.152e+004 ± 1.264e+004[†]	**7.127e+004 ± 1.351e+004**
F13	**6.910e+000 ± 6.191e−001**[‡]	7.166e+000 ± 6.639e−001	5.216e+000 ± 1.223e+000	6.071e+000 ± 1.776e+000	**4.413e+000 ± 4.345e−001**[‡]	4.554e+000 ± 4.721e−001
F14	1.336e+001 ± 1.306e−001	1.332e+001 ± 1.708e−001	1.181e+001 ± 5.779e−001	1.181e+001 ± 6.150e−001	1.311e+001 ± 1.873e−001	1.307e+001 ± 1.541e−001
w/t/l	6/4/5	–	6/8/1	–	7/4/4	–

[†] HLXDE is significantly better than its corresponding HLXDEwoR by the Wilcoxon test at 5% significance level respectively.
[‡] HLXDE is significantly worse than its corresponding HLXDEwoR by the Wilcoxon test at 5% significance level respectively.

Table 26
Results of the multi-problem Wilcoxon's test for HLXDE *vs.* HLXDEwoR for the selected nonseparable functions at 30*D*.

Algorithm	$R+$	$R-$	*p*-Value	$\alpha = 0.05$	$\alpha = 0.1$
HLXDE/rand/1 *vs.* HLXDEwoR/rand/1	61	44	5.72E−01	No	No
HLXDE/best/1 *vs.* HLXDEwoR/best/1	83	22	5.70E−02	No	Yes
HLXCoDE *vs.* HLXCoDEwoR	74	31	1.90E−01	No	No

Table 27
Mean and standard deviation of the best error values obtained by DE/rand/2, DE/best/1, ODE, SaDE and their corresponding HLXDE variants on the functions $f1-f13$ at 100*D*.

Func.	DE/rand/2	HLXDE/rand/2	DE/best/1	HLXDE/best/1
f1	1.126e+005 ± 5.364e+003†	**6.295e+002 ± 1.119e+002**	2.441e+004 ± 4.045e+003†	**1.493e+003 ± 9.303e+002**
f2	8.755e+020 ± 2.806e+021†	**9.900e+002 ± 0.000e+000**	1.062e+002 ± 1.369e+001†	**6.677e+001 ± 1.453e+001**
f3	2.658e+005 ± 2.057e+004†	**2.291e+005 ± 1.831e+004**	**8.205e+003 ± 2.870e+003**‡	1.384e+004 ± 4.553e+003
f4	7.952e+001 ± 1.496e+000	7.880e+001 ± 1.786e+000	4.084e+001 ± 3.088e+000	3.976e+001 ± 2.795e+000
f5	2.918e+008 ± 3.201e+007†	**2.340e+005 ± 4.207e+004**	2.014e+007 ± 7.129e+006†	**2.547e+005 ± 2.058e+005**
f6	1.125e+005 ± 5.552e+003†	**6.644e+002 ± 1.506e+002**	2.715e+004 ± 3.054e+003†	**2.292e+003 ± 8.414e+002**
f7	3.946e+002 ± 2.627e+001†	**6.774e+000 ± 5.117e+000**	1.778e+000 ± 1.738e+000†	**1.583e−001 ± 2.048e−001**
f8	3.248e+004 ± 4.532e+002†	**1.229e+004 ± 9.185e+002**	2.398e+004 ± 9.723e+002†	**1.466e+004 ± 2.144e+003**
f9	1.188e+003 ± 1.480e+001†	**2.811e+002 ± 2.688e+001**	4.033e+002 ± 4.227e+001†	**1.722e+002 ± 3.840e+001**
f10	1.946e+001 ± 1.284e−001†	**6.665e+000 ± 2.353e−001**	1.401e+001 ± 5.337e−001†	**7.665e+000 ± 8.376e−001**
f11	1.014e+003 ± 4.828e+001†	**6.665e+000 ± 1.007e+000**	2.210e+002 ± 3.669e+001†	**1.444e+001 ± 8.373e+000**
f12	4.987e+008 ± 6.708e+007†	**8.516e+000 ± 1.218e+000**	4.914e+006 ± 2.455e+006†	**8.775e+002 ± 3.686e+003**
f13	1.069e+009 ± 1.192e+008†	**1.144e+002 ± 9.974e+001**	3.417e+007 ± 1.375e+007†	**7.932e+004 ± 1.376e+005**
w/t/l	12/1/0	–	11/1/1	–
Func.	ODE	HLXODE	SaDE	HLXSaDE
f1	**4.091e−006 ± 4.795e−006**‡	8.194e−003 ± 3.897e−003	3.184e−009 ± 1.099e−009†	**3.180e−011 ± 1.535e−011**
f2	**1.099e−001 ± 3.695e−002**‡	9.131e−001 ± 2.648e−001	1.557e−006 ± 2.611e−007	1.293e−006 ± 2.630e−007
f3	**1.868e+004 ± 7.203e+003**‡	3.110e+004 ± 9.247e+003	6.216e+003 ± 9.955e+002†	**3.527e+003 ± 7.916e+002**
f4	**3.751e−010 ± 3.005e−010**‡	4.029e−003 ± 3.087e−003	**4.941e+000 ± 1.104e+000**‡	5.261e+000 ± 1.091e+000
f5	**9.496e+001 ± 5.836e−001**‡	9.671e+001 ± 3.601e−001	**1.767e+002 ± 5.292e+001**‡	1.795e+002 ± 5.623e+001
f6*	6.667e−002 ± 2.537e−001	0.000e+000 ± 0.000e+000	[159,453 ± 16752.472]	[157,131 ± 6607.832]
f7	**5.193e−003 ± 1.558e−003**‡	1.347e−002 ± 3.627e−003	2.017e−002 ± 4.233e−003	1.802e−002 ± 3.474e−003
f8	3.261e+004 ± 3.521e+002†	**1.740e+004 ± 1.239e+003**	1.100e+004 ± 1.617e+003†	**4.824e+003 ± 1.040e+003**
f9	5.554e+002 ± 1.267e+002†	**1.589e+002 ± 3.263e+001**	2.499e+002 ± 3.138e+001†	**7.806e+001 ± 1.163e+001**
f10	**1.172e−003 ± 6.595e−004**‡	3.937e−002 ± 1.617e−002	5.868e−006 ± 1.381e−006†	**8.632e−007 ± 2.684e−007**
f11	**5.551e−004 ± 1.993e−003**‡	1.770e−002 ± 1.622e−002	1.396e−003 ± 3.699e−003†	**2.288e−011 ± 1.061e−011**
f12	**3.323e−008 ± 3.507e−008**‡	1.031e−004 ± 1.036e−004	9.322e−012 ± 8.356e−012†	**1.212e−013 ± 5.887e−014**
f13	**3.849e−007 ± 3.199e−007**‡	6.166e−004 ± 4.074e−004	3.662e−004 ± 2.006e−003†	**7.758e−012 ± 3.212e−012**
w/t/l	2/1/10	–	8/3/2	–

* HLXDE and the competitor can obtain the equal optimum value within *MNFES* and *NFES* required to achieve the accuracy level is also shown in square brackets.
‡ HLXDE is significantly worse than its corresponding competitor by the Wilcoxon test at 5% significance level respectively.
† HLXDE is significantly better than its corresponding competitor by the Wilcoxon test at 5% significance level respectively.

4.9.2. Performance on the CEC 2012 optimization problems

A suite of 11 benchmark functions at 1000*D* from the CEC 2012 special session on large-scale global optimization [60] are used here, namely, Shifted Elliptic Function (*LF*1), Shifted Rastrigin's Function (*LF*2), Shifted Ackley's Function (*LF*3), Shifted m-dimensional Schwefel's Problem 1.2 with Single-group (*LF*7), $D/2m$-group (*LF*17) and fully-nonseparable (*LF*19) and Shifted m-dimensional Rosenbrock's Function with Single-group (*LF*8), $D/2m$-group (*LF*18) and fully-nonseparable (*LF*20). The first three functions are used to test the effectiveness of HLX for separable functions and the last eight functions are used to test the effectiveness of HLX for the same function with different degrees of separability. The details can be found in [60]. Here, 25 independent runs are performed for each problem and the maximum number of fitness evaluations is set to 3×10^6 as suggested in [60]. Furthermore, in order to evaluate the influence of grouping, DG is also incorporated into HLX to replace AG. The new HLXDE variant is named as HLXDE-DG. In HLXDE-DG, the value of ϵ is set to 10^{-3}, as suggested in [44]. Four DE algorithms (DE/rand/1, DE/best/1, ODE and CoDE) with different population sizes ($NP = 100$ and 500) are used to provide a deeper analysis. The results are shown in Tables 30 and 31. Additionally, the number of groups decomposed by HLXDE and HLXDE-DG, as well as the real number of groups, are also shown in Table 32.

From the results with $NP = 100$ in Table 30, for the separable functions (i.e., $LF1-LF3$), HLXDE is significantly better than DE in all the cases. For the Schwefel's Problem 1.2 with different degrees of separability (i.e., $LF7, LF12, LF17$ and $LF19$), HLXDE significantly outperforms DE/rand/1 and ODE on no functions and is outperformed by them on three and four

Table 28
Mean and standard deviation of the best error values obtained by DE/rand/2, DE/best/1, ODE, SaDE and their corresponding HLXDE variants on the functions $f1-f13$ at 200*D*.

Func.	DE/rand/2	HLXDE/rand/2	DE/best/1	HLXDE/best/1
f1	3.195e+005 ± 8.486e+003†	**1.149e+004 ± 2.087e+003**	9.301e+004 ± 9.096e+003†	**4.096e+003 ± 1.646e+003**
f2	1.157e+061 ± 4.946e+061†	**1.990e+003 ± 0.000e+000**	2.978e+002 ± 2.497e+001†	**2.321e+002 ± 3.799e+001**
f3	1.053e+006 ± 6.616e+004†	**8.606e+005 ± 6.529e+004**	**9.468e+003 ± 2.995e+003**‡	5.012e+004 ± 8.226e+003
f4	8.917e+001 ± 8.440e−001	8.806e+001 ± 1.042e+000	**4.852e+001 ± 2.628e+000**‡	4.896e+001 ± 3.681e+000
f5	1.044e+009 ± 5.101e+007†	**6.714e+006 ± 1.356e+006**	9.916e+007 ± 1.480e+007†	**1.377e+006 ± 7.418e+005**
f6	3.173e+005 ± 1.066e+004†	**1.164e+004 ± 2.232e+003**	9.740e+004 ± 9.613e+003†	**6.053e+003 ± 2.164e+003**
f7	3.049e+003 ± 1.440e+002†	**1.017e+001 ± 3.815e+000**	1.161e+002 ± 3.049e+001†	**3.956e−001 ± 3.080e−001**
f8	7.018e+004 ± 5.336e+002†	**3.218e+004 ± 2.050e+003**	5.621e+004 ± 1.364e+003†	**3.791e+004 ± 4.035e+003**
f9	2.661e+003 ± 2.816e+001†	**8.028e+002 ± 6.211e+001**	1.110e+003 ± 7.673e+001†	**3.769e+002 ± 5.375e+001**
f10	2.016e+001 ± 8.101e−002†	**1.212e+001 ± 3.820e−001**	1.624e+001 ± 2.991e−001†	**7.655e+000 ± 5.709e−001**
f11	2.876e+003 ± 7.637e+001†	**1.044e+002 ± 1.878e+001**	8.373e+002 ± 8.301e+001†	**3.784e+001 ± 1.480e+001**
f12	2.149e+009 ± 1.053e+008†	**9.380e+004 ± 1.154e+005**	6.074e+007 ± 2.556e+007†	**2.510e+004 ± 5.408e+004**
f13	4.293e+009 ± 2.055e+008†	**2.004e+006 ± 1.108e+006**	2.524e+008 ± 7.154e+007†	**5.328e+005 ± 5.587e+005**
w/t/l	12/1/0	–	11/0/2	–
Func.	ODE	HLXODE	SaDE	HLXSaDE
f1	2.243e−001 ± 1.221e−001†	**2.614e−005 ± 2.344e−005**	2.368e−003 ± 4.177e−004†	**4.555e−006 ± 1.540e−006**
f2	2.417e+000 ± 4.386e−001†	**3.528e−002 ± 1.170e−002**	2.670e−003 ± 2.323e−004†	**5.496e−004 ± 1.033e−004**
f3	7.060e+004 ± 2.885e+004	6.113e+004 ± 2.067e+004	4.229e+004 ± 5.876e+003†	**2.342e+004 ± 4.464e+003**
f4	**3.722e−008 ± 2.290e−008**‡	7.942e−006 ± 6.352e−006	9.358e+000 ± 9.669e−001	9.530e+000 ± 8.325e−001
f5	1.968e+002 ± 7.965e−001†	**1.942e+002 ± 2.667e−001**	7.434e+002 ± 1.051e+002†	**6.263e+002 ± 7.563e+001**
f6	6.800e+000 ± 1.057e+001†	**0.000e+000 ± 0.000e+000**	1.333e−001 ± 3.457e−001	1.500e−001 ± 3.663e−001
f7	1.199e−002 ± 3.463e−003†	**9.184e−003 ± 2.021e−003**	9.493e−002 ± 1.564e−002†	**7.691e−002 ± 1.379e−002**
f8	7.038e+004 ± 5.273e+002†	**3.408e+004 ± 1.753e+003**	3.844e+004 ± 6.769e+002†	**2.254e+004 ± 2.140e+003**
f9	9.603e+002 ± 4.516e+002†	**1.896e+002 ± 4.533e+001**	7.729e+002 ± 2.323e+001†	**2.801e+002 ± 4.450e+001**
f10	3.099e−001 ± 2.078e−001†	**6.858e−004 ± 3.216e−004**	1.726e+000 ± 1.743e−001†	**2.666e−004 ± 8.797e−005**
f11	1.186e−001 ± 1.083e−001†	**5.157e−005 ± 1.132e−004**	1.195e−003 ± 2.207e−003†	**4.948e−004 ± 2.204e−003**
f12	1.312e−004 ± 1.005e−004†	**3.007e−008 ± 3.401e−008**	3.122e−003 ± 7.538e−003†	**1.555e−003 ± 4.786e−003**
f13	2.089e−002 ± 3.149e−002†	**1.143e−006 ± 1.434e−006**	1.804e−003 ± 3.754e−003†	**5.505e−004 ± 2.457e−003**
w/t/l	11/1/1	–	11/2/0	–

‡ HLXDE is significantly worse than its corresponding competitor by the Wilcoxon test at 5% significance level respectively.
† HLXDE is significantly better than its corresponding competitor by the Wilcoxon test at 5% significance level respectively.

Table 29
Results of the multi-problem Wilcoxon's test for DE/rand/2, DE/best/1, ODE, SaDE and their corresponding HLXDE variants on the functions $f1-f13$ at 100*D* and 200*D*, respectively.

Algorithm at 100*D*	$R+$	$R-$	*p*-Value	$\alpha = 0.05$	$\alpha = 0.1$
HLXDE/rand/2 *vs.* DE/rand/2	91	0	2.44E−04	Yes	Yes
HLXDE/best/1 *vs.* DE/best/1	84	7	4.64E−03	Yes	Yes
HLXODE *vs.* ODE	32	59	3.28E−01	No	No
HLXSaDE *vs.* SaDE	74	17	4.79E−02	Yes	Yes
Algorithm at 200*D*	$R+$	$R-$	*p*-Value	$\alpha = 0.05$	$\alpha = 0.1$
HLXDE/rand/2 *vs.* DE/rand/2	91	0	2.44E−04	Yes	Yes
HLXDE/best/1 *vs.* DE/best/1	82	9	8.06E−03	Yes	Yes
HLXODE *vs.* ODE	90	1	4.88E−04	Yes	Yes
HLXSaDE *vs.* SaDE	77	14	2.66E−02	Yes	Yes

functions, respectively, while HLXDE is significantly better than DE/best/1 and CoDE on four and one function, respectively. For the Rosenbrock's function with different degrees of separability (*LF*8, *LF*13, *LF*18 and *LF*20), HLXDE is significantly better than DE/rand/1, DE/best/1, ODE and CoDE on four, four, four and three functions, respectively. As we can see from Table 30, the performance of HLXDE-DG with $NP = 100$ is similar to HLXDE overall. For the results with $NP = 500$ in Table 31, the performances of HLXDE and HLXDE-DG become worse than those with $NP = 100$.

In order to further compare HLXDE with HLXDE-DG, the Wilcoxon signed-rank test at $\alpha = 0.05$ is conducted and summarized in the last row of Tables 30 and 31. HLXDE with $NP = 100$ significantly outperforms HLXDE-DG in 18 cases and is outperformed in 14 cases, while HLXDE with $NP = 500$ is significantly better than HLXDE-DG in 17 cases and is worse in 10 cases. Based on the average number of groups in Table 32, it is interesting to find that HLXDE-DG does not significantly outperform HLXDE in most cases with the correct number of groups (i.e., *LF*12, *LF*17 and *LF*19 in Table 32). In most cases with incorrect number of groups, HLXDE-DG is significantly worse than HLXDE.

Table 30
Mean and standard deviation of the best error values obtained by DE, HLXDE-DG and HLXDE on the CEC2012 functions at 1000D with $NP = 100$. The comparison results between HLXDE and MA-SW-Chains are shown.

Func.	DE/rand/1	HLXDE/rand/1-DG		HLXDE/rand/1	MA-SW-Chains [37]
LF1	1.352e+006 ± 1.398e+006	**1.216e−014 ± 8.432e−015**[†]	=	2.217e−014 ± 1.165e−014[†]	2.10e−014 ± 1.99e−014
LF2	4.824e+003 ± 1.372e+002	4.989e−004 ± 8.986e−004[†]	=	**2.204e−004 ± 1.660e−004**[†]	8.10e+002 ± 5.88e+001[**]
LF3	1.660e+001 ± 3.078e−001	2.690e−009 ± 1.080e−009[†]	=	**2.480e−009 ± 9.521e−010**[†]	7.28e−013 ± 3.40e−013[*]
LF7	**1.537e+005 ± 5.060e+004**	4.188e+005 ± 4.528e+004[‡]	−	7.790e+008 ± 2.366e+008[‡]	1.03e+002 ± 8.70e+001[*]
LF8	4.636e+007 ± 1.273e+007	**3.249e+007 ± 2.912e+006**[†]	−	4.463e+007 ± 1.450e+007[†]	1.41e+007 ± 3.68e+007[*]
LF12	**1.396e+005 ± 1.374e+004**	2.537e+006 ± 1.352e+005[‡]	−	5.091e+006 ± 2.982e+005[‡]	3.62e−006 ± 5.92e−007[*]
LF13	1.334e+006 ± 5.670e+006	2.165e+007 ± 1.381e+007[‡]	+	**2.497e+003 ± 2.577e+003**[†]	1.25e+003 ± 5.72e+002
LF17	**4.243e+005 ± 1.802e+004**	6.978e+005 ± 2.847e+004[‡]	−	1.483e+007 ± 1.066e+006[‡]	1.24e+000 ± 1.25e−001[*]
LF18	1.917e+008 ± 3.496e+008	1.262e+009 ± 5.754e+008[‡]	+	**2.876e+004 ± 3.896e+004**[†]	1.30e+003 ± 4.36e+002[*]
LF19	5.620e+006 ± 7.085e+005	**1.593e+006 ± 8.947e+004**[†]	−	3.189e+007 ± 1.793e+006[‡]	2.85e+005 ± 1.78e+004[*]
LF20	1.192e+008 ± 2.316e+008	2.978e+010 ± 5.779e+009[‡]	+	**9.697e+002 ± 2.307e+002**[†]	1.07e+003 ± 7.29e+001[**]
$+/=/-^1$	–	5/0/6		7/0/4	–
$+/=/-^2$		3/3/5		–	–
Func.	DE/best/1	HLXDE/best/1-DG		HLXDE/best/1	MA-SW-Chains [37]
LF1	1.319e+011 ± 1.107e+010	**1.499e+009 ± 2.400e+009**[†]	=	2.107e+009 ± 2.435e+009[†]	2.10e−014 ± 1.99e−014[*]
LF2	1.679e+004 ± 2.943e+002	3.626e+003 ± 5.222e+002[†]	=	**3.574e+003 ± 6.430e+002**[†]	8.10e+002 ± 5.88e+001[*]
LF3	2.097e+001 ± 3.661e−002	1.565e+001 ± 1.223e+000[†]	=	**1.537e+001 ± 1.155e+000**[†]	7.28e−013 ± 3.40e−013[*]
LF7	2.557e+010 ± 1.134e+010	3.080e+010 ± 8.704e+009[‡]	+	**2.402e+010 ± 6.858e+009**[†]	1.03e+002 ± 8.70e+001[*]
LF8	5.201e+015 ± 2.196e+015	4.577e+015 ± 2.208e+015[†]	+	**8.122e+014 ± 6.964e+014**[†]	1.41e+007 ± 3.68e+007[*]
LF12	6.518e+006 ± 5.583e+005	3.470e+006 ± 4.297e+005[†]	+	**2.574e+006 ± 7.140e+005**[†]	3.62e−006 ± 5.92e−007[*]
LF13	1.080e+012 ± 9.180e+010	9.229e+011 ± 9.180e+010[†]	+	**3.255e+006 ± 1.126e+007**[†]	1.25e+003 ± 5.72e+002[*]
LF17	1.144e+007 ± 6.363e+005	7.839e+006 ± 9.013e+005[†]	+	**4.398e+006 ± 1.029e+006**[†]	1.24e+000 ± 1.25e−001[*]
LF18	2.752e+012 ± 1.634e+011	2.119e+012 ± 1.246e+011[†]	+	**6.355e+005 ± 5.165e+005**[†]	1.30e+003 ± 4.36e+002[*]
LF19	1.185e+007 ± 1.762e+006	1.297e+007 ± 1.935e+006[†]	+	**7.404e+006 ± 9.025e+005**[†]	2.85e+005 ± 1.78e+004[*]
LF20	2.833e+012 ± 1.391e+011	2.023e+012 ± 1.414e+011[†]	+	**1.048e+006 ± 9.923e+005**[†]	1.07e+003 ± 7.29e+001[*]
$+/=/-^1$	–	10/0/1		11/0/0	–
$+/=/-^2$		8/3/0		–	–
Func.	ODE	HLXODE-DG		HLXODE	MA-SW-Chains [37]
LF1	7.092e+007 ± 1.615e+008	8.192e−021 ± 7.039e−021[†]	=	**7.965e−021 ± 7.662e−021**[†]	2.10e−014 ± 1.99e−014[**]
LF2	5.870e+003 ± 2.071e+002	1.061e−004 ± 2.928e−004[†]	=	**2.248e−005 ± 3.401e−005**[†]	8.10e+002 ± 5.88e+001[**]
LF3	1.907e+001 ± 2.441e−001	**4.396e−013 ± 5.439e−013**[†]	=	1.001e−012 ± 1.222e−012[†]	7.28e−013 ± 3.40e−013
LF7	6.417e+005 ± 3.638e+005	**4.362e+005 ± 4.868e+004**[†]	−	6.238e+008 ± 3.156e+008[‡]	1.03e+002 ± 8.70e+001[*]
LF8	1.740e+010 ± 3.684e+010	7.919e+009 ± 3.047e+010[†]	+	**3.890e+007 ± 7.863e+005**[†]	1.41e+007 ± 3.68e+007[*]
LF12	**1.634e+005 ± 1.442e+004**	2.638e+006 ± 1.196e+005[‡]	−	5.107e+006 ± 2.539e+005[‡]	3.62e−006 ± 5.92e−007[*]
LF13	1.244e+009 ± 1.546e+009	2.670e+009 ± 1.277e+009[‡]	+	**7.785e+002 ± 7.186e+002**[†]	1.25e+003 ± 5.72e+002
LF17	**3.708e+005 ± 2.529e+004**	8.358e+005 ± 3.387e+004[‡]	−	1.529e+007 ± 9.463e+005[‡]	1.24e+000 ± 1.25e−001[*]
LF18	5.888e+009 ± 2.903e+009	1.141e+010 ± 4.722e+009[‡]	+	**7.408e+003 ± 1.188e+004**[†]	1.30e+003 ± 4.36e+002
LF19	6.620e+006 ± 1.275e+006	**1.786e+006 ± 6.351e+004**[†]	−	3.082e+007 ± 1.844e+006[‡]	2.85e+005 ± 1.78e+004[*]
LF20	8.525e+009 ± 4.880e+009	4.606e+010 ± 1.322e+010[‡]	+	**1.917e+003 ± 1.097e+002**[†]	1.07e+003 ± 7.29e+001[*]
$+/=/-^1$	–	6/0/5		7/0/4	–
$+/=/-^2$		4/3/4		–	–
Func.	CoDE	HLXCoDE-DG		HLXCoDE	MA-SW-Chains [37]
LF1	1.584e+010 ± 3.201e+008	**2.401e+000 ± 4.726e−001**[†]	=	2.856e+000 ± 8.721e−001[†]	2.10e−014 ± 1.99e−014[*]
LF2	1.460e+004 ± 8.856e+001	**1.453e+000 ± 3.479e−001**[†]	=	1.874e+000 ± 7.520e−001[†]	8.10e+002 ± 5.88e+001[**]
LF3	2.072e+001 ± 2.995e−002	**2.113e−002 ± 4.255e−003**[†]	=	2.114e−002 ± 2.438e−003[†]	7.28e−013 ± 3.40e−013[*]
LF7	**2.130e+010 ± 2.288e+009**	3.160e+010 ± 4.503e+009[‡]	−	4.997e+010 ± 5.679e+009[‡]	1.03e+002 ± 8.70e+001[*]
LF8	**4.616e+007 ± 1.345e+006**	7.848e+007 ± 1.884e+007[‡]	−	1.952e+008 ± 3.938e+007[‡]	1.41e+007 ± 3.68e+007[*]
LF12	8.545e+006 ± 3.058e+005	**3.606e+006 ± 2.124e+005**[†]	−	6.427e+006 ± 2.556e+005	3.62e−006 ± 5.92e−007[*]
LF13	1.528e+011 ± 8.063e+009	9.933e+010 ± 4.050e+009	+	**7.018e+004 ± 1.519e+004**[†]	1.25e+003 ± 5.72e+002
LF17	1.738e+007 ± 5.646e+005	**5.620e+006 ± 1.495e+005**[†]	−	1.682e+007 ± 6.815e+005[†]	1.24e+000 ± 1.25e−001[***]
LF18	1.198e+012 ± 2.901e+010	5.072e+011 ± 1.286e+010[†]	+	**2.566e+005 ± 4.086e+004**[†]	1.30e+003 ± 4.36e+002[*]
LF19	**2.784e+007 ± 1.757e+006**	3.065e+007 ± 1.530e+006[‡]	−	3.249e+007 ± 2.178e+006[‡]	2.85e+005 ± 1.78e+004[*]
LF20	1.252e+012 ± 3.603e+010	5.964e+011 ± 1.419e+010[†]	+	**1.548e+004 ± 2.036e+003**[†]	1.07e+003 ± 7.29e+001[*]
$+/=/-^1$	-	7/1/3		7/1/3	–
$+/=/-^2$		3/3/5		–	–

+, = and − indicate HLXDE is significantly better than, equal to and worse than its corresponding HLXDE-DG by the Wilcoxon test at 5% significance level respectively.
$+/=/-^1$ indicates the Wilcoxon test results between the HLXDE variant and the corresponding original DE algorithm.
$+/=/-^2$ indicates the Wilcoxon test results between HLXDE and HLXDE-DG.
‡ The HLXDE variant is significantly worse than its corresponding DE algorithm by the Wilcoxon test at 5% significance level respectively.
* HLXDE with $NP = 100$ is significantly worse than MA-SW-Chains by a two tailed unpaired t-test at $\alpha = 0.05$ respectively.
† The HLXDE variant is significantly better than its corresponding DE algorithm by the Wilcoxon test at 5% significance level respectively.
** HLXDE with $NP = 100$ is significantly better than MA-SW-Chains by a two tailed unpaired t-test at $\alpha = 0.05$ respectively.

Table 31
Mean and standard deviation of the best error values obtained by DE, HLXDE-DG and HLXDE on the CEC2012 functions at 1000D with $NP = 500$.

Func.	DE/rand/1	HLXDE/rand/1-DG		HLXDE/rand/1
LF1	3.478e+008 ± 2.928e+007	**3.706e+006 ± 3.197e+005**†	=	4.311e+006 ± 9.160e+005†
LF2	1.265e+004 ± 1.192e+002	**2.209e+003 ± 1.446e+002**†	=	2.263e+003 ± 1.960e+002†
LF3	1.435e+001 ± 1.511e−001	**4.562e+000 ± 1.149e−001**†	=	4.817e+000 ± 1.323e−001†
LF7	2.529e+009 ± 4.411e+008	**3.228e+006 ± 3.259e+005**†	−	1.208e+010 ± 6.398e+008‡
LF8	**4.522e+007 ± 6.413e+005**	4.633e+007 ± 5.072e+005	−	4.453e+008 ± 6.730e+007‡
LF12	**4.981e+006 ± 3.197e+005**	5.422e+006 ± 3.496e+005	−	7.357e+006 ± 2.732e+005
LF13	2.082e+008 ± 6.057e+007	7.613e+009 ± 2.266e+009‡	+	**1.523e+006 ± 4.909e+005**†
LF17	**8.260e+006 ± 7.450e+005**	1.014e+007 ± 2.618e+005‡	=	1.865e+007 ± 2.018e+006‡
LF18	2.085e+010 ± 1.358e+009	8.676e+010 ± 7.310e+009	+	**1.675e+007 ± 2.031e+006**†
LF19	3.170e+007 ± 1.436e+006	**2.421e+007 ± 6.257e+006**	−	3.536e+007 ± 1.209e+006
LF20	2.331e+010 ± 3.170e+009	1.744e+011 ± 1.367e+010‡	+	**2.009e+007 ± 2.433e+006**†
$+/=/-^1$	–	4/4/3		6/2/3
$+/=/-^2$		3/4/4		–
Func.	DE/best/1	HLXDE/best/1-DG		HLXDE/best/1
LF1	8.881e+010 ± 6.498e+009	**1.453e+003 ± 2.217e+003**†	=	2.443e+004 ± 4.126e+004†
LF2	1.544e+004 ± 2.593e+002	3.369e+003 ± 1.707e+002†	=	**3.096e+003 ± 6.708e+001**†
LF3	2.081e+001 ± 4.392e−002	1.491e+001 ± 5.001e−001†	=	**1.455e+001 ± 9.195e−001**†
LF7	1.264e+009 ± 1.533e+009	1.772e+009 ± 2.262e+009‡	+	**1.095e+009 ± 8.110e+008**
LF8	3.172e+014 ± 2.006e+014	3.714e+014 ± 2.339e+014	+	**1.401e+014 ± 3.790e+013**†
LF12	4.760e+006 ± 4.611e+005	1.166e+006 ± 3.853e+004†	+	**9.234e+005 ± 8.785e+004**†
LF13	8.245e+011 ± 8.753e+010	7.748e+011 ± 8.412e+010	+	**3.230e+003 ± 1.063e+003**†
LF17	5.316e+006 ± 7.207e+005	4.091e+006 ± 9.809e+005†	+	**2.070e+006 ± 1.340e+005**†
LF18	2.308e+012 ± 1.159e+011	1.943e+012 ± 1.145e+011	+	**9.960e+004 ± 9.748e+004**†
LF19	**2.510e+006 ± 5.021e+005**	4.294e+006 ± 4.246e+005‡	+	3.184e+006 ± 1.871e+005‡
LF20	2.325e+012 ± 8.160e+010	1.910e+012 ± 1.485e+011	+	**1.344e+005 ± 1.128e+005**†
$+/=/-^1$	–	5/4/2		9/1/1
$+/=/-^2$		8/3/0		–
Func.	ODE	HLXODE-DG		HLXODE
LF1	1.080e+008 ± 3.542e+007	7.498e+006 ± 8.084e+005†	=	**6.017e+006 ± 3.928e+005**†
LF2	8.057e+003 ± 2.781e+003	**2.176e+003 ± 2.129e+002**†	=	2.180e+003 ± 1.646e+002†
LF3	1.668e+001 ± 2.306e−001	**4.889e+000 ± 2.845e−001**†	=	5.053e+000 ± 3.015e−001†
LF7	5.829e+009 ± 1.026e+009	**1.120e+007 ± 7.836e+005**†	−	1.615e+010 ± 1.262e+009‡
LF8	4.495e+007 ± 9.558e+005	**4.088e+007 ± 8.043e+005**†	=	4.457e+007 ± 8.437e+005
LF12	5.913e+006 ± 3.718e+005	**5.590e+006 ± 4.744e+005**	−	7.458e+006 ± 2.113e+005
LF13	2.944e+006 ± 1.663e+006	7.953e+007 ± 1.120e+007‡	+	**2.036e+006 ± 1.673e+006**
LF17	1.041e+007 ± 1.004e+006	**1.039e+007 ± 4.029e+005**	−	1.804e+007 ± 2.378e+005
LF18	3.366e+009 ± 1.394e+009	6.893e+009 ± 1.179e+009‡	+	**3.020e+007 ± 1.003e+007**†
LF19	3.278e+007 ± 2.054e+006	**3.104e+007 ± 2.947e+006**	=	3.463e+007 ± 2.079e+006
LF20	3.036e+009 ± 1.166e+009	1.951e+010 ± 1.471e+009‡	+	**3.665e+007 ± 6.975e+006**†
$+/=/-^1$	-	5/3/3		5/5/1
$+/=/-^2$		3/5/3		–
Func.	CoDE	HLXCoDE-DG		HLXCoDE
LF1	3.722e+010 ± 6.356e+008	**1.224e+009 ± 3.275e+008**†	=	1.312e+009 ± 8.549e+007†
LF2	1.650e+004 ± 7.714e+001	**3.441e+003 ± 3.126e+002**†	=	3.457e+003 ± 2.516e+002†
LF3	2.114e+001 ± 1.166e−002	1.229e+001 ± 7.078e−001	=	**1.208e+001 ± 2.054e−001**
LF7	**4.236e+010 ± 5.236e+009**	5.076e+010 ± 3.971e+009	−	5.752e+010 ± 4.595e+009
LF8	**9.402e+008 ± 6.890e+007**	2.959e+010 ± 5.404e+009‡	−	1.065e+011 ± 1.897e+010‡
LF12	9.139e+006 ± 5.150e+005	**6.027e+006 ± 1.371e+005**†	=	7.939e+006 ± 1.071e+005†
LF13	3.764e+011 ± 1.281e+010	3.629e+011 ± 2.265e+010	+	**5.018e+008 ± 3.440e+007**†
LF17	1.902e+007 ± 9.162e+005	**1.265e+007 ± 1.589e+004**†	−	1.907e+007 ± 2.216e+005
LF18	2.067e+012 ± 5.965e+010	1.588e+012 ± 5.828e+010	+	**7.995e+008 ± 4.773e+008**†
LF19	**3.087e+007 ± 1.466e+006**	3.098e+007 ± 1.115e+006	=	3.355e+007 ± 1.014e+006
LF20	2.172e+012 ± 6.935e+010	1.636e+012 ± 1.912e+010	+	**1.381e+009 ± 3.631e+008**†
$+/=/-^1$	–	4/6/1		6/4/1
$+/=/-^2$		3/5/3		–

$+$, $=$ and $-$ indicate HLXDE is significantly better than, equal to and worse than its corresponding HLXDE-DG by the Wilcoxon test at 5% significance level respectively.
$+/=/-^1$ indicates the Wilcoxon test results between the HLXDE variant and the corresponding original DE algorithm.
$+/=/-^2$ indicates the Wilcoxon test results between HLXDE and HLXDE-DG.
‡ The HLXDE variant is significantly worse than its corresponding DE algorithm by the Wilcoxon test at 5% significance level.
† The HLXDE variant is significantly worse than its corresponding DE algorithm by the Wilcoxon test at 5% significance level.

Table 32
Results of the average number of groups obtained by HLXDE and HLXDE-DG, respectively, for the CEC2010 functions. The real number of groups for each function is shown in the last column.

Func.	HLXDE	HLXDE-DG	Real number of groups
LF1	1000	1000	1000
LF2	1000	1000	1000
LF3	1000	1000	1000
LF7	952	52	951
LF8	965.4	21	951
LF12	620	510	510
LF13	998	84	510
LF17	460	20	20
LF18	1000	128	20
LF19	1000	1	1
LF20	1000	191	1

In addition, HLXDE with $NP = 100$ is also compared with MA-SW-Chains [37] which ranked the first during the competition for the CEC 2010 large scale global optimization. Table 30 shows that MA-SW-Chains outperformed HLXDE in 32 cases and is outperformed in six cases. The reasons might be as follows: First, these two algorithms are different in nature. MA-SW-Chains is a memetic algorithm combining EA with a sophisticated local search chains, while HLXDE is a pure EA. Thus, introducing a local search operator would likely enhance the performance of HLXDE. Second, both AG and DG need a large number of fitness evaluations to extract the linkage information for the large-scale problems, which makes the evolutionary process of DE insufficient, especially for the nonseparable functions. Finally, the offspring generation strategy has a great influence on the effectiveness of the group-wise crossover. If the quality of population is poor, the identified BBs cannot work effectively to guide crossover. Therefore, in order to enhance the performance of HLXDE for large-scale problems, other advanced techniques (e.g., parallel mechanism [72] and cooperative co-evolution [44]) and the advanced mutation strategies (e.g., DE with neighborhood and direction information [5]) can be incorporated into HLXDE. This will be studied in the future work.

4.10. Comparison on real-world problems

In order to further test the performance of HLXDE on real-world problems, two problems from the IEEE CEC 2011 competition [10] are used. The first problem is parameter estimation for frequency-modulated sound waves (denoted as P1), which is a highly complex multimodal problem with strong epistasis [10]. The second problem is spread spectrum radar poly-phase code design (denoted as P2), which has numerous local optima and has proven to be an *NP*-hard problem [10]. More details can be found in [10]. The *MNFEs* for each problem is set to 50,000, 100,000 and 150,000 respectively, as suggested in [10]. The results over 25 runs are shown in Table 33.

From Table 33, it can be seen that HLXDE can obtain better solutions than the corresponding DE algorithm in most cases. Specifically, for P1, HLXDE performs better in 22 out of 33 cases. For P2, HLXDE is better than the corresponding DE algorithm in 24 out of 33 cases. These results demonstrate that HLXDE is an effective alternative for solving real-world applications.

5. Conclusion and future research

In evolutionary algorithms (EAs), linkage learning or recognizing building blocks (BBs) play an important role in optimization. The existing work of EA has shown that crossover with linkage learning can effectively improve performance for difficult problems. However, the crossover operator employed in most DE algorithms ignores the consideration of the interactions between pairs of variables. Therefore, to alleviate this drawback and enhance the performance of DE, a novel hybrid linkage crossover (HLX) has been proposed for guiding the crossover process of DE. In HLX, three main operators are designed to explicitly utilize the problem-specific linkage information: linkage matrix construction, adaptive grouping and group-wise crossover. After incorporating HLX into DE, the resulting algorithm, named HLXDE, is presented. In this study, HLX has been incorporated into six original DE algorithms, as well as several advanced DE variants, to evaluate its effectiveness.

Through evaluating and comparing the effectiveness of HLXDE with original DE algorithms, advanced DE variants and four DE variants with different crossover operators, it has been confirmed that HLX can effectively improve the performance of most DE algorithms studied. In addition, the benefit of HLX components, parameter sensitivity and scalability study have also been discussed.

In the future, the present work could be extended in multiple directions. First, other strategies for linkage learning will be incorporated with the crossover operator to guide the search of DE. Second, the sophisticated crossover operators [54] will be introduced to study the utilization of the problem-specific linkages. Third, linkage learning in multiobjective optimization (MOO) is scarce [84], and thus the extension of HLXDE to MOO will also be investigated.

Table 33
Mean and standard deviation of the best error values obtained by HLXDE and the corresponding DE on real-world problems.

Problem	FEs	DE/rand/1	HLXDE/rand/1	DE/best/2	HLXDE/best/2	DE/rand/2	HLXDE-DE/rand/2
P1	50,000	3.878e+000 ± 5.802e+000	**3.753e+000 ± 5.227e+000**	6.966e+000 ± 7.038e+000	**3.501e+000 ± 6.027e+000**	1.658e+001 ± 1.641e+000†	**1.556e+001 ± 2.298e+000**
	100,000	**3.472e−001 ± 1.902e+000**	4.272e−019 ± 1.757e−018	4.529e+000 ± 5.702e+000	**3.688e+000 ± 5.322e+000**	1.434e+001 ± 2.103e+000†	**1.302e+001 ± 1.835e+000**
	150,000	0.000e+0.000 ± 0.000e+000	0.000e+0.000 ± 0.000e+000	**3.082e+000 ± 4.816e+000**	3.646e+000 ± 5.293e+000	1.241e+001 ± 2.926e+000†	**1.061e+001 ± 2.526e+000**
P2	50,000	2.556e+000 ± 1.019e−001	**2.528e+000 ± 1.573e−001**	2.547e+000 ± 1.097e−001	**2.534e+000 ± 1.418e−001**	2.555e+000 ± 8.135e−002†	**2.541e+000 ± 9.904e−002**
	100,000	2.457e+000 ± 1.070e−001	**2.447e+000 ± 1.109e−001**	2.484e+000 ± 1.037e−001	**2.469e+000 ± 1.171e−001**	2.465e+000 ± 1.064e−001†	**2.422e+000 ± 1.053e−001**
	150,000	**2.448e+000 ± 9.865e−002**	2.449e+000 ± 1.157e−001	2.435e+000 ± 8.143e−002	**2.430e+000 ± 9.223e−002**	2.452e+000 ± 1.040e−001†	**2.404e+000 ± 1.273e−001**

Problem	FEs	DE/best/1	HLXDE/best/1	DE/current-to-best/1	HLXDE/current-to-best/1	DE/rand-to-best/1	HLXDE/rand-to-best/1
P1	50,000	1.381e+001 ± 6.464e+000	**1.339e+001 ± 6.179e+000**	1.297e+001 ± 4.958e+000†	**8.694e+000 ± 6.201e+000**	1.381e+001 ± 4.444e+000	**1.299e+001 ± 4.731e+000**
	100,000	1.443e+001 ± 5.383e+000	**1.350e+001 ± 7.117e+000**	1.163e+001 ± 5.588e+000	**1.078e+001 ± 4.358e+000**	1.310e+001 ± 5.031e+000	**1.296e+001 ± 5.399e+000**
	150,000	1.464e+001 ± 4.589e+000	**1.253e+001 ± 6.675e+000**	1.034e+001 ± 4.641e+000	**1.013e+001 ± 5.657e+000**	1.307e+001 ± 5.130e+000	**1.228e+001 ± 5.343e+000**
P2	50,000	1.572e+000 ± 1.870e−001	**1.530e+000 ± 3.099e−001**	2.581e+000 ± 1.383e−001	**2.567e+000 ± 1.292e−001**	2.499e+000 ± 2.179e−001	**2.490e+000 ± 2.586e−001**
	100,000	1.503e+000 ± 1.183e−001	**1.496e+000 ± 1.685e−001**	2.495e+000 ± 1.229e−001	**2.470e+000 ± 1.234e−001**	**1.880e+000 ± 5.592e−001**‡	2.230e+000 ± 4.418e−001
	150,000	1.499e+000 ± 1.598e−001	**1.497e+000 ± 1.749e−001**	2.446e+000 ± 1.308e−001	**2.376e+000 ± 1.227e−001**	**1.729e+000 ± 5.320e−001**‡	2.048e+000 ± 5.111e−001

Problem	FEs	ODE	HLX-ODE	SaDE	HLX-SaDE	MoDE	HLX-MoDE
P1	50,000	3.688e+000 ± 6.097e+000	**1.340e+000 ± 3.246e+000**	**4.355e+000 ± 4.856e+000**	4.939e+000 ± 3.689e+000	1.402e+001 ± 8.051e+000	**1.339e+001 ± 7.460e+000**
	100,000	2.844e+000 ± 4.655e+000	**2.646e+000 ± 4.442e+000**	**1.364e−010 ± 7.473e−010**‡	7.566e−001 ± 9.166e−001	1.502e+001 ± 8.168e+000	**1.335e+001 ± 8.234e+000**
	150,000	**2.826e+000 ± 4.948e+000**	2.869e+000 ± 5.019e+000	**0.000e+000 ± 0.000e+000**‡	6.574e−002 ± 1.801e−001	1.503e+001 ± 6.675e+000	**1.351e+001 ± 8.988e+000**
P2	50,000	**1.714e+000 ± 2.638e−001**	1.795e+000 ± 2.797e−001	2.317e+000 ± 1.060e−001	**2.308e+000 ± 1.253e−001**	1.762e+000 ± 3.194e−001	**1.732e+000 ± 2.360e−001**
	100,000	**1.299e+000 ± 1.880e−001**	1.375e+000 ± 1.794e−001	2.236e+000 ± 1.199e−001	**2.193e+000 ± 1.365e−001**	**1.686e+000 ± 2.730e−001**	1.704e+000 ± 2.704e−001
	150,000	1.240e+000 ± 1.629e−001	**1.236e+000 ± 1.315e−001**	**2.098e+000 ± 1.159e−001**	2.145e+000 ± 1.033e−001	1.687e+000 ± 2.510e−001	**1.673e+000 ± 3.210e−001**

Problem	FEs	CoDE	HLX-CoDE	MDE_pBX	HLX-MDE_pBX
P1	50,000	**6.054e+000 ± 2.990e+000**	7.526e+000 ± 4.249e+000	**4.560e+000 ± 5.788e+000**	5.337e+000 ± 6.474e+000
	100,000	**1.116e+000 ± 2.311e+000**	1.916e+000 ± 3.154e+000	5.593e+000 ± 5.989e+000	**3.722e+000 ± 5.665e+000**
	150,000	**1.476e−001 ± 4.632e−001**	5.774e−001 ± 2.038e+000	4.724e+000 ± 5.949e+000	**4.057e+000 ± 5.574e+000**
P2	50,000	**2.270e+000 ± 1.451e−001**‡	2.345e+000 ± 1.443e−001	2.353e+000 ± 2.827e−001	**2.345e+000 ± 2.626e−001**
	100,000	2.226e+000 ± 1.026e−001†	**2.146e+000 ± 1.823e−001**	2.036e+000 ± 2.876e−001	**2.022e+000 ± 2.488e−001**
	150,000	2.187e+000 ± 8.762e−002†	**2.062e+000 ± 1.678e−001**	**1.965e+000 ± 2.646e−001**	2.035e+000 ± 2.482e−001

‡ The HLXDE variant is significantly worse than its corresponding DE algorithm by the Wilcoxon test at 5% significance level respectively.
† The HLXDE variant is significantly better than its corresponding DE algorithm by the Wilcoxon test at 5% significance level respectively.

Acknowledgements

The authors would like to sincerely thank the Editor and the anonymous reviewers for their constructive comments, which improved the original paper significantly. This work was supported in part by the National Natural Science Foundation of China (61305085), the Natural Science Foundation of Fujian Province of China (2014J05074), the Support Program for Innovative Team and Leading Talents of Huaqiao University (2014KJTD13) and the Fundamental Research Funds for the Central Universities (12BS216).

Appendix A. Supplementary material

Supplementary data associated with this article can be found, in the online version, at http://dx.doi.org/10.1016/j.ins.2015.05.026.

References

[1] J. Alcalá-Fdez, L. Sánchez, S. García, Keel: A Software Tool to Assess Evolutionary Algorithms to Data Mining Problems, 2012. <http://www.keel.es/>.
[2] T. Baeck, D. Fogel, Z. Michalewicz, Handbook of Evolutionary Computation, Taylor & Francis, New York, NY, USA, 1997.
[3] S. Bandyopadhyay, H. Kargupta, G. Wang, Revisiting the gemga: scalable evolutionary optimization through linkage learning, in: the IEEE World Congress on Computational Intelligence, 1998, pp. 603–608.
[4] J. Brest, S. Greiner, B. Boskovic, M. Mernik, V. Zumer, Self-adapting control parameters in differential evolution: a comparative study on numerical benchmark problems, IEEE Trans. Evol. Comput. 10 (6) (2006) 646–657.
[5] Y. Cai, J. Wang, Differential evolution with neighborhood and direction information for numerical optimization, IEEE Trans. Cybern. 43 (6) (2013) 2202–2215.
[6] Y. Cai, J. Wang, Y. Chen, W. Tian, T. Hui, Adaptive direction information in differential evolution for numerical optimization, Soft. Comput. (2014), http://dx.doi.org/10.1007/s00500-014-1517-0.
[7] Y. Chen, W. Peng, M. Jian, Particle swarm optimization with recombination and dynamic linkage discovery, IEEE Trans. Syst. Man Cybern. B Cybern. 37 (6) (2007) 1460–1470.
[8] Y. Chen, T. Yu, K. Sastry, A Survey of Linkage Learning Techniques in Genetic and Evolutionary Algorithms, IlliGAL report, 2007014, 2007.
[9] D. Coffin, R. Smith, Linkage learning in estimation of distribution algorithms, Linkage Evol. Comput. (2008) 141–156.
[10] S. Das, P. Suganthan, Problem Definitions and Evaluation Criteria for CEC 2011 Competition on Testing Evolutionary Algorithms on Real World Optimization Problems, Tech. Rep., Jadavpur Univ., West Bengal, India Nanyang Technological University, Singapore, 2010.
[11] S. Das, P. Suganthan, Differential evolution: a survey of the state-of-the-art, IEEE Trans. Evol. Comput. 15 (1) (2011) 4–31.
[12] D. Devicharan, C. Mohan, Particle swarm optimization with adaptive linkage learning, in: Proc. IEEE Congr. Evol. Comput., 2004, pp. 530–535.
[13] A. Draa, S. Bouzoubia, I. Boukhalfa, A sinusoidal differential evolution algorithm for numerical optimisation, Appl. Soft Comput. 27 (0) (2015) 99–126.
[14] L. Emmendorfer, A. Pozo, Effective linkage learning using low-order statistics and clustering, IEEE Trans. Evol. Comput. 13 (6) (2009) 1233–1246.
[15] L. Eshelman, A. Caruana, J. Schaffer, Biases in the crossover landscape, in: S. JD, (Ed.), Proc of the Third Int Conf on Genetic Algorithms, Morgan Kaufmann Publishers, San Mateo, CA, 1898, pp. 86–91.
[16] K. Fan, J. Lee, T. Yu, T. Ho, Interaction-detection metric with differential mutual complement for dependency structure matrix genetic algorithm, in: IEEE Congress on Evolutionary Computation (CEC), 2010, pp. 1–8.
[17] K. Fan, T. Yu, J. Lee, Linkage learning by number of function evaluations estimation: practical view of building blocks, Inf. Sci. 230 (1) (2013) 162–182.
[18] S. García, A. Fernández, J. Luengo, F. Herrera, A study of statistical techniques and performance measures for genetics-based machine learning: accuracy and interpretability, Soft Comput. 13 (10) (2009) 959–977.
[19] M. Ghasemi, M.M. Ghanbarian, S. Ghavidel, S. Rahmani, E.M. Moghaddam, Modified teaching learning algorithm and double differential evolution algorithm for optimal reactive power dispatch problem: a comparative study, Inf. Sci. 278 (0) (2014) 231–249.
[20] D. Goldberg, K. Deb, H. Kargupta, Rapid, accurate optimization of difficult problems using messy genetic algorithms, in: Proceedings of the Fifth International Conference on Genetic Algorithms, 1993, pp. 59–64.
[21] D. Goldberg, K. Deb, D. Thierens, Toward a better understanding of mixing in genetic algorithms, J. Soc. Instrum. Control Eng. 32 (1) (1993) 10–16.
[22] D. Goldberg, B. Korb, K. Deb, Messy genetic algorithms: motivation, analysis, and first results, Complex Syst. 3 (5) (1989) 493–530.
[23] W. Gong, Z. Cai, Differential evolution with ranking-based mutation operators, IEEE Trans. Cybern. 43 (6) (2013) 2066–2081.
[24] W. Gong, Z. Cai, L. Ling, Enhancing the performance of differential evolution using orthogonal design method, Appl. Math. Comput. 206 (1) (2008) 56–69.
[25] W. Gong, A. Fialho, Z. Cai, H. Li, Adaptive strategy selection in differential evolution for numerical optimization: an empirical study, Inf. Sci. 181 (24) (2011) 5364–5386.
[26] S. Gou, C. Yang, Enhancing differential evolution utilizing eigenvector-based crossover operator, IEEE Trans. Evol. Comput. 19 (1) (2015) 31–49.
[27] M.S.R. Group, C.A. Sci., Orthogonal Design, People Education Pub, Beijing, 1975 (in Chinese).
[28] D. Hartl, E. Jones, Genetics: Principles and Analysis, fourth ed., Jones and Bartlett Publishers, Sudbury, MA, 1998.
[29] J. Holland, Adaptation in Natural and Artificial Systems: An Introductory Analysis with Applications to Biology, Control, and Artificial Intelligence, University of Michigan Press, 1975.
[30] S. Islam, S. Das, S. Ghosh, S. Roy, P. Suganthan, An adaptive differential evolution algorithm with novel mutation and crossover strategies for global numerical optimization, IEEE Trans. Syst. Man Cybern. B Cybern. 42 (2) (2012) 482–500.
[31] D. Kovačević, N. Mladenović, B. Petrović, P. Milošević, DE-VNS: Self-adaptive differential evolution with crossover neighborhood search for continuous global optimization, Comput. Oper. Res. 52 (Part B 0) (2014) 157–169.
[32] C. Lin, A. Qing, Q. Feng, A comparative study of crossover in differential evolution, J. Heuristics 17 (6) (2011) 675–703.
[33] J. Liu, J. Lampinen, A fuzzy adaptive differential evolution algorithm, Soft Comput. 9 (6) (2005) 448–462.
[34] R. Mallipeddi, P. Suganthan, Q. Pan, M. Tasgetiren, Differential evolution algorithm with ensemble of parameters and mutation strategies, Appl. Soft Comput. 11 (2) (2011) 1679–1696.
[35] U. Maulik, I. Saha, Automatic fuzzy clustering using modified differential evolution for image classification, IEEE Trans. Geosci. Remote Sens. 48 (9) (2010) 3503–3510.
[36] E. Mezura-Montes, J. Vel¢zquez-Reyes, C. Coello, Modified differential evolution for constrained optimization, in: Proceedings of the Congress on Evolutionary Computation (CEC 2006), IEEE Press, Sheraton Vancouver Wall Centre Hotel, Vancouver, BC, Canada, 2006, pp. 332–339.
[37] D. Molina, M. Lozano, F. Herrera, Ma-sw-chains: Memetic algorithm based on local search chains for large scale continuous global optimization, in: IEEE Congress on Evolutionary Computation (CEC), 2010, pp. 1–8.
[38] D. Montgomery, Design and Analysis of Experiments, fifth ed., Wiley, New York, 2000.
[39] J. Montgomery, S. Chen, An analysis of the operation of differential evolution at high and low crossover rates, in: 2010 IEEE Congress on Evolutionary Computation (CEC), 2010, pp. 1–8.

[40] R. Mukherjee, G.R. Patra, R. Kundu, S. Das, Cluster-based differential evolution with crowding archive for niching in dynamic environments, Inf. Sci. 267 (20) (2014) 58–82.
[41] F. Neri, V. Tirronen, Recent advances in differential evolution: a survey and experimental analysis, Artif. Intell. Rev 33 (1/2) (2010) 61–106.
[42] A. Nikanjam, H. Sharifi, A. Rahmani, Efficient model building in competent genetic algorithms using DSM clustering, AI Commun. 24 (3) (2011) 213–231.
[43] N. Noman, H. Iba, Accelerating differential evolution using an adaptive local search, IEEE Trans. Evol. Comput. 12 (1) (2008) 107–125.
[44] M. Omidvar, X. Li, Y. Mei, X. Yao, Cooperative co-evolution with differential grouping for large scale optimization, IEEE Trans. Evol. Comput. 18 (3) (2014) 378–393.
[45] M. Pelikan, D. Goldberg, E. Cantú-Paz, Boa: the bayesian optimization algorithm, in: Proceedings of Ge-netic and Evolutionary Computation Conference (GECCO-99), Morgan Kaufmann, San Francisco, CA, 1999, pp. 525–532.
[46] A.P. Piotrowski, Adaptive memetic differential evolution with global and local neighborhood-based mutation operators, Inf. Sci. 241 (0) (2013) 164–194.
[47] V. Plagianakos, D. Tasoulis, M. Vrahatis, A review of major application areas of differential evolution, in: U. Chakraborty (Ed.), Advances in Differential Evolution, Springer-Verlag, Berlin, Germany, 2008, pp. 197–238.
[48] A. Qin, V. Huang, P. Suganthan, Differential evolution algorithm with strategy adaptation for global numerical optimization, IEEE Trans. Evol. Comput. 13 (2) (2009) 398–417.
[49] S. Rahnamayan, H. Tizhoosh, M. Salama, Opposition-based differential evolution, IEEE Trans. Evol. Comput. 12 (1) (2008) 64–79.
[50] J.J. Roňkkoňen, S. Kukkonen, V. Price, Real parameter optimization with differential evolution, in: Proc. IEEE Congr. Evol. Comput. (CEC-2005), IEEE Press, NJ, 2005, pp. 506–513.
[51] A. Salman, K. Mehrotra, C. Mohan, Adaptive linkage crossover, in: Proceedings of ACM Symposium on Applied Computing, 1998, pp. 338–342.
[52] A. Salman, K. Mehrotra, C. Mohan, Linkage crossover for genetic algorithms, in: Proceedings of Genetic and Evolutionary Computation Conference 1999 (GECCO-99), 1999, pp. 564–571.
[53] A. Salman, K. Mehrotra, C. Mohan, Linkage crossover operator, Evol. Comput. 8 (3) (2000) 341–370.
[54] A.M. Sánchez, M. Lozano, P. Villar, F. Herrera, Hybrid crossover operators with multiple descendents for real-coded genetic algorithms: combining neighborhood-based crossover operators, Int. J. Intell. Syst. 24 (5) (2009) 540–567.
[55] R. Storn, K. Price, Differential evolution–a simple and efficient heuristic for global optimization over continuous spaces, J. Global Optim. 11 (4) (1997) 341–359.
[56] P. Suganthan, N. Hansen, J. Liang, K. Deb, Y. Chen, A. Auger, S. Tiwari, Problem definitions and evaluation criteria for the CEC 2005 special session on real-parameter optimization, Tech. Rep. 1-50, Nanyang Technol Universiy, Singapore, 2005.
[57] J. Sun, Q. Zhang, E. Tsang, DE/EDA: a new evolutionary algorithm for global optimization, Inf. Sci. 169 (3) (2005) 249–262.
[58] A. Sutton, M. Lunacek, L. Whitley, Differential evolution and non-separability: using selective pressure to focus search, in: Proc. 9th Annu. Conf. GECCO, 2007, pp. 1428–1435.
[59] G. Syswerda, Uniform crossover in genetic algorithms, in: S. JD, (Ed.), Proc 3rd Int Conf on Genetic Algorithm, Morgan Kaufmann Publishers, San Mateo, CA, 1989, pp. 2–9.
[60] K. Tang, X. Li, P. Suganthan, X. Yang, T. Weise, Benchmark Functions for the CEC2010 Special Session and Competition on Large Scale Global Optimization, Tech. Rep., Nat. Inspired Comput. Appl. Lab., USTC, Anhui, China, 2009.
[61] L. Tang, Y. Dong, J. Liu, Differential evolution with an individual-dependent mechanism, IEEE Trans. Evol. Comput. (2014), http://dx.doi.org/10.1109/TEVC.2014.2360890.
[62] D. Thierens, Analysis and Design of Genetic Algorithms, Ph.D. Thesis, Katholieke Universiteit Leuven, 1995.
[63] C.-K. Ting, W.-M. Zeng, T.-C. Lin, Linkage discovery through data mining, IEEE Comput. Intell. Mag. 5 (1) (2010) 10–13.
[64] D.-H. Tran, M.-Y. Cheng, M.-T. Cao, Hybrid multiple objective artificial bee colony with differential evolution for the time-cost-quality tradeoff problem, Knowl.-Based Syst. 74 (0) (2015) 176–186.
[65] M. Tsuji, M. Munetomo, Linkage analysis in genetic algorithms, Comput. Intell. Paradigms (2008) 251–279.
[66] J. Wang, Y. Cai, Multiobjective evolutionary algorithm for frequency assignment problem in satellite communications, Soft. Comput. 19 (5) (2015) 1229–1253.
[67] J. Wang, J. Liao, Y. Zhou, Y. Cai, Differential evolution enhanced with multiobjective sorting based mutation operators, IEEE Trans. Cybern. 46 (12) (2014) 2792–2805.
[68] Y. Wang, Z. Cai, Q. Zhang, Differential evolution with composite trial vector generation strategies and control parameters, IEEE Trans. Evol. Comput. 15 (1) (2011) 55–66.
[69] Y. Wang, Z. Cai, Q. Zhang, Enhancing the search ability of differential evolution through orthogonal crossover, Inf. Sci. 185 (1) (2012) 153–177.
[70] Y. Wang, B. Li, T. Weise, Estimation of distribution and differential evolution cooperation for large scale economic load dispatch optimization of power systems, Inf. Sci. 180 (12) (2010) 2405–2420.
[71] M. Weber, F. Neri, Contiguous binomial crossover in differential evolution, ICAISC (SIDE-EC) (2012) 145–153.
[72] M. Weber, F. Neri, V. Tirronen, Shuffle or update parallel differential evolution for large scale optimization, Soft Comput. 15 (11) (2011) 2089–2107.
[73] B. Xin, J. Chen, J. Zhang, Hybridizing differential evolution and particle swarm optimization to design powerful optimizers: a review and taxonomy, IEEE Trans. Syst. Man Cybern. C Appl. Rev. 42 (5) (2012) 744–767.
[74] X. Yao, Y. Liu, G. Lin, Evolutionary programming made faster, IEEE Trans. Evol. Comput. 3 (2) (1999) 82–102.
[75] T. Yu, D. Goldberg, Dependency structure matrix analysis: offline utility of the dependency structure matrix genetic algorithm, in: Proceedings of GECCO, 2004, pp. 355–366.
[76] T. Yu, D. Goldberg, K. Sastry, C. Lima, M. Pelikan, Dependency structure matrix, genetic algorithms, and effective recombination, Evol. Comput. 17 (4) (2009) 595–626.
[77] T. Yu, D. Goldberg, A. Yassine, Y. Chen, Genetic algorithm design inspired by organizational theory: pilot study of a dependency structure matrix driven genetic algorithm, in: Proceedings of GECCO 2003, 2003, pp. 1620–1621.
[78] T. Yu, K. Sastry, D. Goldberg, Linkage learning, overlapping building blocks, and systematic strategy for scalable recombination, in: Proceedings of GECCO, 2005, pp. 1217–1224.
[79] W. Yu, M. Shen, W. Chen, Z. J, Differential evolution with two-level parameter adaptation, IEEE Trans. Cybern. 7 (44) (2014) 1080–1099.
[80] D. Zaharie, Control of population diversity and adaptation in differen-tial evolution algorithms, in: R. Matousek, P. Osmera, E. (Eds.), Proc. Mendel 9th Int. Conf. Soft Comput. Brno, Czech Republic, 2003, pp. 41–46.
[81] D. Zaharie, Influence of crossover on the behavior of differential evolution algorithms, Appl. Soft Comput. 9 (3) (2009) 1126–1138.
[82] Z. Zhan, J. Zhang, Y. Li, Y. Shi, Orthogonal learning particle swarm optimization, IEEE Trans. Evol. Comput. (2011).
[83] J. Zhang, A. Sanderson, Jade: adaptive differential evolution with optional external archive, IEEE Trans. Evol. Comput. 13 (5) (2009) 945–958.
[84] Q. Zhang, A. Zhou, Y. Jin, Rm-meda: a regularity model based multiobjective estimation of distribution algorithm, IEEE Trans. Evol. Comput. 12 (1) (2008) 41–63.
[85] J. Zhao, Y. Xu, F. Luo, Z. Dong, Y. Peng, Power system fault diagnosis based on history driven differential evolution and stochastic time domain simulation, Inf. Sci. 275 (0) (2014) 13–29.
[86] S.Z. Zhao, P. Suganthan, S. Das, Empirical investigations into the exponential crossover of differential evolutions, Swarm Evol. Comput. 9 (1) (2013) 27–36.